

This is to certify that the

thesis entitled

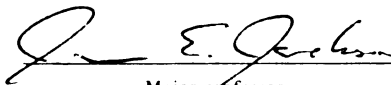
EFFECTS OF VICINAL FUNCTIONAL GROUPS ON  
THE AQUEOUS PHASE HYDROGENATION  
OF LACTIC ACID DERIVATIVES

presented by

Norbert Varga

has been accepted towards fulfillment  
of the requirements for

MS degree in Chemistry



Major professor

Date 11/12/02

**LIBRARY  
Michigan State  
University**

**PLACE IN RETURN BOX** to remove this checkout from your record.  
**TO AVOID FINES** return on or before date due.  
**MAY BE RECALLED** with earlier due date if requested.

DATE DUE	DATE DUE	DATE DUE

EF

**EFFECTS OF VICINAL FUNCTIONAL GROUPS ON  
THE AQUEOUS PHASE HYDROGENATION  
OF LACTIC ACID DERIVATIVES**

**By**

**Norbert Varga**

**A THESIS**

**Submitted to  
Michigan State University  
in partial fulfillment of the requirements  
for the degree of**

**MASTER OF SCIENCE**

**Department of Chemistry**

**2002**

vary

how

heter

and

acids

1200

prop

prop

(2A)

spec

conc

deter

corre

hydr

## **ABSTRACT**

### **EFFECTS OF VICINAL FUNCTIONAL GROUPS ON THE AQUEOUS PHASE HYDROGENATION OF LACTIC ACID DERIVATIVES**

**BY**

**NORBERT VARGA**

Organic acids bearing various functional groups have demonstrated greatly varying reactivity in catalytic hydrogenations. The goal of this project was to determine how reactivity and selectivity of a given organic acid or acid ester in aqueous phase heterogeneous catalytic hydrogenations are affected by different electron-withdrawing and hydrogen-bonding or sterically hindering vicinal substituents

The Ru/C-catalyzed aqueous-phase hydrogenation reactions of various organic acids and esters were run in a high pressure Parr batch reactor at 423, 373 and 348 K and 1200 psi pressure. Nine compounds, namely (1) propionic acid (**PA**), (2) 2-chloropropanoic acid (**2CPA**), (3) lactic acid (**LA**), (4) glycolic acid (**GA**), (5) 2-methoxypropanoic acid (**2MPA**), (6) methoxyacetic acid (**MA**), (7) 2-acetoxypropionic acid (**2APA**), (8) isobutyric acid (**IBA**), and (9) ethyl lactate (**EL**), were studied by <sup>1</sup>H NMR spectroscopic and HPLC chromatographic methods. Substrate and alcoholic product concentrations were monitored with respect to time and the resulting data was used to determine percent conversion of a given organic acid and percent production of the corresponding alcohol. The relationship between molecular structure and efficiency of hydrogenolysis was determined from the selectivity and rate data of each reaction.

Copyrighted by  
NORBERT VARGA  
2002



## Acknowledgements

Great appreciation goes to my advisors, J. E. Jackson and D. J. Miller for providing scientific and financial support with this thesis. Special thanks to my colleagues who provided help when it was needed. Most importantly, my deepest gratitude goes to my friend T. T. O’Kronley who stood by me all along for moral support and helped selflessly in this thesis.

*Vae! Hoc diploma Anglice scriptum est!*

LIS

LIS

LIS

LIS

INT

CH.

CH.

RES

EX

AF

BI

## TABLE OF CONTENTS

LIST OF TABLES.....	vi
LIST OF FIGURES AND IMAGES.....	vii
LIST OF SCHEMES.....	ix
LIST OF ABBREVIATIONS.....	xi
INTRODUCTION.....	1
CHAPTER 1	
1.1 Aqueous Phase Heterogeneous Catalysis.....	3
1.2 Hydrogenation Esters.....	16
1.3 Hydrogenation of Organic Acids.....	31
CHAPTER 2	
RESULTS AND DISCUSSION.....	41
2.1 Hydrogenation of Lactic Acid.....	43
2.2 Hydrogenation of Glycolic Acid.....	47
2.3 Hydrogenation of 2-Methoxypropanoic Acid.....	50
2.4 Hydrogenation of Methoxyacetic Acid.....	54
2.5 Hydrogenation of Isobutyric Acid.....	56
2.6 Hydrogenation of Propanoic Acid.....	58
2.7 Hydrogenation of 2-Chloropropanoic Acid.....	60
2.8 Hydrogenation of Ethyl Lactate.....	65
2.9 Hydrogenation of 2-Acetoxypropanoic Acid.....	67
2.10 Compiled Results.....	71
Conclusion.....	80
EXPERIMENTAL.....	83
General Outline for Hydrogenation Reactions.....	83
Procedure for Handling the Reactor.....	84
Analytical Methods.....	86
Preparation of 2-Methoxypropanoic Acid.....	90
APPENDICES.....	91
BIBLIOGRAPHY.....	115

**List o****Table 1**  
related**Table 1**  
catalyze**Table 2**  
hydroge  
Hydroge  
generate  
a relativ  
**MeOH.****Table 2**  
hydroge  
Hydroge  
generate  
relativel  
**MeOH.****Table 2.**  
Ru C-ca  
The calc  
section.

## List of Tables

<b>Table 1.1.</b> Heats and free energies of formation for diethyl oxalate and related compounds at 1 atm.....	27
<b>Table 1.2.</b> Summary for the hydrogenation of various organic acids, catalyzed by rhenium black. <sup>25</sup> .....	33
<b>Table 2.1.</b> Compiled <sup>1</sup> H NMR results of Ru/C-catalyzed aqueous phase hydrogenations. This table only shows the main products of reactions. Hydrogenation of <b>2APA</b> also generated <b>HOAc</b> and <b>EL</b> hydrogenation generated large quantity of <b>EtOH</b> . Values designated with a * indicate a relatively large degree of uncertainty. Reactions of <b>2MPA</b> also produced <b>MeOH</b> , <b>POL</b> and residual <b>PG</b> .....	73
<b>Table 2.2.</b> Compiled HPLC results of Ru/C-catalyzed aqueous phase hydrogenations. This table only shows the main products of reactions. Hydrogenation of <b>2APA</b> also generated <b>HOAc</b> and <b>EL</b> hydrogenation generated large quantity of <b>EtOH</b> . Values designated with a * indicate a relatively large degree of uncertainty. Reactions of <b>2MPA</b> also produced <b>MeOH</b> , <b>POL</b> and residual <b>PG</b> . The <b>GA</b> was not analyzed by HPLC.....	74
<b>Table 2.3.</b> The calculated <sup>1</sup> H NMR results for the aqueous phase Ru/C-catalyzed hydrogenation of organic acids and esters at 423 K and 1200 psi. The calculations are described in the Analytical Methods of the Experimental section. The relative rates of product formation are the ratios of k(product).....	79

## List of Figures and Images

<b>Figure 1.1.</b> The schematic representation of the addition of hydrogen to the substrate as the molecule enters the porous catalyst and adsorbs on its internal surface. <sup>6</sup> .....	7
<b>Figure 1.2.</b> Two modes of adsorption of unsaturated alcohols to the catalyst surface: (1) Ni interacts with the lone pair of electrons of the hydroxyl functionality, (2) Pd interacts with carbinol carbon by haptophilic affect. <sup>7,8</sup> .....	8
<b>Figure 1.3.</b> On top, adsorption is controlled by the relative position of the large substituent on the chiral center. On the bottom, hydrogen bonding controls the addition of hydrogen, but just as in the top figure, the less hindered side adsorbs to the catalyst surface. <sup>6</sup> .....	9
<b>Figure 1.4.</b> The direct attachment of the formyl group to the catalyst surface. <sup>35</sup> .....	18
<b>Figure 1.5.</b> Mechanism for the gaseous byproduct formation from diethyl oxalate. <sup>46</sup> .....	28
<b>Figure 2.1.</b> A magnified region of the lactic acid mixture showing the doublets of the corresponding acid and esters.....	44
<b>Figure 2.2.</b> Selected <sup>1</sup> H NMR spectra of LA hydrogenation in which PG is produced. For stacked spectra detailing the LA hydrogenation each hour, please see Appendix 1.1.....	45
<b>Figure 2.3.</b> Spectrum (I) is the starting material (GA) and its cyclic ester. Spectrum (II) shows EG, the final product of GA hydrogenation after six hours.....	48
<b>Figure 2.4.</b> Intra-molecular hydrogen bonding of glycolic and lactic acid have a relative fixed geometry compared to propanoic acid.....	50
<b>Figure 2.5.</b> <sup>1</sup> H NMR spectrum of the hydrogenation of 2MPA. The reaction produced a mixture of 2MPOL and 2MPA after six hours.....	52
<b>Figure 2.6.</b> <sup>1</sup> H NMR spectra of 2MPA hydrogenation in which 2MPOL is produced along with small amount of PG and residual amount of MeOH and POL. For stacked <sup>1</sup> H NMR spectra detailing 2MPA hydrogenation each hour, please see Appendix 3.1.....	53

THE  
2  
1911



<b>Figure 2.7.</b> <sup>1</sup> H NMR spectra of <b>MA</b> hydrogenation. Spectrum (I) shows the starting material and spectrum (II) corresponds to the reaction mixture containing <b>MA</b> , <b>2METOH</b> and <b>MeOH</b> after six hours. Stacked spectra detailing <b>MA</b> hydrogenation each hour are found in Appendix 4.1.....	55
<b>Figure 2.8.</b> <sup>1</sup> H NMR spectra of <b>IBA</b> hydrogenation. Spectra (I) shows the starting material, spectra (II) is the mixture of <b>IBA</b> and <b>IBUOL</b> after six hours. For stacked <sup>1</sup> H NMR spectra detailing <b>IBA</b> hydrogenation, see Appendix 5.1.....	57
<b>Figure 2.9.</b> <sup>1</sup> H NMR spectrum of <b>PA</b> hydrogenation. Spectrum (I) shows the starting material, spectrum (II) corresponds to the mixture of <b>PA</b> and <b>POL</b> . For stacked spectra detailing <b>PA</b> hydrogenation, please see Appendix 6.1.....	59
<b>Figure 2.10.</b> (I) is the <sup>1</sup> H NMR spectrum of <b>2CPA</b> pre-reaction mixture. (II) is taken after six hours and is the spectrum of <b>PA</b> . For stacked <sup>1</sup> H NMR spectra detailing <b>2CPA</b> hydrogenation, see Appendix 7.1.....	61
<b>Figure 2.11.</b> <sup>1</sup> H NMR spectra of <b>EL</b> hydrogenation. Spectrum I is <b>EL</b> and spectrum II is the mixture of <b>PG</b> and ethanol after a six hour reaction time. For stacked <sup>1</sup> H NMR spectra detailing <b>EL</b> hydrogenation, see Appendix 8.1.....	66
<b>Figure 2.12.</b> Hydrogenation of <b>2APA</b> at 423 K and 1200 psi produces <b>PG</b> , ethanol and <b>HOAc</b> . Spectrum I is the starting material ( <b>2APA</b> ) and Spectrum II is the product mixture after six hours. For stacked <sup>1</sup> H NMR spectra of <b>2APA</b> , see Appendix 9.1.....	68
<b>Figure 2.13.</b> Percent conversion of <b>LA</b> , <b>IBA</b> , <b>2MPA</b> , <b>MA</b> , <b>GA</b> , <b>PA</b> , <b>EL</b> and <b>2APA</b> in aqueous phase hydrogenation reactions at 423 K and 1200 psi, as determined by <sup>1</sup> H NMR.....	75
<b>Figure 2.14.</b> Percent conversion of <b>LA</b> , <b>IBA</b> , <b>2MPA</b> , <b>MA</b> , <b>PA</b> and <b>EL</b> in aqueous phase hydrogenation reactions at 423 K and 1200 psi, as determined by HPLC.....	76
<b>Figure 2.15.</b> Percent production of <b>LA</b> , <b>IBA</b> , <b>2MPA</b> , <b>MA</b> , <b>GA</b> , <b>PA</b> , <b>EL</b> and <b>2APA</b> and <b>2CPA</b> in aqueous phase hydrogenation reactions at 423 K and 1200 psi, as determined by HPLC.....	77
<b>Figure 2.16.</b> Percent production of <b>LA</b> , <b>IBA</b> , <b>2MPA</b> , <b>MA</b> , <b>PA</b> , <b>EL</b> and <b>2APA</b> in aqueous phase hydrogenation reactions at 423 K and 1200 psi, as determined by HPLC.....	78
<b>Image 1.</b> The Series 4560 Parr Mini Reactor interfaced with a control panel that monitors both pressure and temperature.....	86

## List of Schemes

<b>Scheme 1.1.</b> Chemoselective hydrogenation of an aromatic carboxylic acid to an aldehyde. <sup>6</sup> .....	5
<b>Scheme 1.2.</b> Selectivity determined by the catalyst. Platinum hydrogenates exclusively the olefin moiety of the molecule whereas Zn or Fe selectively hydrogenates the carbonyl carbon. <sup>6</sup> .....	6
<b>Scheme 1.3.</b> Chemoselectivity influenced by steric hindrance. <sup>6</sup> .....	6
<b>Scheme 1.4.</b> Enantioselective hydrogenation of diketo ester to a $\beta$ -hydroxy ester by cinchonidine-modified Pt/Al <sub>2</sub> O <sub>3</sub> catalyst.....	10
<b>Scheme 1.5.</b> Proposed mechanism for the hydrogenolysis of methyl formate to form two moles of methanol.....	17
<b>Scheme 1.6.</b> Adkins hydrogenated esters with 1.5 eq. of copper-chromium oxide at 330 atm of H <sub>2</sub> and 398 K, producing the corresponding alcohols with 80% yield.....	21
<b>Scheme 1.7.</b> The selected reactions by Adkins show that copper-chromium oxide selectively reduces the phenyl-substituted ester at the carbonyl functionality, whereas W-6 Raney nickel, or all tested Raney nickels indiscriminately reduced all unsaturated carbon-carbon bonds, resulting in cyclohexyl functionalities.....	22
<b>Scheme 1.8.</b> The hydrogenations of esters produced yields in excess of 80%. Even though the temperatures did not exceed 373 K, reaction conditions required 1.5 equivalent of W-6 Raney nickel catalyst and 330 atm pressure of H <sub>2</sub> gas.....	24
<b>Scheme 1.9.</b> The two step process of hydrogenolysis of diethyl oxalate to ethylene glycol.....	26
<b>Scheme 1.10.</b> The hydrogenation at two different pressures, producing two different results.....	29
<b>Scheme 1.11.</b> Solvent effects strongly influence the hydrogenation of lactic acid and succinic acid, using rhenium heptoxide reduced in situ. <sup>25</sup> .....	34
<b>Scheme 1.12.</b> The hydrogenation of lactic acid, 2-chloropropanoic acid, malic acid and tartaric acid gave good to moderate yields. The stereochemistry of the substrate was largely retained after hydrogenation resulting in high ee's.....	38
<b>Scheme 1.13.</b> The proposed mechanism of lactic acid hydrogenation. <sup>2</sup> .....	39

THE  
2  
1911



<b>Scheme 2.1.</b> Hydrogenation of lactic acid to generate propylene glycol.....	43
<b>Scheme 2.2.</b> Hydrogenation of glycolic acid that generates ethylene glycol.	
<b>Scheme 2.3.</b> The hydrogenation of <b>2MPA</b> to generate <b>2MPOL</b> .....	51
<b>Scheme 2.4.</b> Hydrogenation of methoxyacetic ( <b>MA</b> ) to generate 2-methoxyethanol ( <b>2METOH</b> ).....	54
<b>Scheme 2.5.</b> Summary of <b>2CPA</b> hydrogenation reactions at varying temperatures and under controlled conditions.....	64
<b>Scheme 2.6.</b> Hydrogenation of <b>2CPA</b> at 348 and 423 K and 1200 psi.....	67
<b>Scheme 2.7.</b> The reaction mechanism for alcohol formation from $\alpha$ -substituted organic acids in aqueous medium under heterogeneous catalytic conditions.....	71

# List

(LA)-  
(PG)-  
(MA)-  
(2ME)-  
(GA)-  
(EG)-  
(2MP)-  
(2MP)-  
(MeO)-  
(EtOH)-  
(IBA)-  
(IBUC)-  
(PA)--  
(POL)-  
(2CPA)-  
(2CPO)-  
(EL)--  
(2APA)-  
(HOAc)-  
(THF)-  
(HDO)-  
(D<sub>2</sub>O)--  
(HCl)--

## List of Abbreviations

(**LA**)---lactic acid  
(**PG**)---propylene glycol  
(**MA**)---methoxyacetic acid  
(**2MEOH**)---2-methoxyethanol  
(**GA**)---glycolic acid  
(**EG**) ---ethylene glycol  
(**2MPA**)---2-methoxypropanoic acid  
(**2MPOL**)---2-methoxypropanol  
(**MeOH**)---methanol  
(**EtOH**)---ethanol  
(**IBA**)---isobutyric acid  
(**IBUOL**)---isobutanol  
(**PA**)---propanoic acid  
(**POL**)---n-propanol  
(**2CPA**)---2-chloropropanoic acid  
(**2CPOL**)---2-chloropropanol  
(**EL**)---ethyl lactate  
(**2APA**)---2-acetoxypropanoic acid  
(**HOAc**)---acetic acid  
(**THF**)---tetrahydrofuran  
(**HDO**)---partially deuterated water  
(**D<sub>2</sub>O**)---deuterium oxide (deuterated water)  
(**HCl**)---hydrochloric acid

THE  
19



# Introduction

Organic acids bearing various functional groups have demonstrated greatly varying reactivity in catalytic hydrogenations. The goal of this project was to determine how reactivity and selectivity toward hydrogenation of a given organic acid or acid ester are affected by different electron-withdrawing and hydrogen-bonding or sterically hindering vicinal substituents. The reactions in this work were run in aqueous medium under mild conditions, using a carbon-supported ruthenium catalyst, to generate value-added chemicals, such as propylene glycol which can be produced by lactic acid hydrogenation. These organic acids and esters are also important feedstocks of the renewable resource-based chemical industry that uses environmentally friendly chemical processes also termed “green chemistry”.

The existence and constant evolution of green chemistry is a result of an environmental consciousness that has impacted all strata of society. Although much work remains to be done to improve the environment, political attitudes, practices in the chemical industry and consumer habits have been making tremendous progress. While the demand for synthetically produced material has increased, the chemical industry has been finding alternative ways that are not only economically sound but are within the realm of “benevolent” chemical processes. The renewable resource-based chemical industry is in the vanguard of these efforts.

Organic acids compose a major class of renewable-resource feedstock chemicals. They are commonly obtained from fermentation of biomass-derived glucose, which comes in turn from starch hydrolysis.<sup>1</sup> Though corn is currently the most important



starch cro  
importan  
I  
because  
glycol. w  
block for  
H  
organic s  
hydrogen  
highly eff  
Miller to p  
and the ef  
the much p  
because bo  
published H  
both.<sup>2</sup>

The  
by Jackson a  
hydrogenati  
OCH<sub>3</sub> or OAc  
substituents or

starch crop, other grains as well as non-cereal crops (e.g. potatoes) represent other important sources of biomass-derived carbohydrate starting materials.<sup>1</sup>

The hydrogenated derivatives of organic acids and esters have great importance because they can serve as building blocks of many syntheses. For example, propylene glycol, which is a hydrogenation product of lactic acid, is a useful molecular building block for the syntheses of a number of pharmaceutical compounds.

Hydrogenolyses of esters often involving stepwise processes and the use of organic solvents, have been successfully practiced in industry. While esters undergo hydrogenolysis more easily than organic acids, lactic acid (LA) has been an exception. Its highly efficient direct hydrogenolysis, relative to propanoic acid, prompted Jackson and Miller to probe the relationship between the molecular structure of various organic acids and the efficiency of hydrogenation under mild conditions.<sup>2</sup> Their research investigates the much preferred aqueous condensed-phase processes over vapor-phase processes because both the feed purity and temperature requirements are less demanding than many published hydrogenations that have been run at either high temperatures or pressures or both.<sup>2</sup>

The ease of aqueous phase Ru/C-catalyzed hydrogenation of LA, demonstrated by Jackson and Miller, laid the ground work for further investigation into the hydrogenation of organic acids bearing a vicinal substituent X (X= H, CH<sub>3</sub>, Cl, OH, OCH<sub>3</sub> or OAc). The goal of this thesis was to elucidate the relative importance of substituents on the efficiency of aqueous phase Ru/C-catalyzed hydrogenation.

THE  
2  
3



# Chapter 1

## 1.1. Aqueous Phase Heterogeneous Catalysis

The essential component in the hydrogenation of an organic acid or ester is the catalyst which can be one of two types: (1) homogeneous or (2) heterogeneous. It is important to note that a complete review of both types of catalysts even in the context of ruthenium, the only catalytic species used in this work, is virtually impossible, given the vast amount of knowledge that has been amassed throughout the years in the science of catalysis. Hence only a limited review of heterogeneous catalysis directly pertaining to this work is provided here.

Although stereochemical control remains a great challenge in synthetic organic chemistry, optimization of reactivity and selectivity to targeted products are of primary importance, in order to afford an efficient and practical use of these reactions.<sup>3</sup>

Homogeneous catalysts have served as useful agents for selective hydrogenations. They must meet two criteria for efficient synthesis: (1) they must possess a high turnover number (TON), (2) high turnover frequency (TOF).<sup>3</sup> Equally important is our ability to handle them easily and safely that conforms to environmentally friendly protocol.<sup>3</sup> With this in mind, ruthenium metal, which is the cheapest precious metal, is an excellent candidate as it has demonstrated superb catalytic activity.<sup>3</sup>

THE  
2  
3



The molecular fine tuning of homogeneous catalysts allow ever increasing stereo control in selective hydrogenations and maximization of product yields.<sup>4</sup> Tuning heterogeneous catalyst on the other hand is more challenging. The question then arises; “Why use heterogeneous catalysts?” As opposed to homogeneous catalysts they are easy to handle and are also easy to separate from the reaction mixture. In addition, they can also be recovered and regenerated after use which makes them immensely appealing to industry.<sup>4</sup>

As opposed to homogeneous catalysis, in which reactants and the catalyst are in one phase (liquid-phase), heterogeneous catalysis involves reactants and the catalyst that are in different phases.<sup>5</sup> This necessarily means that heat and mass transfer must pass through different phases for reaction to occur.<sup>5</sup> For instance, regardless of the activity of the catalyst, a hydrogen molecule must ultimately reach either the external or internal surface of the catalyst where hydrogenation takes place.<sup>5</sup> Following an H<sub>2</sub> molecule, one could see that eight essential steps must happen in the heterogeneous catalytic hydrogenation reaction. Firstly, the H<sub>2</sub> molecule must diffuse from the bulk gas phase to the gas/liquid interface; (2) then it must be absorbed and diffused in the bulk liquid phase; (3) in the liquid phase the H<sub>2</sub> along with other reactants must transfer to the external surface of the catalyst particle; (4) the reactants must then diffuse into the porous catalyst where (5) they adsorb on the catalyst surface; (6) at the surface of the catalyst hydrogenation takes place; (7) the products desorb and transfer away from the catalyst and (8) diffuse into the liquid phase or gas phase.<sup>5</sup>

Selective hydrogenation of a substrate is one of the main challenges in heterogeneous catalytic reactions. Of particular concern is the development of effective

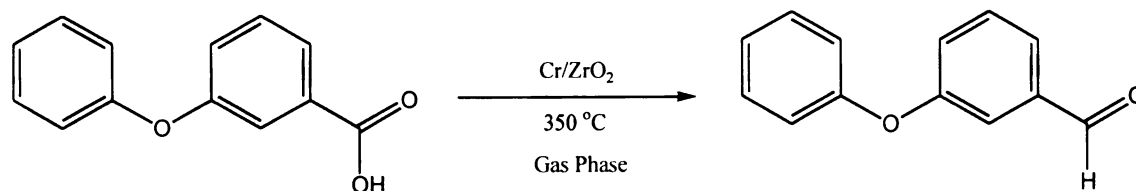
THESE

2

2



systems that can control either enantioselectivity or diastereoselectivity.<sup>6</sup> In addition, great interest lies in the chemoselective hydrogenation of unsaturated acids and esters to the corresponding unsaturated alcohols.<sup>6</sup> One example of chemoselectivity is the heterogeneous catalytic hydrogenation of a carboxylic acid to an aldehyde (Scheme 1.1).<sup>6</sup>



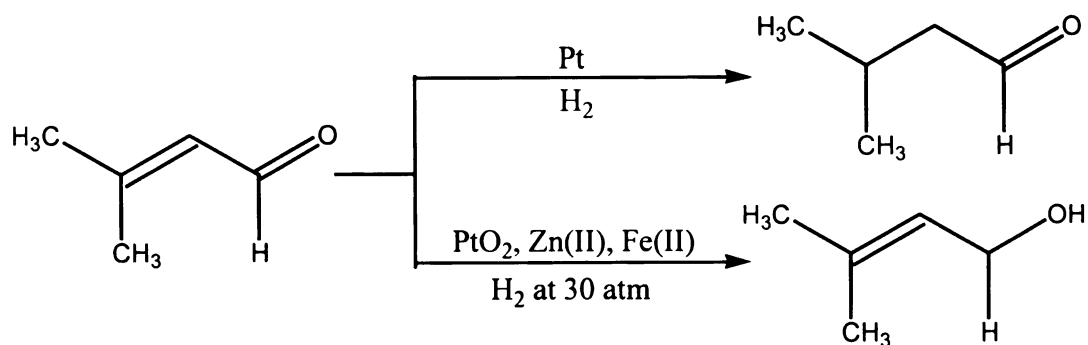
**Scheme 1.1.** Chemoselective hydrogenation of an aromatic carboxylic acid to an aldehyde.<sup>6</sup>

In this reaction two types of selectivity are of interest: (1) the preference toward reducing the carbonyl carbon instead of the unsaturated carbons in the phenyl rings and (2) partial hydrogenation of the carboxylic acid to the corresponding aldehyde instead of an alcohol. The synthetic importance of partial hydrogenation is manifested in conversion of an alkyne to a *cis* alkene instead of the generation of saturated species.<sup>6</sup> The choice of catalyst is a determining factor in chemoselectivity and the result is normally the formation of two different products from the same starting material (Scheme 1.2).<sup>6</sup>

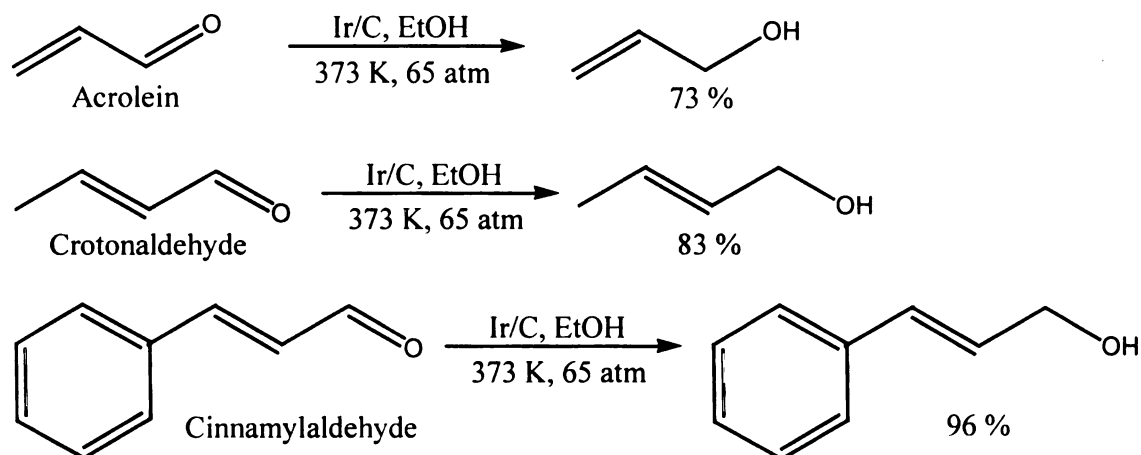
Steric hindrance can also influence the selectivity, normally resulting in preferential hydrogenation of one site over the other. For example, hydrogenation by carbon-supported iridium under identical reaction conditions results in higher product yields for  $\alpha,\beta$ -unsaturated alcohols as the steric bulk close to the olefinic moiety increases (Scheme 1.3).<sup>6</sup>

THE  
D.C.





**Scheme 1.2.** Selectivity determined by the catalyst Platinum hydrogenates exclusively the olefin moiety of the molecule whereas Zn or Fe selectively hydrogenates the carbonyl carbon.<sup>6</sup>



**Scheme 1.3.** Chemoselectivity influenced by steric hindrance.<sup>6</sup>

The stereochemistry of the product is greatly influenced by the adsorption of the substrate on the catalyst surface. As shown in Figure 1.1, molecule can be hydrogenated from the top or the bottom face of the alkene functional group.<sup>6</sup> The facial discrimination is relative to which side of the molecule adsorbs on the catalyst surface.<sup>6</sup>

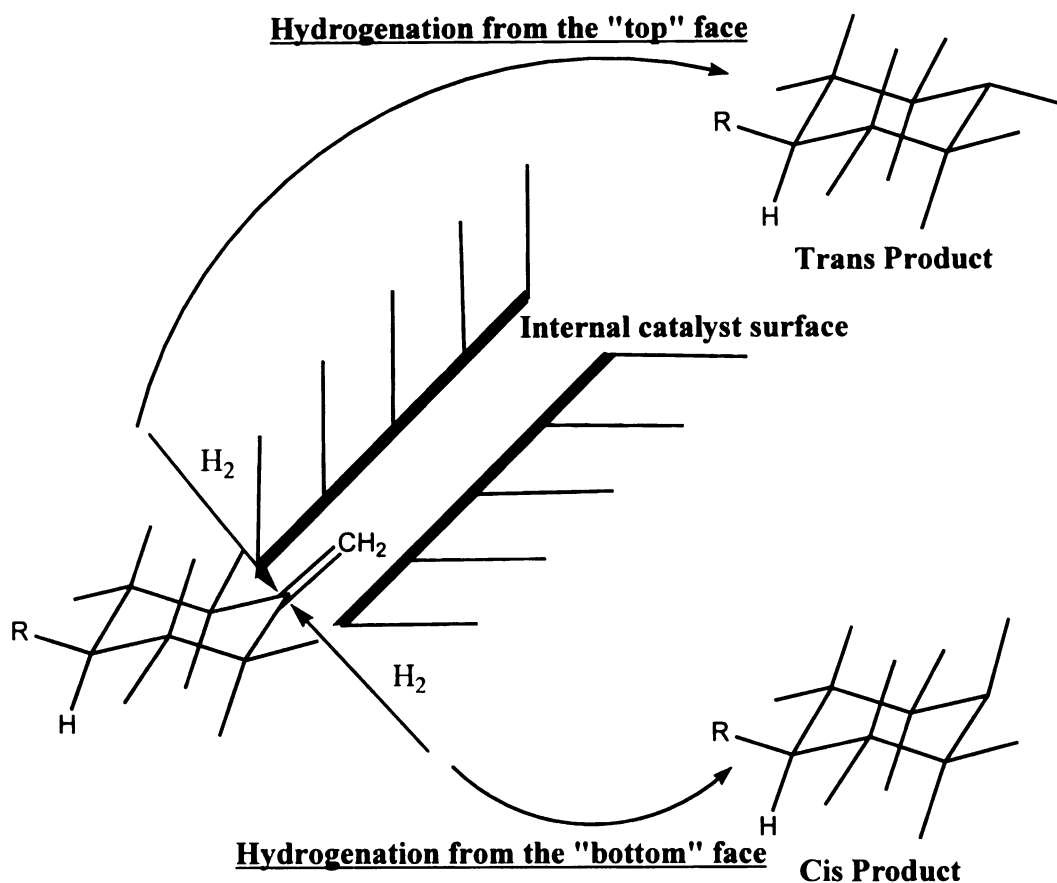


**Figure 1.1.** The schematic representation of the addition of hydrogen to the substrate as the molecule enters the porous catalyst and adsorbs on its internal surface.<sup>6</sup>

Vicinal bulky substituents and hydrogen bonding functional groups, such as hydroxyl or amine groups, can determine the direction of adsorption on the catalyst surface.<sup>7,8</sup> For example, the hydroxyl group can interact with the catalyst surface to determine from which direction the alkene will be adsorbed to the catalyst surface (Figure 1.2)<sup>6</sup> The mode of interaction between the catalyst's orbitals and the hydroxy group is believed to depend on the type of metal as well. For example, it has been proposed that the orbitals of a nickel catalyst interact with the lone pair of electron of the

hydroxyl group, giving trans product, whereas the palladium's orbitals interact with the carbinol carbon, giving cis product (Figure 1.2).<sup>9</sup>

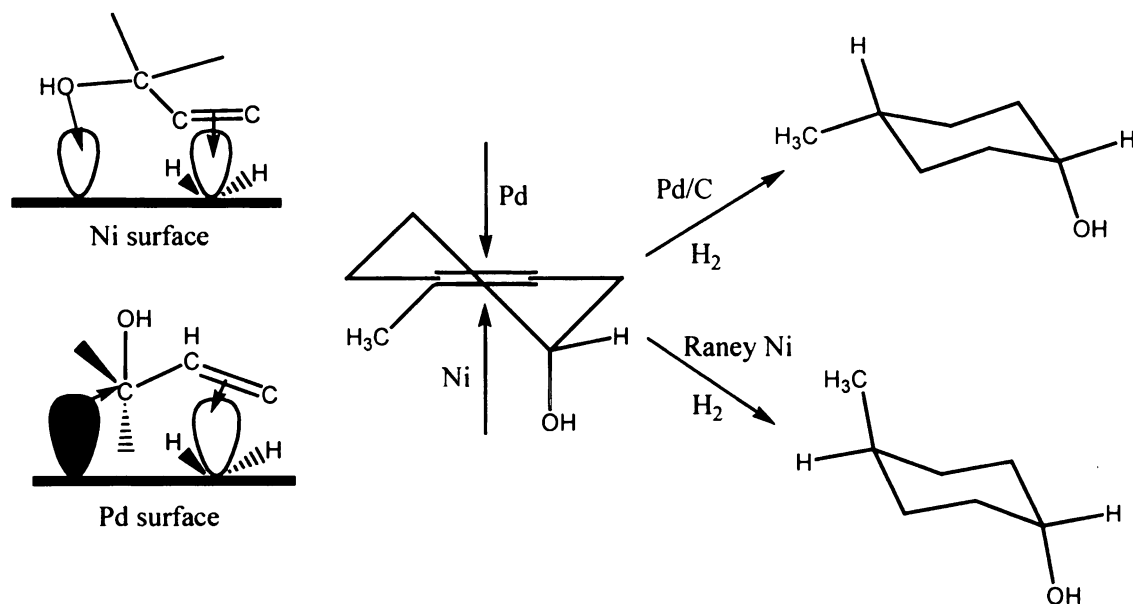


**Figure 1.2.** Two modes of adsorption of unsaturated alcohols to the catalyst surface: (1) Ni interacts with the lone pair of electrons of the hydroxyl functionality, (2) Pd interacts with carbinol carbon by haptophilic effect.<sup>7,8</sup>

Adsorption to the catalyst surface can influence the diastereoselectivity as well. The diastereoselective hydrogenation of ketones is influenced by the presence of a chiral center of the molecule that can direct the hydrogen addition to the substrate.<sup>6</sup> It has been proposed that Cram's Rule can be applied in heterogeneous catalytic hydrogenations to explain the stereoselectivity of hydride transfer to the carbonyl functionality. In this process the hydrogen is transferred to the carbonyl carbon from the less sterically hindered face of the molecule (Figure 1.3).<sup>6,10</sup> The degree of adsorption to the catalyst surface is influenced by the relative size of the other two substituents attached to the

chiral center.<sup>6</sup> Hydrogen bonding of a carbonyl with a vicinal -OH or -NH group can influence the direction of hydrogen addition.<sup>6</sup> In principle, the molecule is fixed in one plane and the adsorption takes place from the less sterically hindered side where the smaller substituent is situated (Figure 1.3).<sup>6</sup>

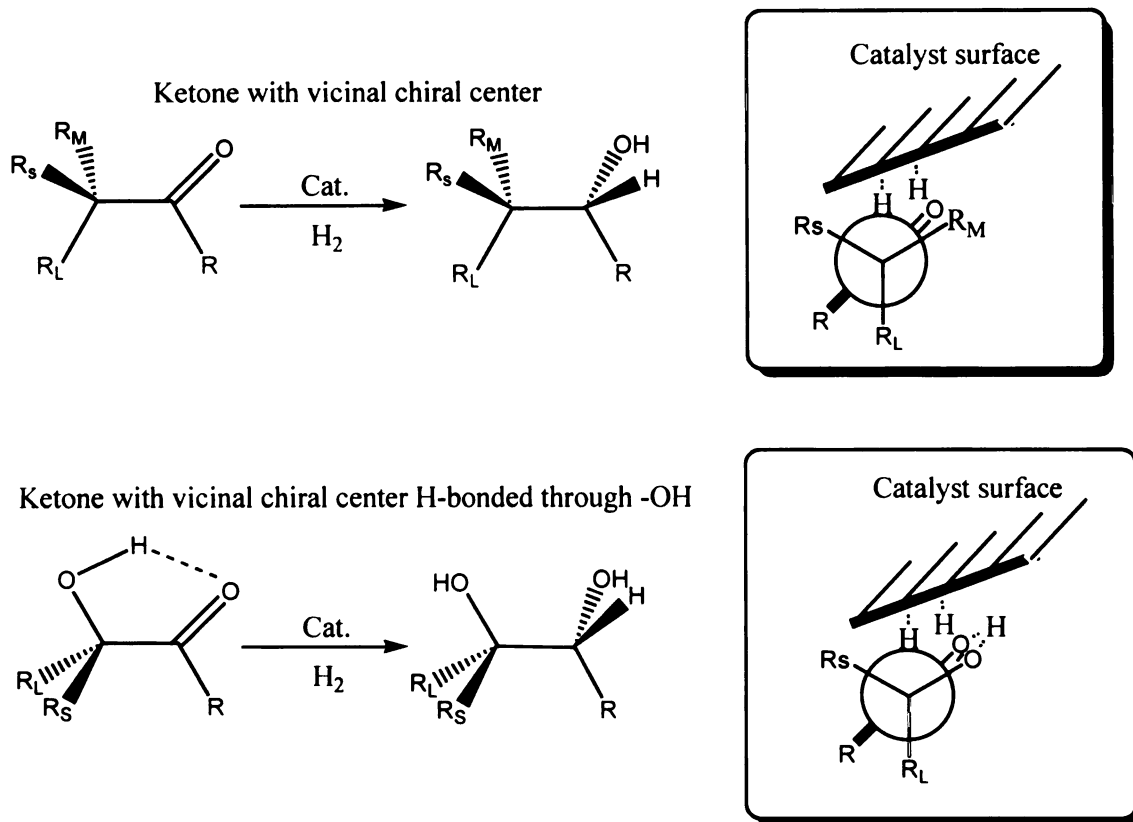


**Figure 1.3.** On top, adsorption is controlled by the relative position of the large substituent on the chiral center. On the bottom, hydrogen bonding controls the addition of hydrogen, but just as in the top figure, the less hindered side adsorbs to the catalyst surface.<sup>6</sup>

Chiral directing groups that reside on the substrate molecule can be essential for the diastereoselectivity in such hydrogenation reactions. Although Cram's Rule has worked



well for predic

reaction at the

In the

performed usi

Alternatively,

enantioselecti

without hydro



**Scheme 1.4.**  
cinchonidine-r

Althou

of H<sub>2</sub> from the

too.<sup>4</sup> One of t

inside the reac

profoundly aff

hydrogenation

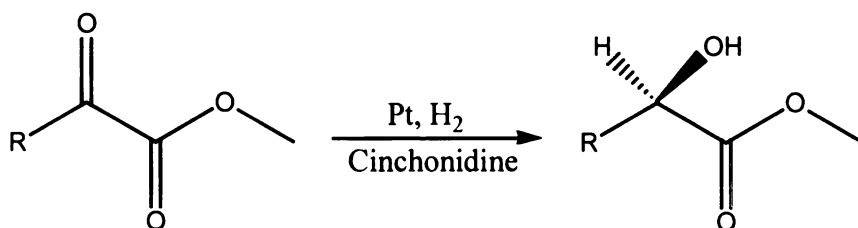
selectivity for

1000 rpm.<sup>13</sup>

well for predicting stereoselectivity in homogeneous catalytic reactions, the details of the reaction at the catalyst surface in heterogeneous catalysis have not been elucidated.

In the early fifties, enantioselective, heterogeneous catalytic hydrogenation was performed using metal catalysts with quartz or silk fibroin serving as chiral support.<sup>11,12</sup>

Alternatively, cinchonidine-modified Pt/Al<sub>2</sub>O<sub>3</sub> catalysts can be employed to enantioselectively hydrogenate a generic diketo ester to the corresponding R ester without hydrolysis (Scheme 1.4).<sup>6,4</sup>



**Scheme 1.4.** Enantioselective hydrogenation of diketo ester to a β-hydroxy ester by cinchonidine-modified Pt/Al<sub>2</sub>O<sub>3</sub> catalyst.

Although the choice of a heterogeneous catalyst is vital, mass transfer limitations of H<sub>2</sub> from the gas phase to the liquid phase can severely influence enantioselectivity too.<sup>4</sup> One of the ways to minimize diffusion limitations is by varying the stirring speeds inside the reactor.<sup>4</sup> Blackmond et al. has demonstrated that increasing the stirring speed profoundly affects the optical yields for the Pt/Al<sub>2</sub>O<sub>3</sub>-catalyzed liquid-phase hydrogenation of ethyl pyruvate to R and S ethyl lactate.<sup>13-16</sup> In their work the selectivity for (R)-lactic acid increased as the stirring speed was increased from 400 to 1000 rpm.<sup>13</sup>



With an increase of  $H_2$  pressure, from 1 to 40 atm, the enantiomeric excess also increased for the R enantiomer.<sup>17</sup> This preference for the R enantiomer was believed to be due to the difference in the rate determining step for the formation of the R and S enantiomers.<sup>17</sup> An alternative explanation for this selectivity lies in the assumption of a steady-state approximation that allows the determination of the surface concentration of the ethyl pyruvate that is adsorbed on modified catalytic sites.<sup>4,15</sup>

The reaction rate in heterogeneous catalytic hydrogenations is another important factor. Mass transfer limitations, however, can skew rate determinations. To avoid this problem, the absence of all transport limitation is assumed to determine the kinetics of these reactions. Based on this assumption, the rate of reaction increases with an increasing number of active sites, if the reaction is not sensitive to the structure of the catalyst.<sup>4</sup> Hence, there is a linear relationship between the active site density and the number of metal atoms on the surface.<sup>4</sup> In the hydrogenation of citral, Singh et al. compared the catalytic activity of Group VIII metals supported on  $SiO_2$ ,  $Al_2O_3$  and  $TiO_2$  and found that Pd on silica support shows the greatest catalytic activity at 300 K and 1 atm, when all mass transport limitations are absent.<sup>18</sup> Tests were also carried out by  $TiO_2$ -supported Pt, and they found that the hydrogenation rate is strongly influenced by the particle size of the Pt catalyst due to metal-support interaction.<sup>18</sup>

Just as in organic synthesis, solvent effects have an impact on heterogeneous catalytic hydrogenation reactions as well. Although these effects are incompletely understood, the rational behind them is based on systematic correlations of solvent polarity or dielectric constant with the rates of reactions and distribution of products.<sup>19,20</sup> Because the solvent can interact with the metal support, unraveling the solvent effects in

THE  
S.



these reactions are more difficult as compared to homogeneous catalysis. However, it was found that polar and nonpolar substrates hydrogenate at different rates in solvents of varying polarity.

Polar solvents seem to increase the adsorption of non-polar substrates to the catalyst surface whereas non-polar solvents increase the adsorption of a polar reactant to the catalyst surface.<sup>4,6</sup> In a study of competitive hydrogenation of cyclohexene and acetone, Scholten et al. demonstrated that the selectivity of Ru-catalyzed liquid-phase hydrogenation of cyclohexene to cyclohexane was enhanced by addition of ethanol.<sup>4</sup> Conversely, the addition of cyclohexane increased the selectivity in the hydrogenation of acetone to isopropanol.<sup>4,21</sup> Furthermore, addition of ethanol in acetone hydrogenations produced poor yields.<sup>4,21</sup> They proposed that ethanol strongly increased the rate of desorption from the catalyst surface and simultaneously impeded the rate of hydrogenation.<sup>21</sup> This finding was also confirmed in the gas-phase hydrogenation of benzene in which ethanol was introduced. Using FTIR spectroscopic methods to characterize the interaction between the alcohol and the olefin, they observed that the –OH group of ethanol formed a hydrogen bonding adduct with the alkene functional group of the substrate.<sup>4</sup> Based on this finding, they proposed that the increased desorption rate was due to a weakened overlap of the olefin  $\pi$  electrons with the Ru catalyst.<sup>4,21,22</sup> In addition, the synergy between  $H_2$  concentration and the solvent effect has profound impact on the concentration of the adsorbed hydrogen on the catalyst surface. Using 5% Pt/C at 300 K and 1 atm, Cervený et al. demonstrated a linear relationship between the concentration of adsorbed hydrogen on the catalyst and liquid-phase hydrogen concentration, optimized in various solvents.<sup>4</sup>



Although  
 be reported in  
 Using citral as  
 catalyst, there  
 are easier to be  
 kinetic studies  
 temperature ra  
 product distrib  
 does not at all  
 found that the  
 conversion at  
 298 K to 423  
 also observed  
 hydrogenation  
 benzene adsor  
 observed an a  
 activity.<sup>4</sup>

Reactive  
 useful to hydro  
 temperatures (c  
 Furthermore, c  
 Pt/SiO<sub>2</sub> or Pt  
 as the tempera

Although a review of the kinetic descriptions of heterogeneous catalysis will not be reported in this thesis, a few highlights pertinent to this project need to be addressed. Using citral as the target model for parallel hydrogenation reactions by supported Pt catalyst, thermodynamic considerations suggest that non-conjugated terminal C=C bonds are easier to hydrogenate than conjugated C=C followed by C=O bond.<sup>4</sup> Based on kinetic studies of citral hydrogenation by Pt supported on TiO<sub>2</sub> or SiO<sub>2</sub>, in the temperature range of 298 to 423 K, it was found that increasing temperatures can effect product distributions and it can also cause a peculiarity in the kinetics of this reaction that does not at all adhere to simple Arrhenius behavior.<sup>4,18</sup> Using Pt/SiO<sub>2</sub> at 20 atm, it was found that the turnover frequency for H<sub>2</sub> uptake was significantly lower for citral conversion at 423 K than at 298 K. This means that as the temperature is increased from 298 K to 423 K, the rate of hydrogenation significantly decreases.<sup>18</sup> Other groups have also observed a significant decrease in the reactivity in heterogeneous catalytic hydrogenation of benzene, which was thought to be due to a lower concentration of benzene adsorbed on the catalyst surface at higher temperatures.<sup>4</sup> Because Singh et al. observed an activity minimum, they argued against the latter proposition of decreased activity.<sup>4</sup>

Reaction kinetics can also be altered by the metal-support interactions and can be useful to hydrogenate C=O bonds selectively.<sup>4</sup> Group VIII metals were reduced at high temperatures (over 700 K), and their interaction with TiO<sub>2</sub> support was studied. Furthermore, citral hydrogenation was also studied under similar conditions, using Pt/SiO<sub>2</sub> or Pt/TiO<sub>2</sub> catalysts, and a twofold decrease in turnover frequency was observed as the temperature was raised from 473 K to 773 K.<sup>4</sup> Haller et al. proposed that this

unusual kinetic behavior is due a partial loss of oxygen from the support, rendering it a partially unsaturated cation with its coordination bonds still intact.<sup>4</sup> The oxygen vacancy is the greatest at the metal-support interface that facilitates the partial reduction of the support. The support can in turn migrate onto the metal catalyst surface and virtually block the chemisorption of H<sub>2</sub> on the metal.

If the support can have such a profound impact, how does the metal catalyst affect the kinetics? The choice of metal appears to have the greatest affect. Virtually three orders of magnitude of initial turnover frequency was observed amongst Group VIII metals in citral hydrogenation.<sup>4</sup> Using the silica support for each catalyst, the lowest initial turnover frequency was observed for cobalt followed by nickel, rhodium, ruthenium, osmium, iridium, platinum and palladium, respectively, at 300 K and 1 atm pressure.<sup>4</sup> This trend was attributed to percent d character of the metal that is defined as the contribution of d electrons to the spd hybrid orbitals.<sup>4,23</sup> The relationship between the catalytic activity and the percent d character of a Group VIII metal is not well understood.<sup>4</sup> In addition, various group VIII metals generated different product distribution in the hydrogenation of citral.<sup>4</sup> Based on extended Huckel calculations, Delbecq and Sautet proposed that this difference is due to the relative geometry and strength of adsorption, which in turn depends on two important interactions: the relative contributions of stabilizing two-electron donation/backdonation and four-electron destabilizing interactions between the catalyst and the substrate.<sup>4</sup> Finally, crystallite size effects seem to affect the kinetics of some hydrogenation reactions.<sup>4</sup> These effects can be understood from the structure sensitivity of the turnover frequency.<sup>4</sup> More specifically, a change in the size of metal crystallite in the range of 1-10 nm and a change

in the available crystal plane can effectively decrease or increase the turnover frequency of the catalyst.<sup>24</sup>

Hydrogenation reactions involving C-C, C-O and C-N scission are sensitive to the structure of the catalyst, whereas C-H bond formation and scission including hydrogenation reaction are structure insensitive.<sup>4</sup> Apparently, metal atoms crowd the support surface with varying coordination that lead to inhomogeneity in the potential energy surface. This phenomenon has rendered the explanation for structure insensitivity elusive.<sup>4</sup>

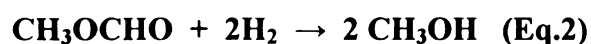
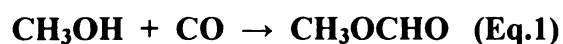
Although heterogeneously catalyzed selective hydrogenations are useful there is still plenty of work to be done in improving the diastereoselectivity and enantioselectivity of these reactions. At present there is still a great potential in homogeneous catalysts from the synthetic point of view as they can be molecularly tuned to improve both stereoselectivity and product yields. The caveat though is how to remove homogeneous catalysts effectively from the reaction mixture, minimize environmental hazards that they may pose, and make their use more cost effective. Because heterogeneous catalysis can circumvent these problems they can provide an excellent alternative to conventional stoichiometric hydride reductions.



## 1.2. Hydrogenation of Esters

By the middle of the 1930's numerous heterogeneous catalytic hydrogenations of esters had been published. The economic feasibility of these processes were quite questionable as they were done under stringent conditions, requiring high temperatures and pressures up to 700 K and 350 atm and the use of organic solvents such as dioxane.<sup>25</sup>

The pioneering work of Christiansen to generate methanol via the hydrogenolysis of methyl formate provided an alternative route to the common industrial process in which CO was hydrogenated over Cu/Zn catalyst at 523 K and 99 atm.<sup>26</sup> The catalytic hydrogenation of methyl formate to form methanol, with  $\Delta H(298\text{K}, 1\text{atm}) = -47.5$  kJ/mol, is an exothermic process, making this alternative route thermodynamically feasible.<sup>27</sup> Christiansen developed a two step process that initially involved the generation of a methyl formate intermediate (Equation 1) by reacting carbon monoxide with methanol in the presence of a dissolved alkali metal such as sodium.<sup>28</sup> From one mole of formate two moles of methanol were produced by catalytic hydrogenation, using a copper-based catalyst (Equation 2).<sup>26,28</sup>



The generation of methanol from methyl formate was the focus of several studies. Evans examined the kinetics of the copper chromite catalyzed hydrogenolysis of methyl formate in the temperature range of 373 to 500 K at atmospheric pressure. He observed

over 90 °

He also fo

ratio of hy

Ce

hydrogene

methanol

pressure. 7

of 428 to

kJ mol un

undergoe

cleavage

then proo

1.5),<sup>26,32</sup>

H<sub>3</sub>C

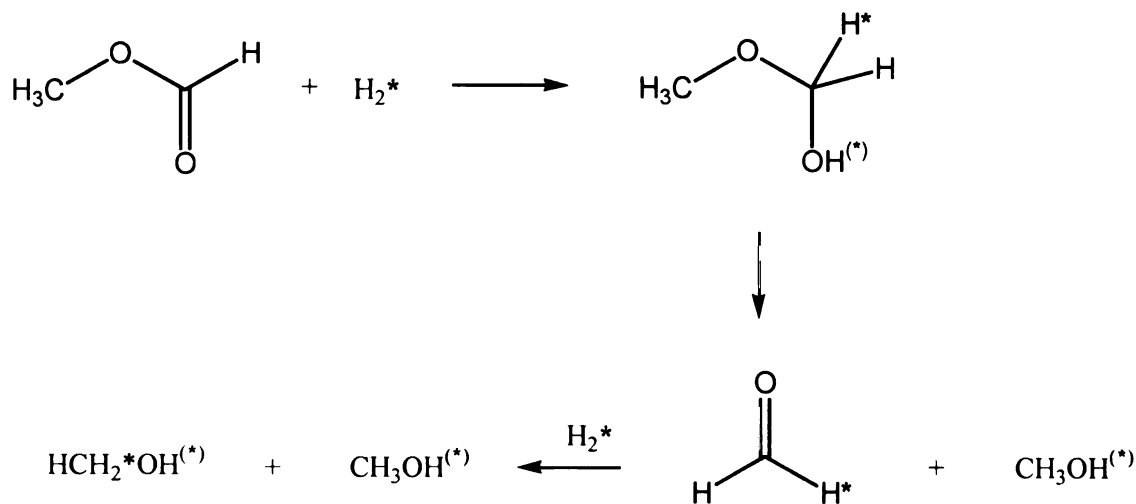
HCH

**Scheme**  
moles of

over 90 % selectivity to methanol while below 90 % conversion of methyl formate.<sup>29,30</sup>

He also found that the selectivity for methanol was not influenced by temperature or the ratio of hydrogen to methyl formate.<sup>29,30</sup>

Cervený et al. demonstrated that the carbonylation of methanol and hydrogenolysis of methyl formate could be carried out in a one pot reaction to generate methanol in liquid phase in the temperature range of 373 and 500 K and at atmospheric pressure.<sup>26,31</sup> Sorum and Onsager studied this reaction in the narrow temperature range of 428 to 458 K and at 70 atm pressure and determined that activation energy is 53 kJ/mol under these conditions.<sup>32</sup> They proposed a mechanism in which the reaction undergoes a rate limiting formation of a hemiacetal intermediate followed by a rapid cleavage to generate formaldehyde and methanol. The hydrogenation of formaldehyde then produces one mol of methanol which is the net yield of this reaction (Scheme 1.5).<sup>26,32</sup>



**Scheme 1.5.** Proposed mechanism for the hydrogenolysis of methyl formate to form two moles of methanol.

1

Monti et al. found that the very same reaction, carried out in a temperature range of 408 to 473 K and pressure of 17 to 45 atm, has an energy of activation of 62 kJ/mol.<sup>32</sup> Although a relatively high selectivity for methanol was demonstrated in the gas phase reaction, some degree of inhibition by CO was also observed.<sup>26,33</sup> This was not a great concern, but they found that CO poisoning can be lowered by increasing the temperature.<sup>34</sup>

Trimm et al. studied the hydrogenation of methyl formate by in-situ IR spectroscopy, using silica-supported copper as catalyst.<sup>26,35</sup> They found that the rate of conversion is directly related to the intensity of the IR absorbance at  $1666\text{ cm}^{-1}$ , assigned to the formyl group directly bound to the copper (Figure 1.4).<sup>35</sup>

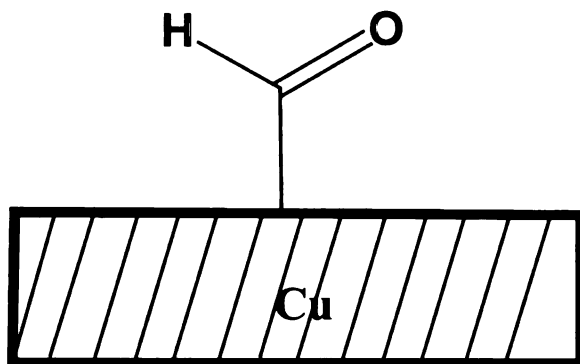
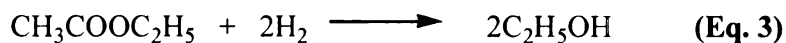


**Figure 1.4.** The direct attachment of the formyl group to the catalyst surface.<sup>35</sup>

One of the earliest examples of the hydrogenation of higher esters was demonstrated by Lazier.<sup>36</sup> In the temperature range of 473 to 673 K and pressure range of 50 to 250 atm, butyl alcohol was obtained from the hydrogenolysis of butyl butyrate

with high selectivity, using a copper oxide/zinc oxide catalytic mixture.<sup>36</sup> The liquid-phase hydrogenolysis of butyl acetate was compromised by competing transesterifications in studies with barium-promoted copper chromite catalyst in the temperature range of 450 to 530 K and pressure from 50 to 200 atm.<sup>26,37</sup> Grey et al. described the use of an anionic ruthenium hydride complex for the hydrogenolysis of esters run neat or using solvents such as toluene or THF. Although decarbonylation and transesterification reactions compromised his reactions, producing low yields, he was able to demonstrate the feasibility of mild conditions for hydrogenolysis (T = 373 K, P = 6.2 atm)<sup>38,39</sup>

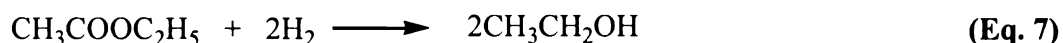
Ethyl acetate has been a primary target of hydrogenolysis. Two patents and several studies describe the application of bimetallic rhodium catalyst (Sn/Rh) and Raney Copper catalyst, claiming 90 % conversion to ethanol in the temperature range of 473 to 560 K and pressures of 1 to 50 atm.<sup>40</sup> However, ethanol yields from ethyl acetate hydrogenolysis (Eq.3) can be compromised under such conditions by the formation of acetaldehyde which is in equilibrium with ethanol (Eq.4).<sup>26,40</sup>



Using Sn/Rh catalyst mixtures, Ferreti demonstrated that an increase of Sn/Rh ratio increases the rate of hydrogenation of ethyl acetate to ethanol, but the competing acetaldehyde formation is not affected.<sup>41</sup> Furthermore, transesterification reactions were

observed during the hydrogenation of higher esters such as methyl propanoate and methyl butanoate, at temperatures close to 500 K.

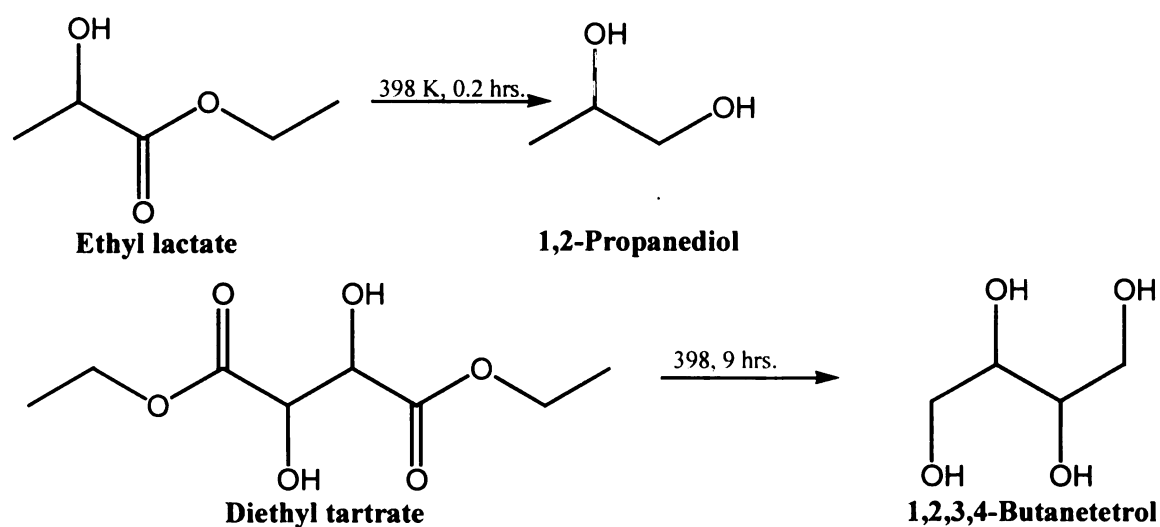
Mechanistically similar to the Christiansen hydrogenolysis of methyl formate, Claus et al. provided an interesting route to ethanol formation. Using a copper catalyst, methyl acetate was hydrogenated to methanol and ethanol at 40 atm and 500K. They proposed that the first step involves the formation of ethanol and methanol (Equation 5). Subsequently the ethanol undergoes a transesterification with another methyl acetate to form ethyl acetate and methanol (Equation 6). Finally, ethyl acetate is reduced to two moles of ethanol (Equation 7).<sup>42</sup>



Yan et al. and Evans et al. proposed that the mechanism of the hydrogenolysis of various acetates involves the dissociative adsorption of acetate to the catalytic surface via the acyl fragment.<sup>26,37</sup> This hypothesis was confirmed by Trimm et al. who conducted isotopic labeling studies on methyl formate and found that the hydrogenation of the acyl fragment is a relatively slow step. They proposed that an alkoxy fragment associated to the catalytic surface quickly forms an alcohol whereas the adsorbed acyl fragment is slow to release, undergoing rate limiting hydrogenation to the corresponding alcohol or aldehyde.<sup>26,37</sup> Though the latter process must have been expected to lower the

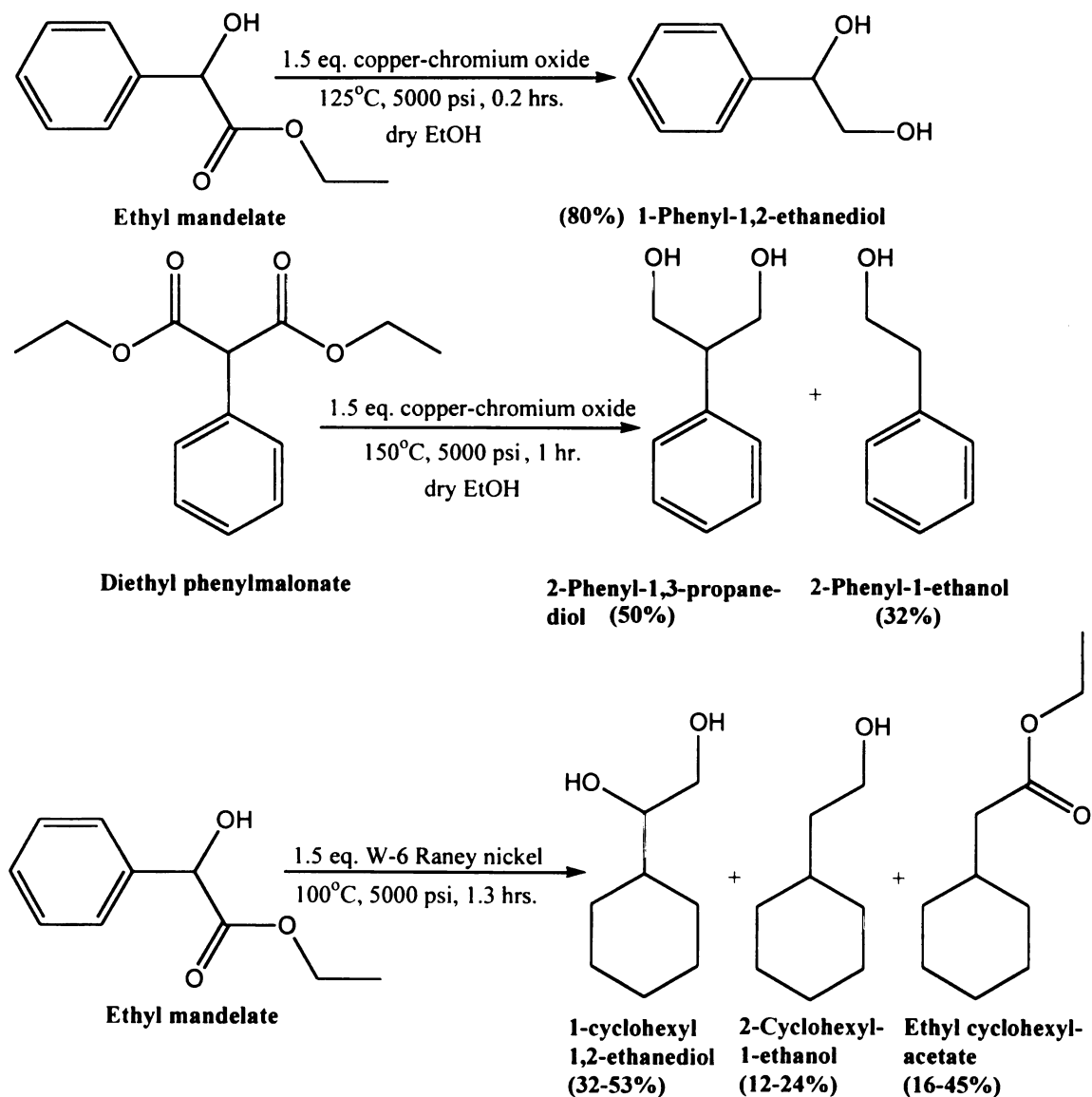
yield, Agarawal, using Cu suspended on silica, demonstrated that acetaldehyde is hydrogenated three orders of magnitude faster than ethyl acetate.<sup>43</sup>

As demonstrated in the 1930's high temperatures (up to 485 K) were required in copper-chromium oxide catalyzed hydrogenations of ethyl lactate to generate propylene glycol and ethanol.<sup>44,45</sup> These temperatures were high enough to racemize or even pyrolyze esters. Such high temperatures are impractically expensive for any useful process; thus lowering temperatures became an important issue. For example, Mozingo and Folkers successfully hydrogenated malonates, acetoacetates and benzoates at 430 K for 13 hours, using copper-chromium oxide in the ratio of 20 to 50 weight percent to esters and reporting 40 % yields.<sup>43</sup> Adkins used their findings to demonstrate that increasing copper-chromium oxide loading up to one or even 1.5 equivalent of the ester in a temperature range of 621 to 673 K would improve the product yield beyond 40% in the hydrogenation of esters (Scheme 1.6).



**Scheme 1.6.** Adkins hydrogenated esters with 1.5 eq. of copper-chromium oxide at 330 atm of H<sub>2</sub> and 398 K, producing the corresponding alcohols with 80% yield.

While Raney nickel indiscriminately reduces the aromatic ring of phenyl-substituted esters in all cases, giving cyclohexyl-substituted alcohols, copper-chromium oxide only reduces the phenyl-substituted esters at the carbonyl functionality (Scheme 1.7). Aside from this limitation on selectivity, Raney nickel is useful in reducing esters



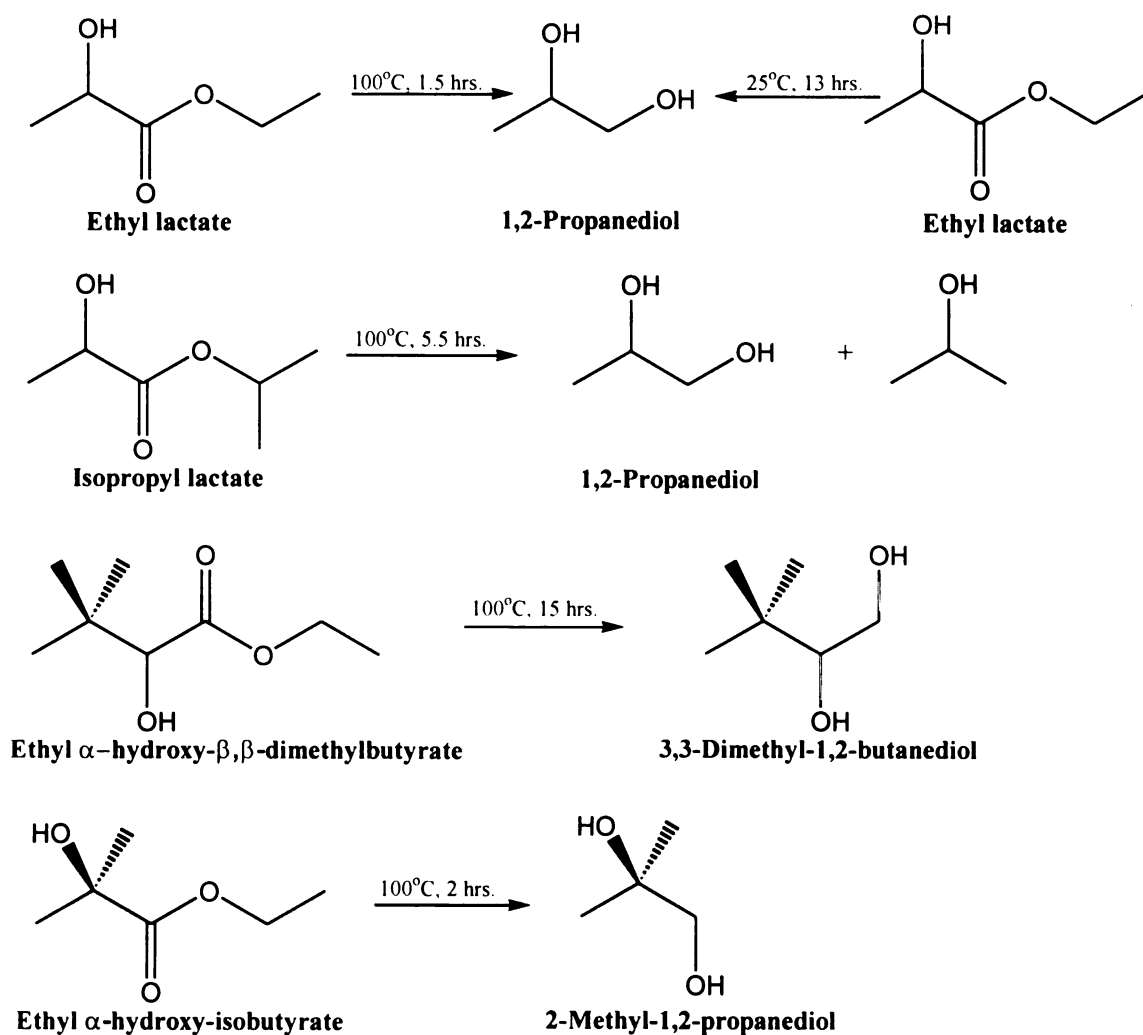
**Scheme 1.7.** The selected reactions by Adkins show that copper-chromium oxide selectively reduces the phenyl-substituted ester at the carbonyl functionality, whereas W-6 Raney nickel, or all tested Raney nickels indiscriminately reduced all unsaturated carbon-carbon bonds, resulting in cyclohexyl functionalities.

because the hydrogenation can proceed to completion at room temperature, producing 80% product yield.<sup>44</sup> Depending on the substrate and catalyst, however, the amount of time can vary. Various types of Raney nickels, designated as W-1 through W-8 have been widely used in industry (W designation refers to the preparation technique of Raney nickel, varying temperatures, NaOH:alloy ratios, digestion temperatures with respect to time and washing process).<sup>44,45</sup> For example, W-6 Raney nickel requires 14 and 25 hours in the reduction of 5-carbomethoxy-2-pyrrolidone and ethyl N-phenylglycinate to the corresponding amino alcohols, respectively. On the other hand reductions of the same substrate by W-5 Raney nickel to the corresponding amino alcohols required less time (0.8-9.0 hours). Adkins did point out that at the time of testing W-6 Raney nickel catalysts were not completely developed yet. In fact, when tested, W-6 Raney nickel catalyzed a reduction of N-phenylglycinate that went with extreme violence at 373 K. Thus temperature control poses a safety concern, making lower temperatures a practical necessity and safety requirement.

At conditions employing 1.5 equivalent of W-6 Raney nickel to esters at 330 atm and 373 K, quantitative yields of 1,2-propanediol (1.5 hrs.) and 1,2,3,4-butanediol (10 hrs.) were produced from ethyl lactate and diethyl tartrate, respectively (Scheme 1.8). Under identical conditions, 3,3-dimethyl-1,2-butanediol from ethyl  $\alpha$ -hydroxy- $\beta,\beta$ -dimethylbutyrate (373 K for 15 hours) and 2-methyl-1,2-propanediol from ethyl  $\alpha$ -hydroxy-isobutyrate (373 K for 2 hours) form (Scheme 1.8).<sup>44,45</sup>

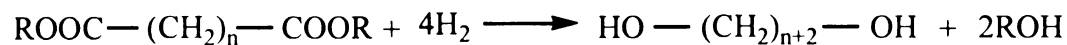
Adkins observed that temperature, pressure and catalyst loading have a profound effect on the rate of hydrogenation. When investigating the rate of conversion of ethyl lactate he found that while at room temperature 5.5 hours were required to achieve 75 %

conversion, the same reaction required less than an hour at 373 K. It is important to note that this reaction was carried out using 1.5 equivalent of catalyst (Raney nickel W-6).<sup>44,45</sup> When the hydrogen pressure was increased from 230 to 330 atm, conversion of ethyl lactate was accomplished in substantially less time.<sup>44,45</sup>



**Scheme 1.8.** The hydrogenations of esters produced yields in excess of 80%. Even though the temperatures did not exceed 373 K, reaction conditions required 1.5 equivalent of W-6 Raney nickel catalyst and 330 atm pressure of H<sub>2</sub> gas.

Adkins was the first to demonstrate that dibasic esters can be hydrogenated to the corresponding diol by the scheme below:

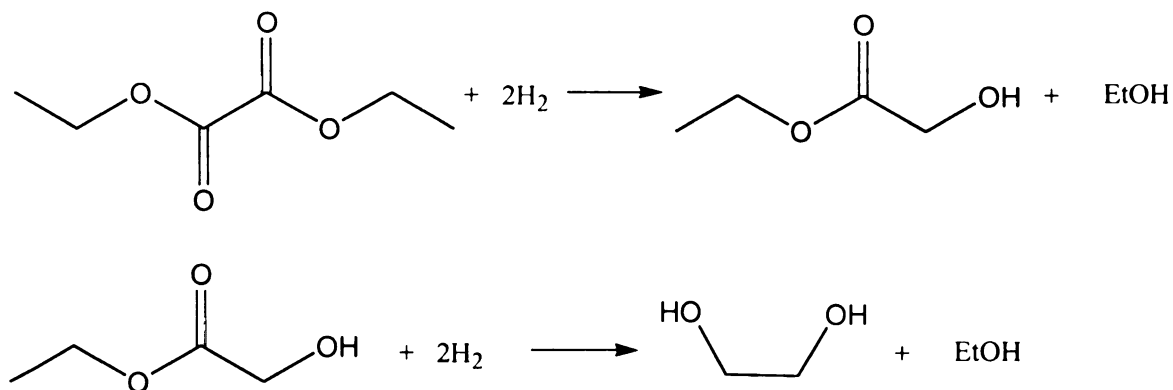


Dibasic esters that have two carbons separating the carbalkoxy groups produced 80-90 % yield of diol, whereas less than 40 % yield was observed for malonates to produce 1,3-propanediol.<sup>26,46,47</sup>

An immensely important compound to the chemical industry is ethylene glycol. It has use not only as antifreeze but as a component in hydraulic fluids, alkyd resins and polyester fibers.<sup>46</sup> The industrial production of ethylene glycol involves the process in which ethylene is oxidized to ethylene oxide over a silver catalyst which in turn is treated with aqueous acid to produce ethylene glycol.<sup>46</sup> Trimm et al. suggested an alternative route for producing ethylene glycol from diethyl oxalate that is cheaply available as a byproduct from aluminum production. They studied the gas phase hydrogenolysis of diethyl oxalate over a series of copper-based catalysts. They observed up to 99% conversion with 85% selectivity to ethylene glycol in the ion-exchanged Cu/SiO<sub>2</sub>-catalyzed hydrogenolysis of diethyl oxalate at 513 K and 6 atm. They also observed some polymerization of the ethyl glycolate intermediate that had formed during the reaction. These polymerization side products presented a challenge as they caused a partial deactivation of the catalyst.<sup>46</sup>

Trimm et al. proposed that the hydrogenolysis of diethyl oxalate involves two steps. First ethyl glycolate and one equivalent of ethanol are generated. In the second

step the ethyl glycolate is further reduced to ethylene glycol and another equivalent of ethanol (Scheme 1.9).<sup>46</sup> The choice of catalyst was either Raney copper or copper supported on either silica, alumina, MgO or TiO<sub>2</sub>. Trimm et al. determined that the deactivation of catalyst caused by the polymerization of ethyl glycolate can be minimized by increasing the surface area of the silica-supported copper catalyst.<sup>46</sup> They proposed that diethyl oxalate quickly adsorbs in a dissociative fashion on the copper surface to generate an ethoxy species, which in turn reacts with hydrogen to form ethanol. The remaining keto-acyl fragment reacts more slowly to yield ethyl glycolate.<sup>46</sup> The dissociative adsorption of alkoxy and acyl fragments have been previously proposed in studies done on acetates and higher esters.<sup>48,49</sup>



**Scheme 1.9.** The two step process of hydrogenolysis of diethyl oxalate to ethylene glycol.

Thrimm et al. also examined the thermodynamic feasibility of diethyl oxalate hydrogenolysis to produce the diol.<sup>46</sup> The heats and free energies of formation of reactants and products were calculated and are reported in Table 1.1.<sup>46</sup> From these values the equilibrium constants of the possible reactions in diethyl oxalate

hydrogenolysis were calculated. These calculations demonstrated the feasibility of diethyl oxalate hydrogenolysis to ethylene glycol with high conversion at relatively low pressures (1-6 atm).<sup>46</sup>

Name	Formula	$\Delta H_f$ (kJ/mol)	$\Delta G_f$ (kJ/mol)
Diethyl oxalate	$C_2H_5OOC COOC_2H_5$	-768	-562
Ethylene glycol	$HO(CH_2)_2OH$	-385	-301
Ethyl glycolate	$HOCH_2COOC_2H_5$	-576	-431
Ethanol	$C_2H_5OH$	-235	-168

**Table 1.1.** Heats and free energies of formation for diethyl oxalate and related compounds at 1 atm.<sup>46</sup> Note that entries for ethanol have been switched, as the Trimm paper incorrectly reported these values from the CRC Handbook.

Other than the polymerization of ethyl glycolate on the catalytic surface, gaseous byproducts can also be generated. Trimm et al. proposed a reaction mechanism for the decarbonylation of ethyl glycolate in which CO, CO<sub>2</sub> and C<sub>2</sub>H<sub>4</sub> are generated, which process is proposed to be the same for diethyl oxalate (Figure 1.5). He observed that the generation of gaseous byproducts depends on the partial pressure of the diethyl oxalate or ethyl glycolate. Contamination from CO, CO<sub>2</sub> and C<sub>2</sub>H<sub>4</sub> can be minimized and a 99% conversion with 85% selectivity to ethylene glycol can be achieved at 513K and 6 atm by increasing the concentration of ethyl glycolate.<sup>46</sup>

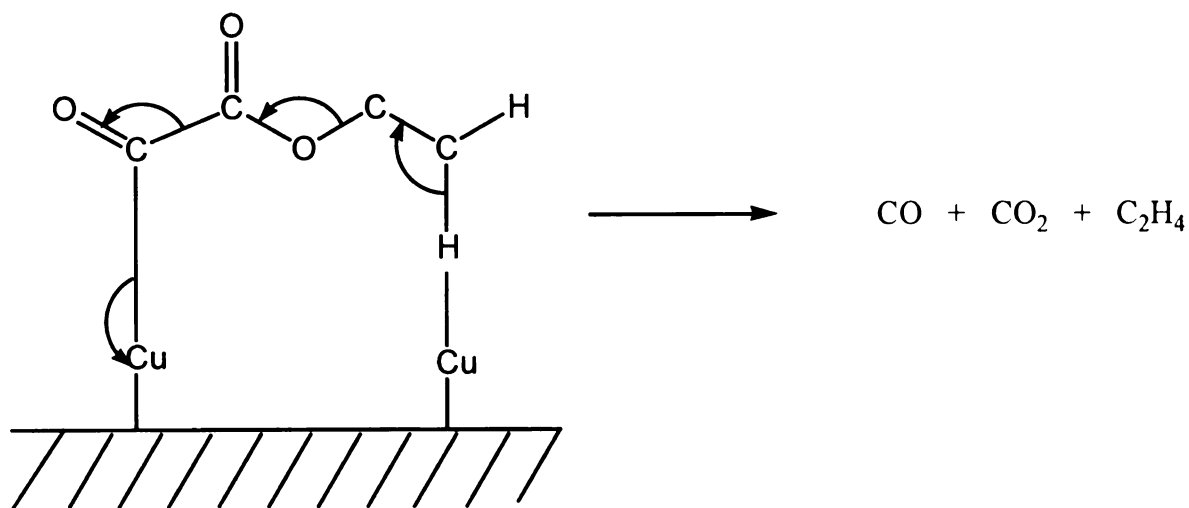
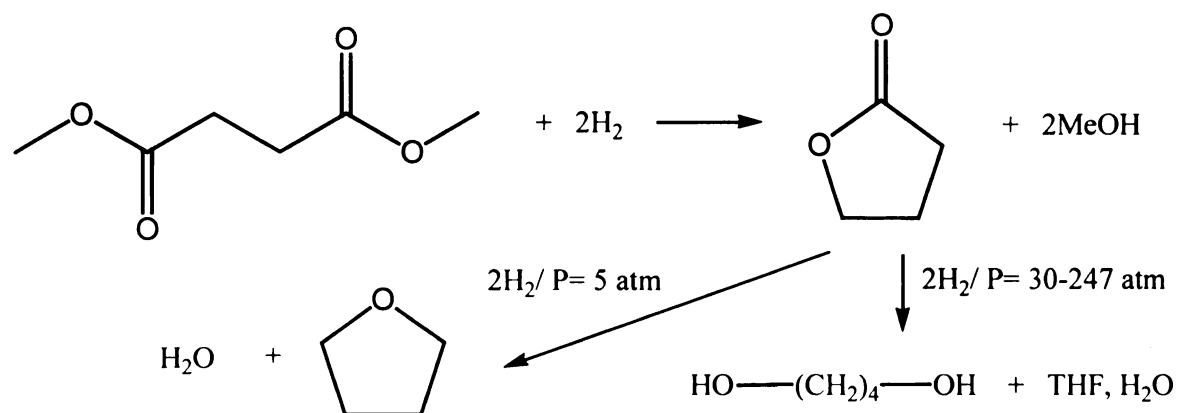


**Figure 1.5.** Mechanism for the gasous byproduct formation from diethyl oxalate.

As previously established, hydrogenation of dibasic esters presents a major challenge in that they can easily form undesired cyclization products at higher temperatures.<sup>47</sup> For example, dimethyl succinate preferentially generates  $\gamma$ -butyrolactones and methanol at low pressures and high temperature. At 5 atm H<sub>2</sub> pressure  $\gamma$ -butyrolactone further reacts to generate THF and water, whereas at pressures above 300 atm it generates 1,4-butanediol, THF and water (Scheme 1.10).<sup>47,50</sup> As Trimm et al. showed that it is possible to develop a process in which controlled quantities of THF and 1,4 butanediol are generated via what is thought to be a  $\gamma$ -butyrolactone intermediate.<sup>47,51-54</sup> Furthermore, the formation of the desired final product (1,4-butanediol) at low temperature and higher pressure is thermodynamically favored.<sup>47</sup>

Various copper catalysts, such as Raney copper, have been successfully used in the hydrogenation of dialkyl succinates.<sup>47</sup> Patent applications only demonstrate the use

of copper/zinc oxide, silica-supported copper and especially copper chromite. Addition of zinc oxide to the copper chromite mixture increased the catalytic activity for the

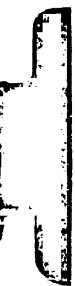


**Scheme 1.10.** The hydrogenation at two different pressures, producing two different results.

conversion of dimethyl succinate to produce  $\gamma$ -butyrolactone.<sup>47</sup> Coprecipitated copper/zinc oxide showed a one order of magnitude greater rate of conversion of dimethyl succinate with respect to per unit surface area of copper than copper chromite or silica-supported copper catalysts used by themselves.<sup>47</sup> Using coprecipitated copper/zinc oxide in the hydrogenation of dimethyl succinate,  $\gamma$ -butyrolactone (**GBL**) intermediate is generated along with methanol (Scheme 1.10). Starting with **GBL**, the reaction takes different routes as pressures are varied. While at 5 atm, THF and water are generated from **GBL**, at higher pressures (30-247 atm) a substantial amount of 1,4-butanediol is formed along with negligible amounts of THF and water.<sup>47</sup>

3

The hydrogenation of esters is a non-trivial process that often requires high temperatures and pressures. In this section a variety of catalysts has been discussed for such processes. Although esters normally can be hydrogenated more than the corresponding free organic acids, development of even more effective methodologies for their reduction is an active research area.



## 1.3 Hydrogenation of Organic Acids

Although there are numerous published examples of the hydrogenation of organic acids to value-added chemicals, their fundamental chemistry and the economics of their hydrogenation have been much less discussed. Nevertheless, hydrogenation of organic acids under mild conditions still has a lot of promise even though they are typically much more difficult to hydrogenate than esters. Studies by Adkins showed that esters hydrogenate more poorly in the presence of free acids.<sup>55</sup> For example, he obtained well above 90% yields for the hydrogenation of caproate esters over copper-barium-chromium oxide between the temperature range of 423 to 473 K and 200-300 atm. pressure in 35 minutes. In contrast, hydrogenation of free caproic acid in ethanol and n-butanol produced only 10 and 15 % yields, respectively. Hydrogenation of n-butyl caproate in the presence of caproic acid suppressed the product yield and produced only 75 % hexanol for the same amount of time.<sup>55</sup>

In 1959 rhenium “black” was reported as an effective catalyst for the hydrogenation of organic acids to the corresponding alcohols, under much less stringent conditions than had previously been done.<sup>25</sup> Various forms of copper catalysts employing chromium, cadmium, cobalt-nickel and ferrous metals coupled with non-ferrous metals had been used to hydrogenate carboxylic acids in the temperature range of 393 to 673 K and the pressure range of 30 to 400 atm.<sup>25,56,57</sup> Adams et al. demonstrated that cadmium-nickel salts of organic acids over copper chromite catalyst produce alcohols under dry conditions at 513 K and 235 atm.<sup>58</sup> When discussing rhenium catalysts, it is important to note that they show lower activity toward the reduction of

alkene functionality than platinum, palladium or nickel.<sup>25</sup> However, they must be in a high ratio to substrate to hydrogenate an organic acid, such as maleic or cinnamic acid, effectively.<sup>25</sup> Of particular interest is the hydrogenation of maleic acid with rhenium black that exclusively afforded succinic acid in various solvents under varying temperatures and pressures and with different reaction times (Table 1.2).

Rhenium “black” derived from rhenium heptoxide afforded ethanol in the hydrogenation of acetic acid with reaction times of 2.5 hours to 60 hours, depending on the type of solvent used (Table 1.2).<sup>25</sup> In general, the catalyst prepared in water produced very poor yields in the hydrogenation of acetic acid and succinic acid. While the hydrogenation of maleic acid over water-prepared catalyst produced low yields of succinic acid, the catalyst prepared in ethanol or dioxane afforded 100 % yield (Table 1.2). The introduction of water for the preparation of the catalyst and the reduction of substrate is noteworthy because it proved that solvent effects must be taken into account and that they can be a dominant factor in hydrogenolysis.<sup>59</sup>

It also became obvious that an increase in temperature or pressures does not necessarily lead to higher conversion rates and selectivity. Broadbent also demonstrated with rhenium “black” that higher catalyst loading does not necessarily lead to better product yields and that the solvent used in the preparation of the catalyst and the hydrogenation can profoundly affect the product yields of these reactions (Table 1.2).<sup>25</sup> For example, hydrogenation of acetic acid produced 68 % yield when acetic acid was used for the catalyst preparation, but ethanol used in the preparation of the same catalyst caused a drop in the product yield to 38 %.<sup>25</sup>

Substrates	Solvents for Catalyst Prep.	Gram of Cat./ Mole of Substrate	Solvent for Reduction	Avg. Temp. (K)	Avg. Pressure (atm.)	Time (hr.)	% Yield	Main Product
Acetic acid	Dioxane	1.0	None	420	355	9	40	Ethanol
Acetic acid	Acetic acid	0.2	None	433	129	60	68	Ethanol
Acetic acid	Ethanol	1.1	None	419	258	15	38	Ethanol
Acetic acid	Water	1.1	None	448	275	2.5	27	Ethanol
Maleic acid	Dioxane	2.6	Dioxane	421	177	2.5	100	Succinic Acid
Maleic acid	Acetic acid	2.5	Dioxane	431	163	12	93	Succinic Acid
Maleic acid	Ethanol	1.1	Water	424	254	4	100	Succinic Acid
Maleic acid	Water	1.0	Water	473	194	8	0	Succinic Acid
Succinic acid	Water	1.1	Water	478	272	12	39	Tetrahydrofuran

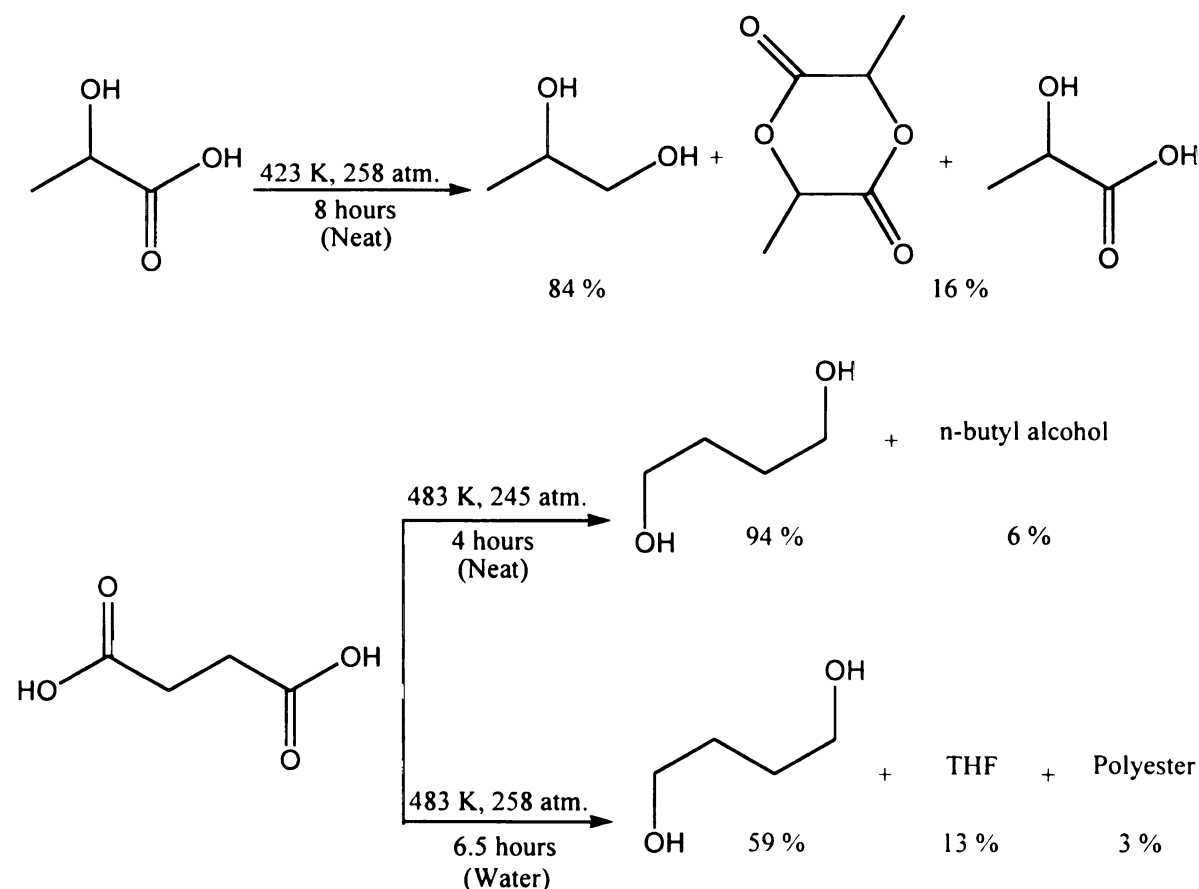
**Table 1.2.** Summary for the hydrogenation of various organic acids catalyzed by rhenium black.<sup>25</sup>

Rhenium heptoxide with catalyst loading similar to that of rhenium “black” afforded good results especially when water was used for hydrogenation. For example, acetic acid in water was converted to ethanol with 100 % yield in 10 hours at 423 K and 168 atm.<sup>25</sup> Furthermore, the hydrogenation of trifluoroacetic acid, which contains three very strongly electron-withdrawing atoms, required longer reaction time (18.5 hours) and higher pressure (300 atm) and temperature (480 K) to generate the corresponding trifluoroethanol. Under the same conditions but even longer reaction times (27 hours), trichloroacetic acid did not afford any product.<sup>25</sup> Hydrogenolysis of succinic acid produced 94 % 1,4-butanediol and 6 % n-butyl alcohol when the reaction was run neat. When water was added the 1, 4 butanediol yield dropped to 59 % and 13 % tetrahydrofuran were produced. The hydrogenation of lactic acid using rhenium

heptoxide produced 84 % propylene glycol in an eight hour reaction time at high pressure and temperature (Scheme 1.11).<sup>25</sup>

A large array of hydrogenolysis by rhenium heptoxide reduced in situ was demonstrated by Broadbent. The beauty of these reactions was their simplicity as they avoided the initial preparation of rhenium black catalyst. However, they often required very long reaction times and either very high temperatures or pressures, or both.

Broadbent's work, however, was pivotal in that he was able to demonstrate that various organic acids, such as acetic acid, can indeed be reduced in good to excellent yields.



**Scheme 1.11.** Solvent effects strongly influence the hydrogenolysis of lactic acid and succinic acid using rhenium heptoxide reduced in situ.<sup>25</sup>

In a 1988 patent Kitson described heterogeneous catalytic hydrogenation of various organic acids with 2-12 carbon backbones, using either molybdenum or tungsten coupled with a second component that could be palladium, rhodium or ruthenium on carbon support. Just as Broadbent did, Kitson also observed trans-esterification products from the hydrogenolysis of various organic acids.<sup>60</sup> For example, the hydrogenation of acetic acid produced ethyl acetate and the hydrogenation of propanoic acid produced not only propanol but propyl propanoate.<sup>60</sup> These reactions were carried out at relatively high temperatures from 180-250 °C, pressures above 10 atm and relatively high catalyst loading, producing very poor conversions of substrates. The catalyst composition and method of preparation determined the degree of conversion as well as the selectivities for the corresponding alcohols and ester by-products. When the catalyst was tested for acetic acid hydrogenation, both the temperature variation and catalyst composition affected the conversions and selectivities of these reactions. For example, a mixture of 2.5 weight percent palladium and 5 weight percent tungsten on carbon support produced a 16.5% conversion of acetic acid with an 84.3% selectivity toward ethanol at 462 K, whereas the very same catalyst produced a 44.6 % conversion at 521 K with 82.7 % selectivity to ethanol. Palladium on carbon support produced marginal conversion (0.3 %) and no products of any kind under the same conditions, and when tungsten was excluded only 0.6% conversion was observed. Similar results were obtained from mixtures of molybdenum and palladium using carbon support. Again exclusion of Pd lead to no reaction, but a mixture of 2.5 weight % molybdenum and 5% palladium produced 58% conversion and 83% selectivity toward ethanol.<sup>60,61</sup>

In the literature to this point, high selectivity was attainable only under the conditions that Kitson had described, using catalytic mixtures supported on various inert materials, such as carbon, silicas, aluminas, but the conversions of substrates remained low.<sup>62</sup> Various combinations of Group VIII metals, such as palladium and ruthenium, with rhenium seemed promising. Of particular interest was palladium in various mole percent compositions with rhenium. In the hydrogenation of acetic acid, a mixture of 2.5 % Pd with 5 % Re afforded both lower conversion and selectivity when the temperature was lowered. Under the same conditions, lowering the Re content of the catalytic mixture to 2.5 % yielded a dramatic drop in conversion but the selectivity to ethanol essentially remained the same. The Kitson patent was intended to demonstrate that heterogeneous catalytic systems composed of two metals and supported on high surface area inert material such as carbon can produce high selectivities even though the percent conversions remained low. In hydrogenating acetic acid and propanoic acid, esterification products such as ethyl acetate and propyl propionate were also formed and their ratios to the corresponding alcohol from the reductions of carboxylic acids can be increased by lower conversion per pass in gas phase, whereas at high conversion per pass or continuous co-feeding of water would generate more of the corresponding alcohol.<sup>62</sup>

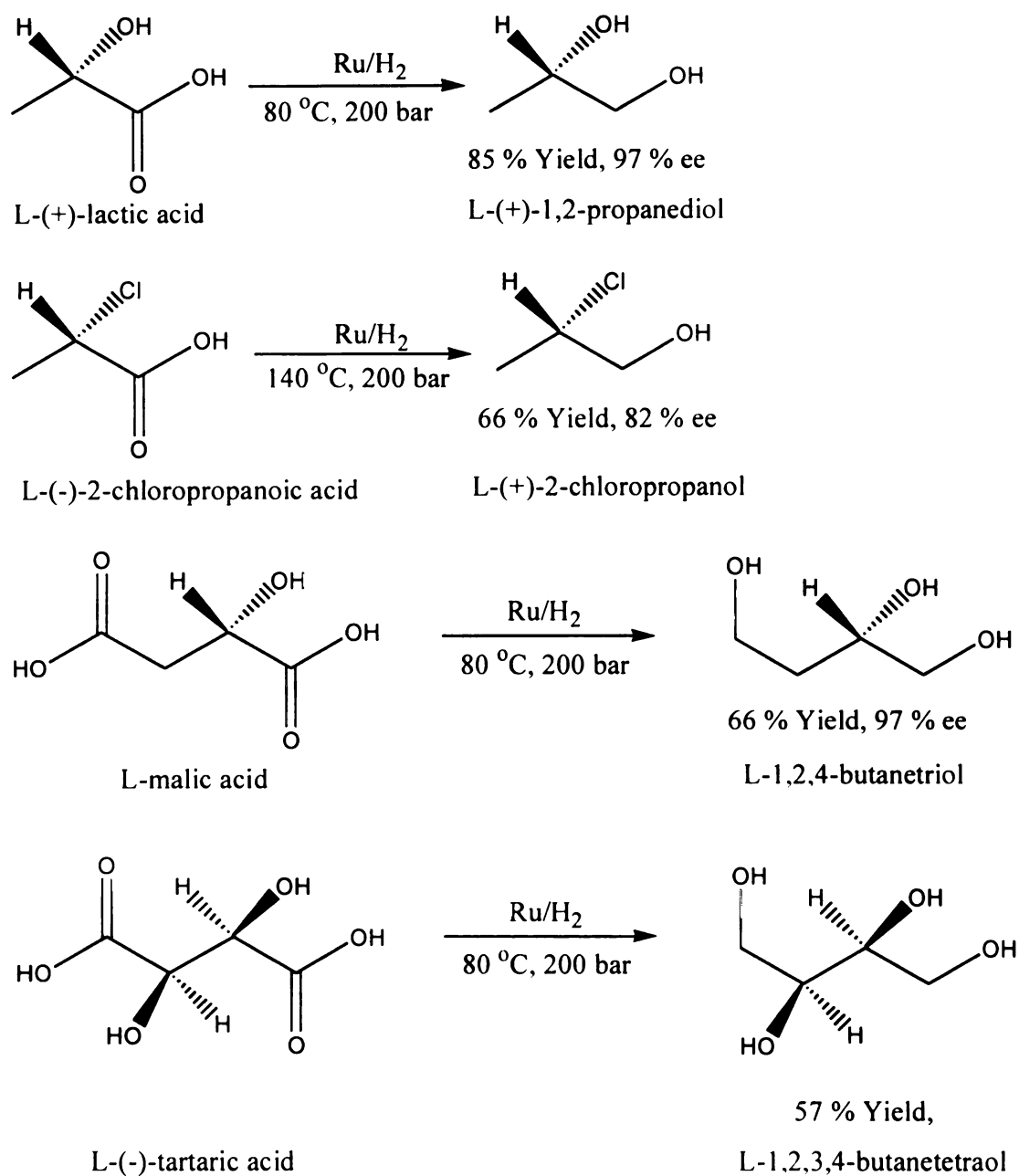
Antons described the preparation of optically active alcohols from optically active carboxylic acids, employing catalyst either by itself (elemental ruthenium, ruthenium oxide, hydroxide or halide) or on a support such as carbon, aluminum oxide or silicon dioxide.<sup>63</sup> Of greatest pertinence to this thesis were the hydrogenations of short organic acids with vicinal substituents such as optically active lactic acid and 2-chloropropanoic acid to propylene glycol and 2-chloropropanol (Scheme 1.12).<sup>63</sup> Although the

enantiomeric excess was well above 90 %, relatively poor yields were obtained.

Nevertheless, the quantity of Ru required and the ease of handling these Ru catalysts are much more cost effective than conventional reducing agents such as lithium aluminum hydride and sodium borohydride.<sup>63</sup> For the hydrogenolysis of lactic acid it was also observed that with increasing temperatures, 383 to 413 K, the enantiomeric excess of propylene glycol dropped from 93 % to 71 %.

Optically active propylene glycol and 1,2,3,4-butanetetrol can also be prepared from optically active lactic and tartaric acids, using ruthenium/rhenium mixtures prepared from ruthenium oxide and rhenium heptoxide. Although this colloidal mixture outperformed ruthenium black by producing up to 99 % ee, the yields did not improve beyond 80 %.<sup>64</sup> Nevertheless, combinations of finely dispersed ruthenium oxide with metals such osmium, iron, rhodium, copper, zinc/germanium, gallium and trimetallic species of ruthenium with two other metals such as rhenium/silver, rhenium/copper, and rhenium/tin seem promising and are under investigation.<sup>64</sup>

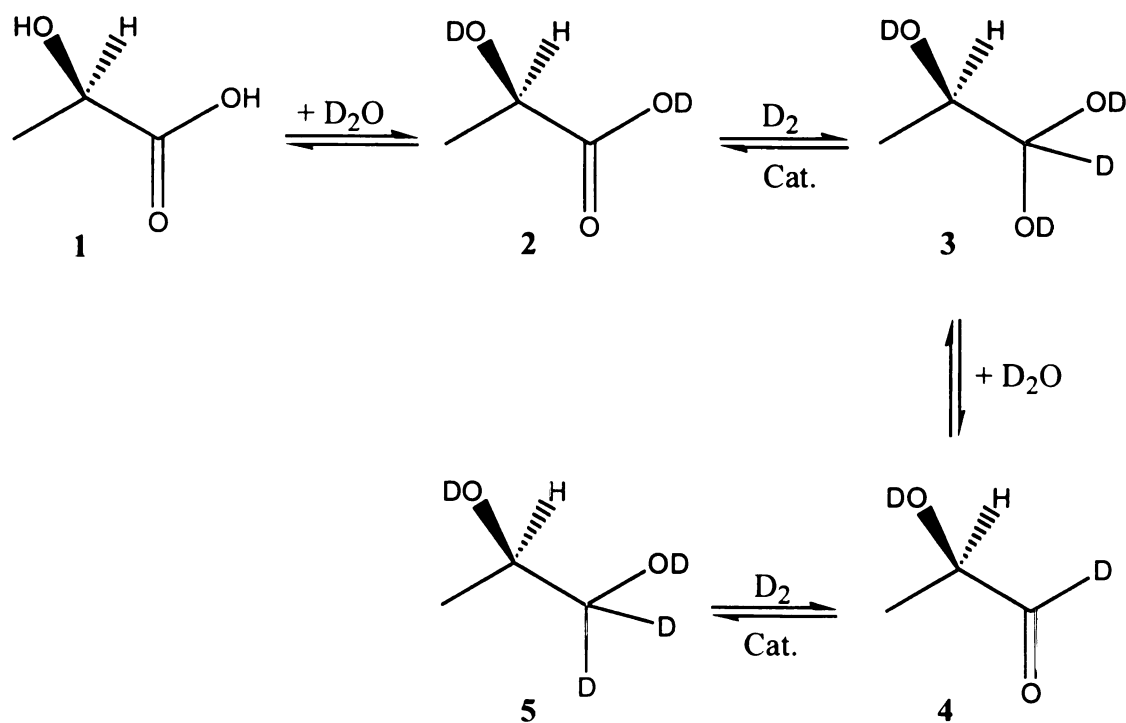
The numerous examples of patent applications do provide various methodologies for catalytic hydrogenations of organic acids, demonstrating ever-increasing yields and selectivities, but they do not go into the mechanistic aspects of the chemistry behind all these processes. Using <sup>1</sup>H and <sup>13</sup>C NMR spectroscopic methods for H/D exchange, the hydrogenation of lactic acid, a particularly important organic acid, was mechanistically investigated by Kovacs et al.<sup>2</sup> The determination of H/D exchange in both the solvent and the hydrogenation product, propylene glycol, is a prerequisite in order to understand the hydrogenation mechanism of lactic acid.



**Scheme 1.12.** The hydrogenation of lactic acid, 2-chloropropionic acid, malic acid and tartaric acid gave good to moderate yields. The stereochemistry of the substrate was largely retained after hydrogenation resulting in high ee's.

Control experiments, in which a heterogeneous ruthenium catalyst was used under the same reaction conditions, when neither lactic acid nor propylene glycol was

present, demonstrated rapid H/D exchange between H<sub>2</sub> and D<sub>2</sub>O. Propylene glycol, the hydrogenation product of lactic acid, also underwent catalytic H/D exchange at the C<sub>1</sub> and C<sub>2</sub> positions, and more slowly at C<sub>3</sub>. The NMR splitting patterns of <sup>13</sup>C coupled to deuterium and the chemical shift differences between the deuterated and the corresponding protiated carbon sites proved valuable in determining the location and the extent of H/D exchange in both lactic acid and propylene glycol.<sup>2</sup>



**Scheme 1.13.** The proposed mechanism of lactic acid hydrogenation.<sup>2</sup>

Kovacs et al. proposed that hydrogenation only occurs at the C<sub>1</sub> position of lactic acid. This mechanism involves the formation of an acetal intermediate (3) followed by a

dehydration to obtain aldehyde (4) that further hydrogenates to the corresponding alcohol (5) (Scheme 1.13).<sup>2</sup> Because the optical activity at the C<sub>2</sub> position of lactic acid was retained in these reactions, alternative routes involving keto-enol tautomerization were excluded. However, as deuterium incorporation was observed at the C<sub>2</sub> position of propylene glycol, Kovacs et al. proposed that H/D exchange takes place after the propylene glycol is formed and occurs via a surface-bound intermediate.<sup>2</sup>

The efficient and selective aqueous phase hydrogenation of organic acids in general presents a greater challenge than that of esters. Ruthenium and copper chromite are relatively efficient catalysts for organic acid hydrogenations, but they work at relatively high pressures and temperatures.<sup>6</sup> In aqueous-phase hydrogenation, ruthenium supported on activated carbon produced 95 % conversion of lactic acid and 90 % selectivity to propylene glycol at optimal reaction conditions (423 K and 99-140 atm).<sup>65</sup>

## Chapter 2

### Results and Discussion

The Ru/C-catalyzed aqueous-phase hydrogenation reactions of ethyl lactate and various organic acids bearing -OH, -OMe, -OCOCH<sub>3</sub>, -H or -CH<sub>3</sub> substituent, vicinal to the carboxy functional group, were run in a high pressure Parr batch reactor under mild conditions (348 to 423 K and 1200 psi). Three-carbon backbone compounds bearing  $\alpha$ -substituent X (X = -H, -Cl, -OH, -OCH<sub>3</sub>, -OAc, -CH<sub>3</sub>) and two-carbon backbone compounds bearing  $\alpha$ -substituent X (X = -OH, -OCH<sub>3</sub>) were studied by <sup>1</sup>H NMR spectroscopy and HPLC. While <sup>1</sup>H NMR analysis of the samples required the use of either t-butyl alcohol or dioxane as internal standards, for HPLC analysis ethanol was used. In the text <sup>1</sup>H NMR peaks were designated as follows: singlet (s), doublet (d), triplet (t), quartet (q), quintet (quint), sextet (sext), septet (sept), multiplet (m), doublet of a doublet (d/d).

Substrate and alcohol product concentrations were monitored with respect to time and the resulting data were used to determine the percent conversion of a given organic acid and the percent production of the corresponding alcohol. The relationship between molecular structure and the efficiency of hydrogenation of organic acids or esters was determined from the selectivity and rate data of each reaction. This work has demonstrated that various vicinal functional groups can influence the reactivity of organic acids.

While a hydroxy functional group can hydrogen-bond inter- or intra-molecularly, the methoxy functional group has only electron-withdrawing ability. With this in mind,

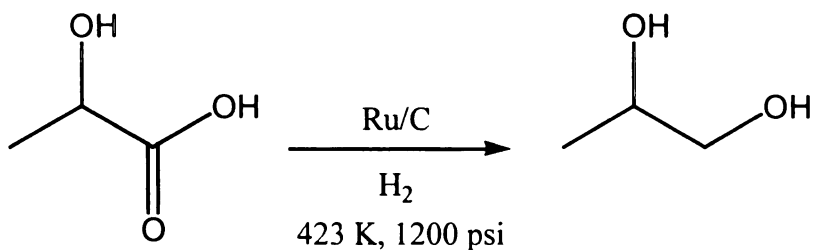
various electron-withdrawing groups (-OAc, -Cl or -OMe) at the C2 position of a given organic acid were varied and tested and compared to -OH bearing substrates for their effect on the reactivity in hydrogenation reactions.

The ester functionality does present a problem as it can easily hydrolyze in hydrogenation reactions and the resulting rate data contain both hydrolysis of the alkoxy fragment and the hydrogenation of the acyl fragment. The chlorine substituent at the C2 position was also of concern as it was readily removed from the substrate in Ru/C-catalyzed aqueous phase hydrogenation reactions. Hence the loss of chlorine rendered the substrate functionally void at the C2 position.

Finally, steric effects may also play a role in the reactivity of these organic acids as the substrates must adsorb on the catalyst surface for reduction to take place. In theory, the relatively bulky -OAc or -OMe group may adversely influence the adsorption of the substrate on the catalyst surface as free rotation around the sigma bond between C1 and C2 carbon is evident. The momentary presence of a bulky substituent close to the  $sp^2$  carbon of the carboxyl functionality may hinder the delivery of hydride.

## 2.1. Hydrogenation of Lactic Acid

The hydrogenation reaction of lactic acid (LA) was run at 423 K and 1200 psi for six hours. The product from lactic acid hydrogenation, detectable by  $^1\text{H}$  NMR and HPLC, was only propylene glycol (PG) (Scheme 2.1). The  $^1\text{H}$  NMR peaks of products and reactants from lactic acid were referenced to t-butyl alcohol at 1.22 ppm. Lactic acid was purchased and used as a mixture consisting of approximately 15 % self-esterification products (lactyl lactate; and di-lactide which is a cyclic dimer of LA) and approximately 80 to 85% LA and residual amount of water (see Figure 2.1 for  $^1\text{H}$  NMR spectrum). Unfortunately, purification by distillation of this mixture, even at low pressures and temperatures, is non-conductive because its constituents are azeotropic. Furthermore, polymerization of LA during distillation, even at lower temperatures, is quite significant.



**Scheme 2.1.** Hydrogenation of lactic acid to generate propylene glycol.

Lactyl lactate has two doublets: one at 1.498 and the other at 1.420 ppm. A weak doublet of the di-lactide is evident at 1.554 ppm (Figure 2.1). In addition, three quartets of lactic acid and its esterification products are visible on the spectrum. The most upfield quartet at 3.380 ppm belongs to LA, whereas the more downfield quartets of the esterification products generate weak signals and one of them is at the HDO peak. These quartets could not be used for integration due to their close proximity to the HDO, especially when  $^1\text{H}$  NMR spectra are obtained from a water suppression experiment. In addition, quartets run across a relatively long base line, thus integration values can easily

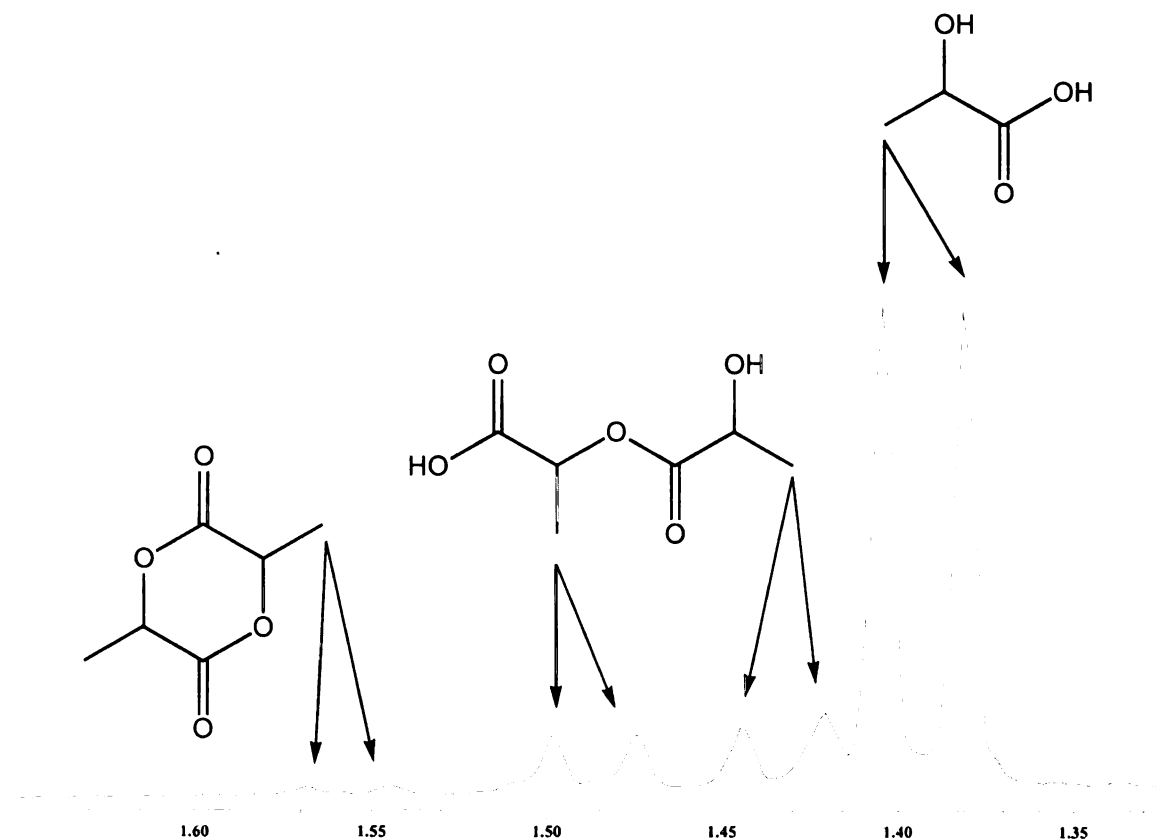


**Figure 2.1.** A magnified region of the lactic acid mixture showing the doublets of the corresponding acid and esters.

be skewed. It must be noted that one of the main errors for calculating concentrations can come from long base-line integration that can effectively increase the calculated concentrations of the samples.

LA ( $\delta$  4.364 1H(q)/[B]; 1.404 3H(d)/[A]) has a prominent and easily distinguished doublet at 1.404 ppm that was monitored to determine the  $^1\text{H}$  NMR concentration of the reactant (Figure 2.2). The esters from the starting material completely hydrolyzed to LA or directly hydrogenated to form PG within two hours of

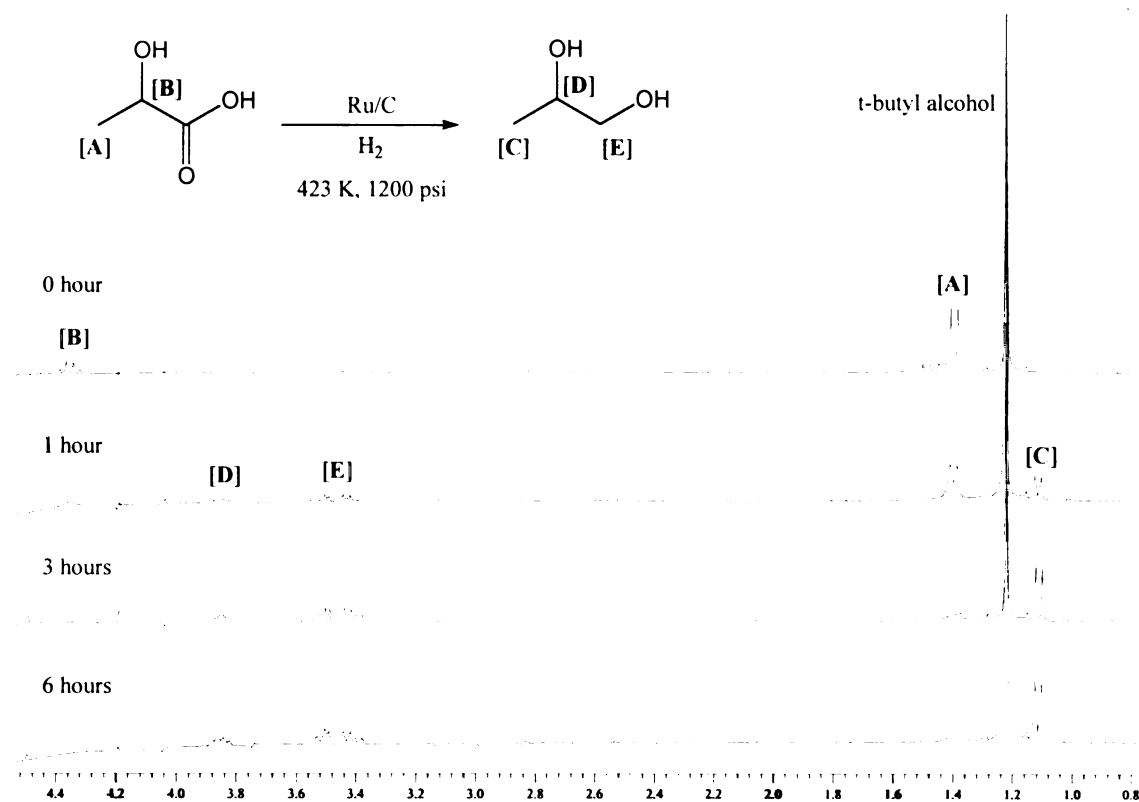


**Figure 2.2.** Selected  $^1\text{H}$  NMR spectra of LA hydrogenation in which PG is produced. For stacked spectra detailing the LA hydrogenation each hour, please see Appendix 1.1.

reaction time as their characteristic doublets and quartets were no longer visible in the  $^1\text{H}$  NMR spectrum. The product **PG** ( $\delta$  3.84 1H(m)/[**D**]; 3.49 2H(d/d)/[**E**]; 1.12 3H(d)/[**C**]) has a doublet at 1.12 ppm that was monitored for concentration change (Figure 2.2).

The  $^1\text{H}$  NMR results for the percent conversion of **LA** and production of **PG** differ significantly from the HPLC results (Figure 2.13-2.16). The  $^1\text{H}$  NMR concentration profiles of the hydrogenation of **LA** reveal that the starting material is almost completely used up after five hours (Appendix 1.2 and 1.3). Although the conversion of the starting material approaches  $100\pm 7\%$ , only  $72\pm 11\%$  **PG** was produced after six hours. On the other hand, the presence of **LA** was evident from the HPLC chromatogram even after six hours (for HPLC concentration profile, see Appendix 1.3). HPLC experiments indicate 87% conversion of **LA** to 67% **PG** within this time frame. A large number of different samples handled by HPLC may cause a discrepancy in the chromatogram as a different type of sample from a former run may show up and may have a retention time that is similar or even identical with that of the analyte.

As patent literature has demonstrated, close to 100 % conversion is possible for **LA** under the same conditions.<sup>2, 63-65</sup> While the  $^1\text{H}$  NMR results of this work concur with published results, the values for percent conversion of production, obtained from HPLC, should be considered with a hint of skepticism. Ideally the values obtained from either analytical method should be very close. Furthermore, the concentration versus time profile of HPLC results (Appendix 1.3) shows an exponential decay that corresponds well to first order behavior. On the other hand, the concentration profile, based on  $^1\text{H}$  NMR experiment, does not closely follow the first order behavior.

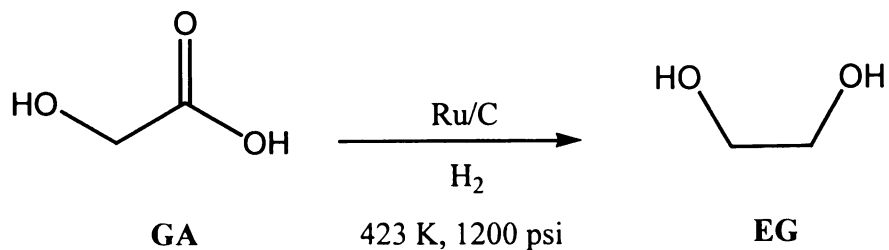
The agreement between  $^1\text{H}$  NMR and HPLC with respect to selectivity to **PG** as the final product is satisfactory. The selectivity to **PG** is 82 and 77 % based on  $^1\text{H}$  NMR and HPLC, respectively. Foreign peaks for side products on the  $^1\text{H}$  NMR spectrum and additional humps on the HPLC chromatogram were not observed even after six hours. However, gaseous byproduct formation, such as  $\text{CO}_2$ , should be considered as decarboxylation reactions at this temperature and time period are possible.

Two control experiments were run: one under  $\text{H}_2$  without the catalyst and the other under He with Ru/C catalyst. There was no evidence of product formation. Although some degree of decarboxylation may occur, the  $^1\text{H}$  NMR spectra did not show any products and the concentration of the **LA** starting material was invariant.

## 2.2. Hydrogenation of Glycolic Acid

The hydrogenation reactions of glycolic acid (**GA**) were run at 423 K and 1200 psi. The product from **GA** hydrogenation, detectable by  $^1\text{H}$  NMR, was only ethylene glycol (**EG**) (Scheme 2.2). The peaks of products and reactants from **GA** were referenced to t-butyl alcohol at 1.22 ppm. Two singlets of **GA** appear in the  $^1\text{H}$  NMR spectrum. One of the peaks is at 4.050 ppm accounting for the two ethylene protons of glycolic acid and a small singlet at 4.181 ppm that belongs to a cyclic di-ester which is the dimerized derivative of glycolic acid. The singlet of glycolic acid was monitored to

determine  $^1\text{H}$  NMR concentrations. The singlet of ethylene glycol at 3.510 ppm was monitored to determine the product concentration (Figure 2.3).



**Scheme 2.2.** Hydrogenation of glycolic acid that generates ethylene glycol.

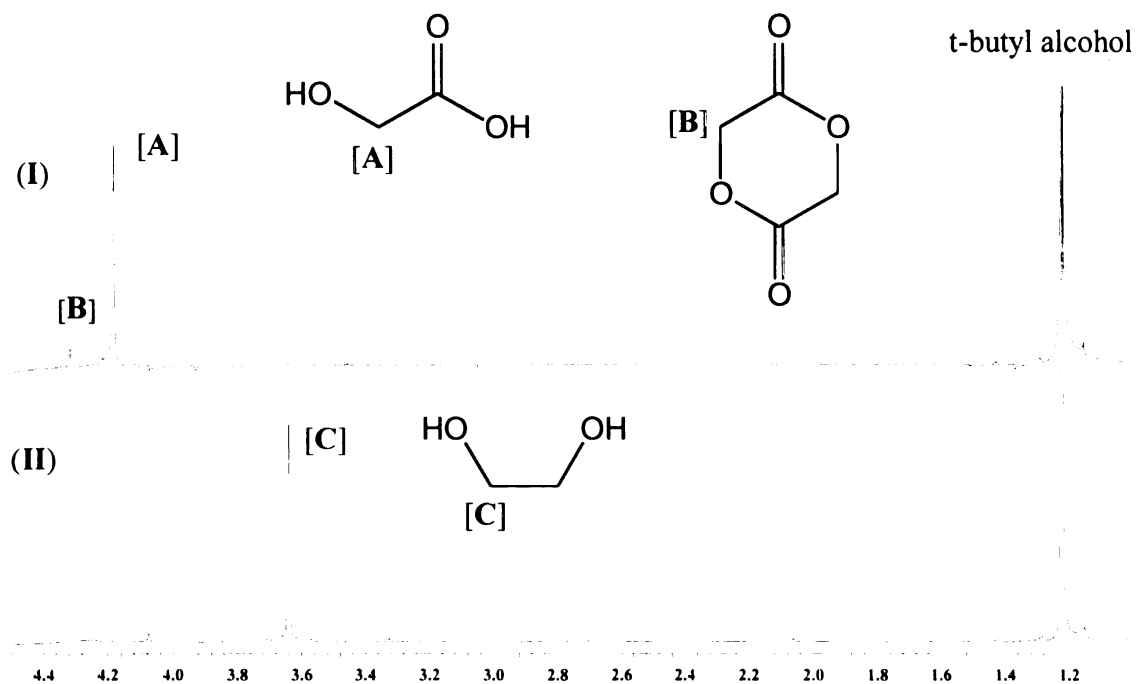


**Figure 2.3.** Spectrum (I) is the starting material containing (GA) and its cyclic ester. Spectrum (II) shows EG, the final product of GA hydrogenation after six hours. For stacked spectra detailing the hydrogenation of GA each hour, please see Appendix 2.1.

The concentration profiles for the hydrogenation reaction of GA, determined by  $^1\text{H}$  NMR, reveal that the starting material is completely used up after five hours (see

Appendix 2.2 for  $^1\text{H}$  NMR concentration profile). Although the conversion of the starting material approaches  $100\pm 7\%$ , only  $60\pm 5\%$  EG is produced.

**GA** is a one carbon shorter analogue of **LA**. **GA** hydrogenation has demonstrated that the selectivity to **EG** (62 %) is quite different from that of **LA** hydrogenation to **PG** (82 %).  $^1\text{H}$  NMR did not show the presence of any hydrogenation byproducts, such as methanol or ethanol, but gaseous byproducts, such as CO and  $\text{CO}_2$ , may have formed during the reaction. HPLC analysis was not carried out on **GA** because of technical difficulties.

Lactic acid and glycolic acid are important target compounds in this work as their vicinal hydroxy functional group can intra-molecularly hydrogen-bond to the carboxy group. The reactivity of **LA** and **GA** is dramatically increased by the  $-\text{OH}$  functional group as compared to simple unsubstituted propanoic acid. Conceivably, the  $-\text{OH}$  substituent induces a fixed intra-molecular geometry, while it simultaneously induces the  $\text{sp}^2$  carbon of the adjacent carboxy functionality, which favors its rehybridization to  $\text{sp}^3$  (Figure 2.4). Considering this increased reactivity, glycolic acid should react at a similar rate as lactic acid in these reactions.

In addition, the  $-\text{OH}$  functionality can form an inter-molecular hydrogen bonding with water that may also play a role in an increased reactivity of these compounds as compared to propanoic acid that is less capable of hydrogen bonding. As solvent effects can stabilize the transition state of a reaction, strongly hydrogen bonding water could facilitate the interaction between the substrate and the active site of the catalyst.

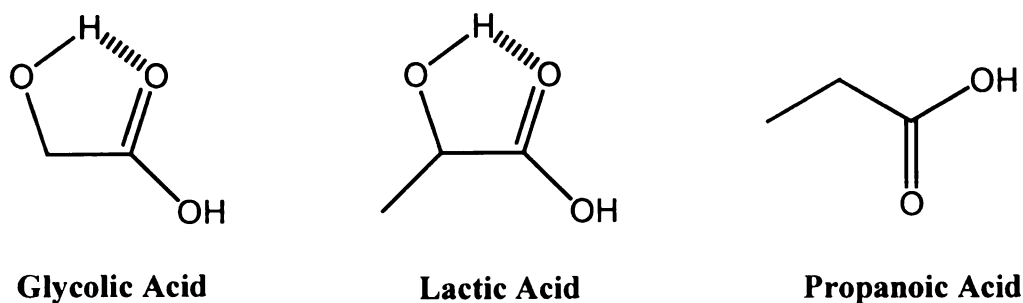
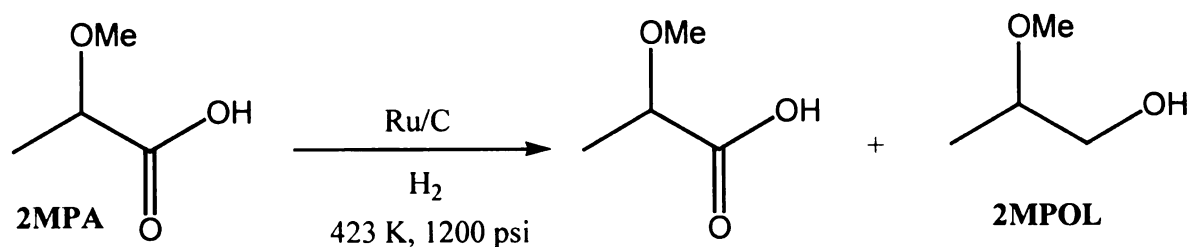


**Figure 2.4.** Intra-molecular hydrogen bonding of glycolic and lactic acid have a relative fixed geometry compared to propanoic acid..

Comparing the rate of conversion of **LA** to **GA** from  $^1\text{H}$  NMR experiments, it is clear that **LA** hydrogenates at a marginally faster rate (Data Table 2.3). However, both compounds are completely reacted after five hours. Similarly to **LA**, under  $\text{H}_2$  without the catalyst, controlled reaction of **GA** did not produce any products.

### 2.3. Hydrogenation of 2-Methoxypropanoic Acid

The hydrogenation of 2-methoxypropanoic acid (**2MPA**) was carried out at 423 K and 1200 psi for six hours (Scheme 2.3). The  $^1\text{H}$  NMR spectrum of the reactant and the product was referenced to t-butyl alcohol at 1.22 ppm. Three peaks belong to 2-methoxypropanoic acid ( $\delta$  1.38 3H(d)/[A], 3.360 3H(s)/[C] and 4.00 1H(q)/[B]). The main product of the hydrogenation of **2MPA**, detectable by  $^1\text{H}$  NMR, was 2-methoxypropanol (**2MPOL**) ( $\delta$  1.092 ppm 3H(d)/[D]; 3.350 3H(s)/[F]; 3.40-3.62 2H(m)/[G]; 3.40-3.62 1H(m)/[E]) (see Figure 2.5).



**Scheme 2.3.** The hydrogenation of **2MPA** to generate **2MPOL**.

The doublet [A] of **2MPA** and the doublet [D] of **2MPOL** were monitored for the concentration change in the six hour period (see Appendix 3.1 for  $^1\text{H}$  NMR spectra, and Appendix 3.2 and 3.3 for concentration profiles). The pre-reaction mixture contained an estimated 5% **LA** which was a byproduct of **2MPA** synthesis. Because **LA** and **2MPA** are azeotropes, the removal of the remaining **LA** from the **2MPA** mixture proved very difficult and severely reduced the product yield after each attempt. Hence, the pre-reaction mixture contained 5% **LA** relative to **2MPA**. The starting material (**2MPA**) was not completely used up in the six hour hydrogenation reaction. Both  $^1\text{H}$  NMR and HPLC showed that the reaction mixture contained **2MPOL**, a substantial amount of **2MPA**, a small amount of **PG** and a residual amount of methanol (**MeOH**) and n-propanol (**POL**) after six hours (see Figure 2.6). The  $^1\text{H}$  NMR results were non-conclusive as they showed  $43\pm 3\%$  conversion and 55% production of **2MPOL**. Percent error could not be established for **2MPOL** production because only one set of  $^1\text{H}$  NMR data was conclusive for product formation. The discrepancy between the conversion and production values is likely due to integration error. HPLC analysis gave more reasonable values with 48 % conversion of **2MPA** and 47 % production of **2MPOL**.

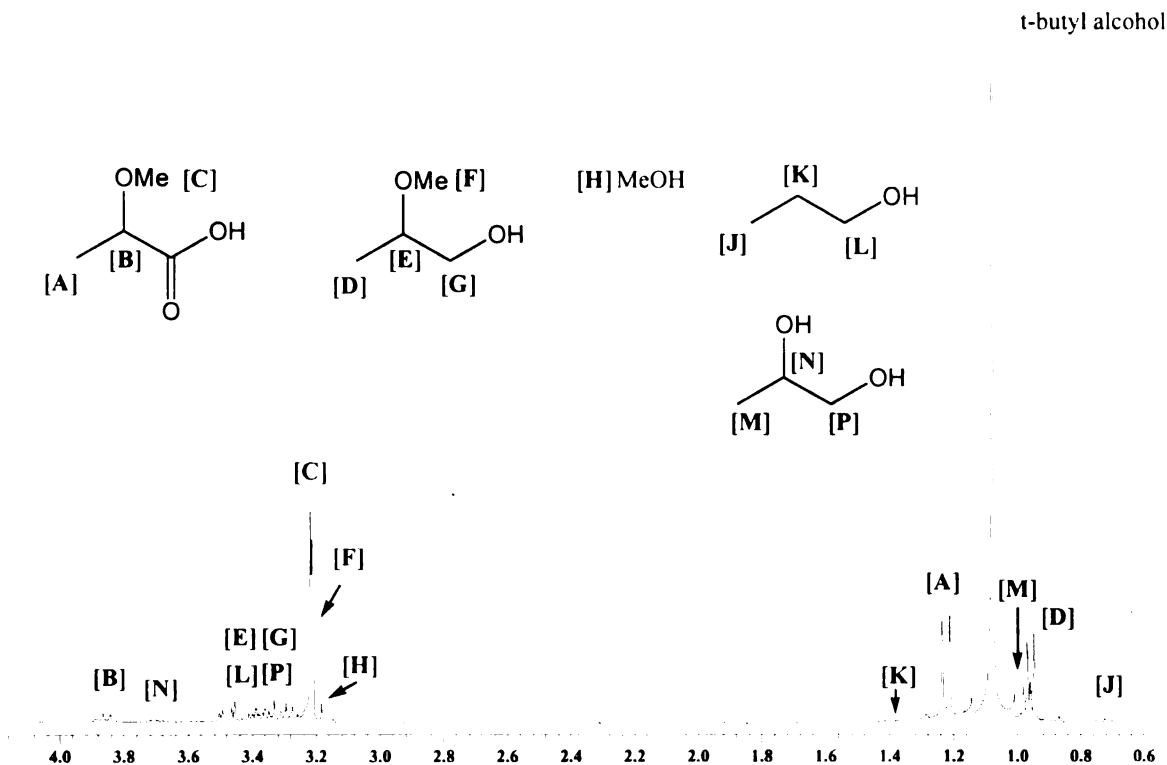


**Figure 2.5.**  $^1\text{H}$  NMR spectrum of the hydrogenation of 2MPA. The reaction produced a mixture of **2MPOL** and **2MPA** after six hours.

While HPLC shows 98 % selectivity to **2MPOL**,  $^1\text{H}$  NMR results show an impossibly high selectivity which is greater than 100%. Hence, only HPLC could be considered for the selectivity. Although this degree of selectivity is encouraging, it seems to be higher than expected as some hydrolysis of the methoxy functionality must take place. Residual amount of **MeOH** and **POL** are also formed and are clearly visible on the  $^1\text{H}$  NMR spectrum and HPLC. Upfield triplet of **POL** at 0.82 ppm and **MeOH** at 3.32 at ppm are evident. The amount of **MeOH** and **POL** formed in this reaction is estimated at 5 % based  $^1\text{H}$  NMR results.

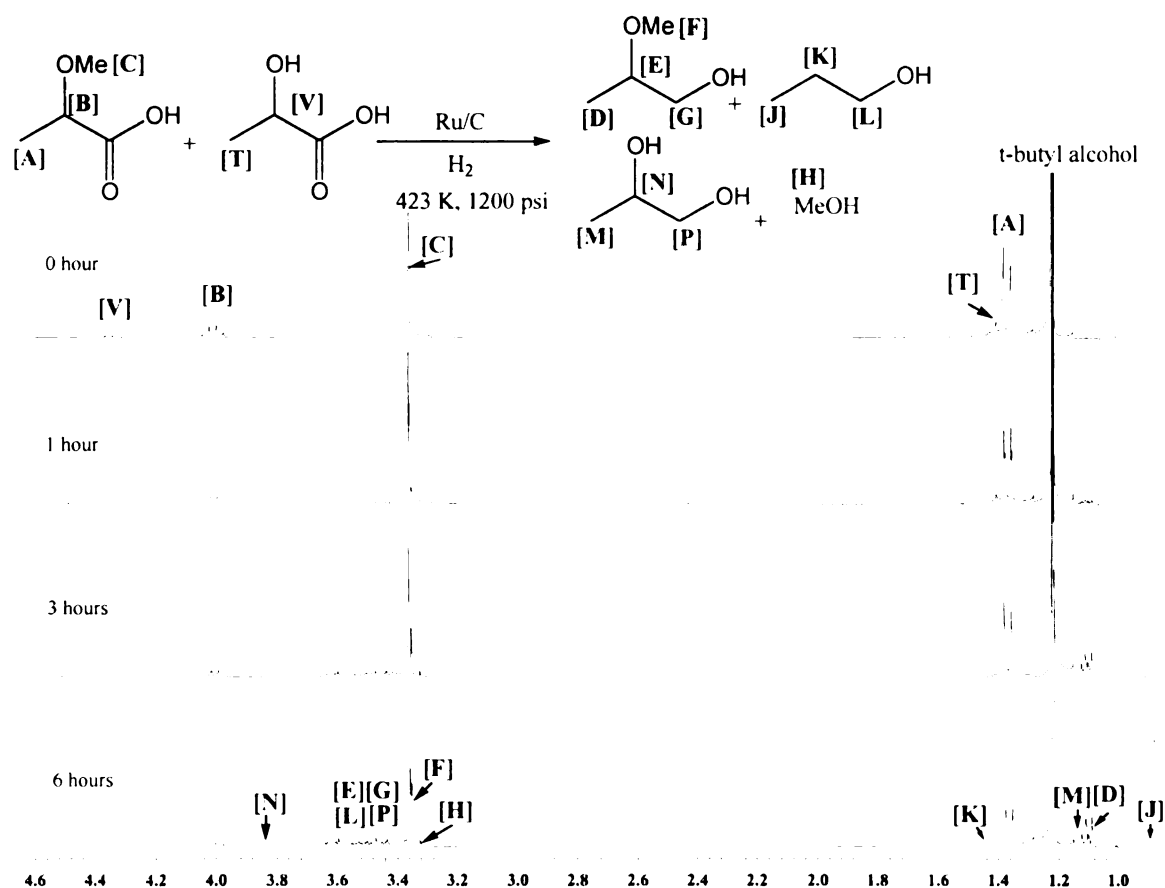
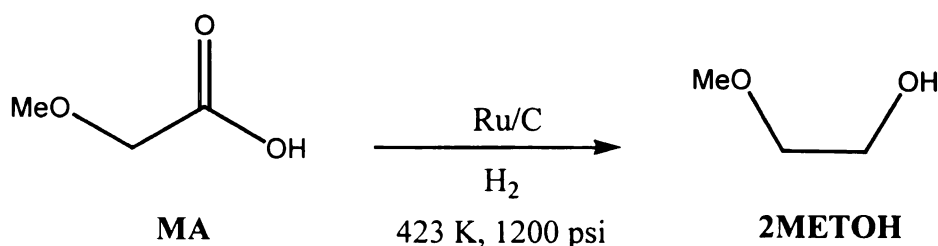


**Figure 2.6.**  $^1\text{H}$  NMR spectra of **2MPA** hydrogenation in which **2MPOL** is produced along with small amount of **PG** and residual amount of **MeOH** and **POL**. For stacked  $^1\text{H}$  NMR spectra detailing **2MPA** hydrogenation each hour, please see Appendix 3.1.

Two types of control experiments were run for **2MPA** at 423 K and 1200 psi for six hours: one without the catalyst under  $\text{H}_2$  and another under  $\text{He}$  with the catalyst. Product formation was not observed in either of these experiments. Furthermore, the gas pressure did not change in the control reactions, also confirming that gas was not consumed nor generated.

## 2.4. Hydrogenation of Methoxyacetic Acid

Methoxyacetic acid (**MA**) was reduced at 423 K and 1200 psi to 2-methoxyethanol (**2METOH**) (scheme 2.4). The  $^1\text{H}$  NMR spectrum of **MA** ( $\delta$  3.402 3H(s)/[**B**]; 4.105 2H(s)/[**A**]) and **2METOH** ( $\delta$  3.402 3H(s)/[**C**]; 3.706-3.553 4H(m)/[**D**] and [**E**]) was referenced to t-butyl alcohol at 1.22 ppm. The methoxy singlet of the starting material shifts to 3.405 ppm after reaction has taken place (Figure 2.7).



**Scheme 2.4.** Hydrogenation of methoxyacetic acid (**MA**) to generate 2-methoxyethanol (**2METOH**).

A small singlet at 3.322 ppm, corresponding to **MeOH** singlet, is seen in the  $^1\text{H}$  NMR spectrum. Although the presence of **MeOH** was confirmed by a peak enhancement technique in which a small quantity of **MeOH** was added to the sample to produce an intense and sharp singlet at 3.322 ppm, the presence of ethanol cannot be clearly seen. This is because the small triplet and quartet of ethanol (**EtOH**) are indeed overlapped with product and reactant peaks as well as the standard itself. Based on relative peak intensities, 6 % of **MeOH** is estimated to be in the reaction mixture.

HPLC analysis showed residual quantities of **MeOH** and **EtOH** that estimated at less than 2 % of the generated product mixture.

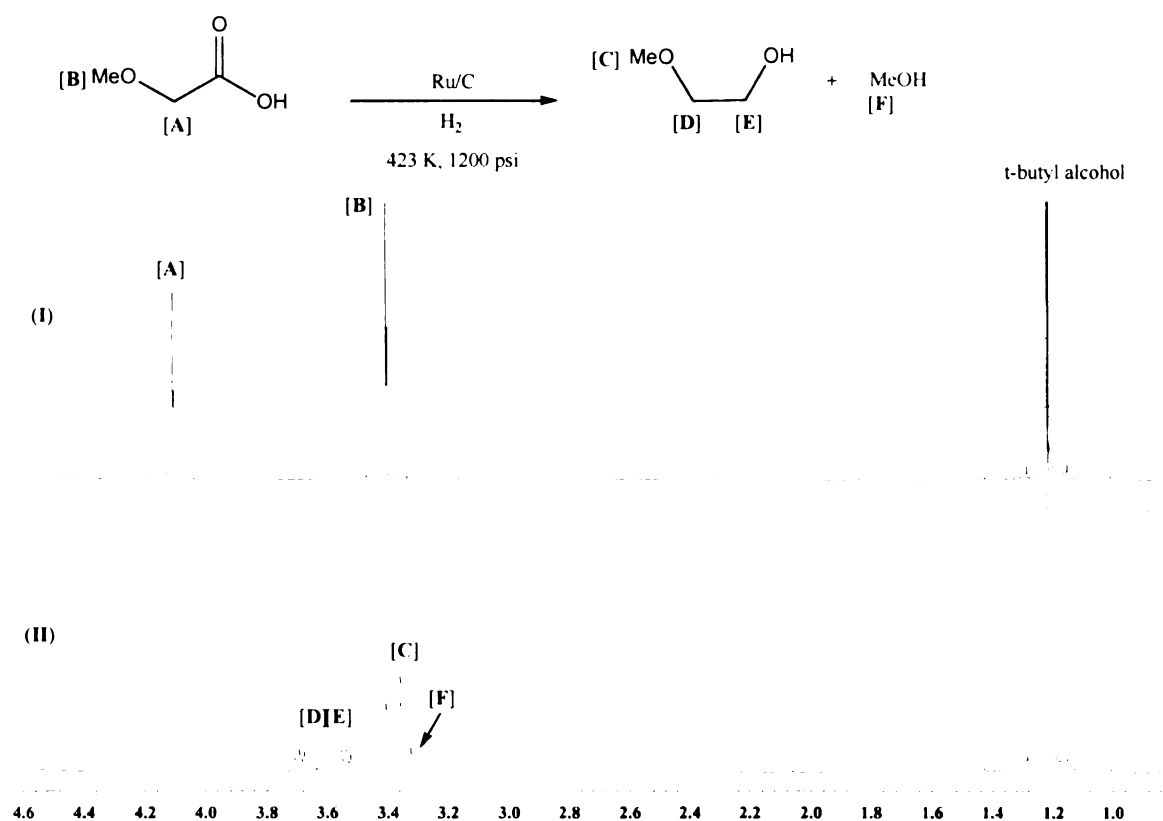


**Figure 2.7.** <sup>1</sup>H NMR spectra of MA hydrogenation. Spectrum (I) shows the starting material and spectrum (II) corresponds to the reaction mixture containing MA, 2METOH and MeOH after six hours. Stacked spectra detailing MA hydrogenation each hour are found in Appendix 4.1.

The concentration profile of this reaction shows that a substantial amount of the starting material is still present in the reaction mixture after six hours (see Appendix 4.2. and 4.3 for concentration profiles). Based on <sup>1</sup>H NMR, 78±7% conversion is calculated that is in contrast with the HPLC results that demonstrate only 64±11% conversion after six hours. The percent production of 2METOH was calculated at 46 % by <sup>1</sup>H NMR and

44 % by HPLC. The selectivity to **2METOH** was 53 and 69 % as determined <sup>1</sup>H NMR and HPLC, respectively.

The calculated percent conversions of **MA** and **2MPA** compared to **LA** and **GA** reveal that the hydrogenations of **LA** and **GA** go at faster rates than do their methoxy-substituted analogues. Furthermore, comparing **MA** with **2MPA**, it is evident that **MA** hydrogenates twice as fast as **2MPA** (see Table 2.3).

A control experiment for **MA** hydrogenation was run under H<sub>2</sub> without the catalyst. During this reaction the hydrogen pressure was stable, indicating that hydrogen was not being used up. This was confirmed by <sup>1</sup>H NMR that showed that the product did not form and the starting and the final concentration of **MA** was the same in a six hour run.

## 2.5. Hydrogenation of Isobutyric Acid

Hydrogenation of isobutyric acid (**IBA**) was carried out at 423 K and 1200 psi to produce isobutyl alcohol (**IBUOL**). The <sup>1</sup>H NMR spectrum of **IBA** ( $\delta$  1.134 6H(d)/[A]; 2.607 1H(hept)/[B]) and **IBUOL** ( $\delta$  0.861 6H(d)/[C]; 1.718 1H(m)/[D]; 3.334 2H(d)/[E]) was referenced to t-butyl alcohol at 1.22 ppm. The doublet of **IBA** (1.134 ppm) and the doublet of **IBUOL** (0.861 ppm) were monitored for the concentration change (Figure 2.8).

The concentration profile of the hydrogenation of **IBA** reveals that a significant amount of the starting material is still present after six hours (see Appendix 5.2 and 5.3 for concentration profiles). The results from  $^1\text{H}$  NMR and HPLC are in close agreement for the values of percent conversion and percent production at each time interval. For example, after four hours,  $^1\text{H}$  NMR and HPLC showed 40 and 39 % conversion, respectively. After six hours,  $^1\text{H}$  NMR indicated that  $52\pm 8$  % percent of the starting material had been converted, but only  $25\pm 10$  % **IBUOL** had been produced and these results matched those in HPLC analysis. The relatively low production of **IBUOL** could be due to gaseous byproduct formation such as  $\text{CO}_2$ ,  $\text{CO}$  and propane, as decarboxylation and decarbonylation reactions are quite possible at 423 K for a six hour period. Value of selectivity to **IBUOL** was 48% as determined by  $^1\text{H}$  NMR and HPLC, respectively.

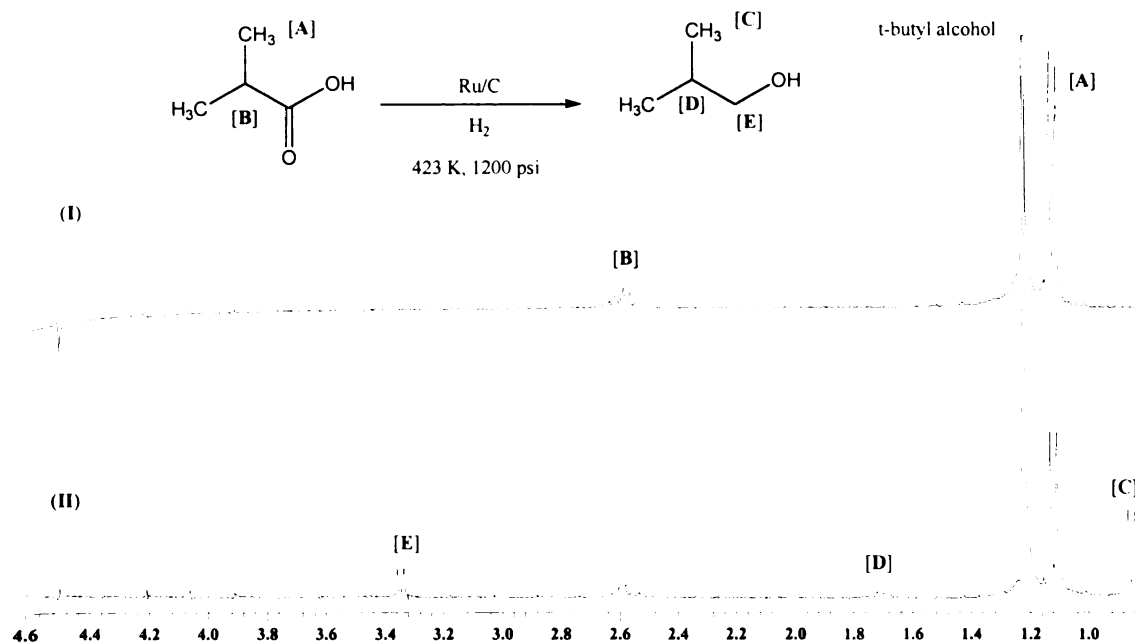


**Figure 2.8.**  $^1\text{H}$  NMR spectra of **IBA** hydrogenation. Spectrum (I) shows the starting material, spectrum (II) is the mixture of **IBA** and **IBUOL** after six hours. For stacked  $^1\text{H}$  NMR spectra detailing **IBA** hydrogenation, see Appendix 5.1.

In a control experiment, run under H<sub>2</sub> without catalyst, it was clear that hydrogenation was not taking place, as H<sub>2</sub> pressure was relatively stable all throughout the reaction. <sup>1</sup>H NMR spectrum only showed the characteristic peaks of **IBA** after six hours. Concentration profiles also demonstrated that under such conditions, reaction did not take place as the initial and final concentration of **IBA** was invariant.

## 2.6 Hydrogenation of Propanoic Acid

The hydrogenation of propanoic acid (**PA**) was carried out at 423 K and 1200 psi. The product detectable by <sup>1</sup>H NMR and HPLC was n-propanol (**POL**). The spectrum of **PA** ( $\delta$  1.062 3H(t)/[**A**]; 2.351 2H(q)/[**B**]) and **POL** ( $\delta$  0.864 3H(t)/[**C**]; 1.531 2H(sext)/[**D**]; 3.529 2H(t)/[**E**]) was referenced to t-butyl alcohol at 1.22 ppm (Figure 2.9). The triplet of **PA** at 1.062 ppm and the triplet of **POL** were monitored for concentration change. Concentration profile of this reaction shows a slow decrease of the concentration of the starting material and a correspondingly slow increase of the concentration of **POL** (see Appendix 6.2 and 6.3 for concentration profile).

Conversion values, determined by <sup>1</sup>H NMR and HPLC, were in good agreement; 35 $\pm$ 5% and 33 %, respectively. While <sup>1</sup>H NMR showed 18 $\pm$ 6% production of **POL** after six hours, HPLC indicated that this value is only 14 %. The discrepancy may be due to the integration error of the triplet in the <sup>1</sup>H NMR spectrum. The selectivity was 51 and 42 %, as determined by <sup>1</sup>H NMR and HPLC, respectively. Similarly to **IBA**

hydrogenation, decarboxylation and decarbonylation could be side reactions that may occur to a great degree in which CO<sub>2</sub>, CO and ethane are produced.

In a control experiment, run under H<sub>2</sub> without catalyst, product formation was not observed. This result is expected as **PA** is relatively slow to reduce to **POL** compared to other functionalized organic acids with very poor yields in catalytic hydrogenation. Furthermore, the invariant concentration of **PA** during the control experiment indicated that gaseous byproduct formations are unlikely.

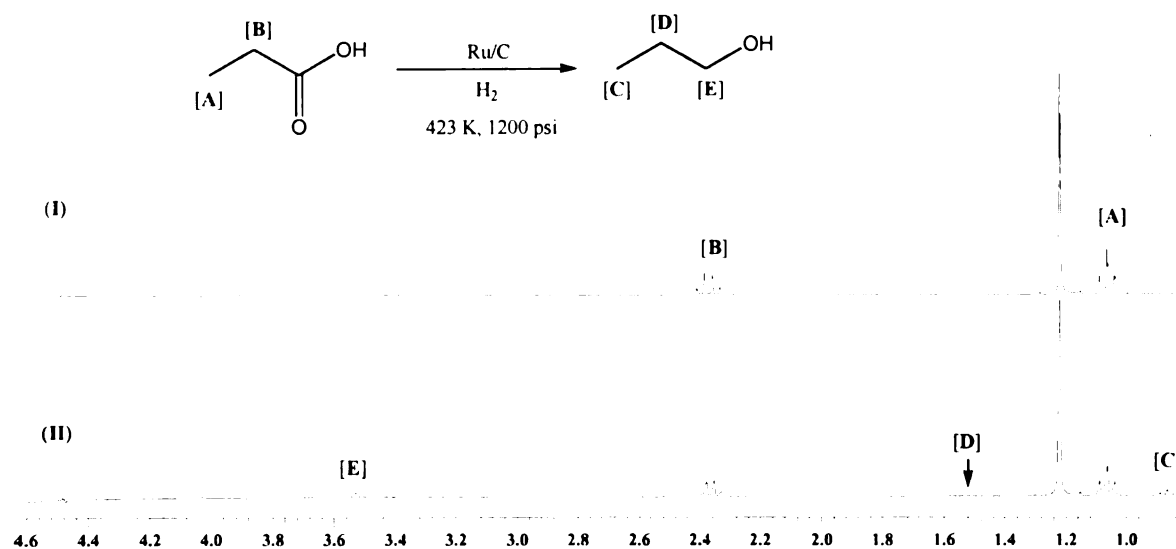


**Figure 2.9.** <sup>1</sup>H NMR spectrum of **PA** hydrogenation. Spectrum (I) shows the starting material; spectrum (II) corresponds to the mixture of **PA** and **POL**. For stacked spectra detailing **PA** hydrogenation, please see Appendix 6.1.

It is important to contrast the hydrogenation of **PA** with **IBA**. Clearly, the rate of conversion of **IBA** to **IBOL** is substantially faster than the conversion of **PA** to **POL**. However, the selectivity to the corresponding alcohol is higher for **PA** hydrogenation than that of **IBA** (selectivities are 51% and 48% for **PA** and **IBA**, respectively). Based

on HPLC analysis, the rate of product (**POL**) formation from **PA** was slower than **IBUOL** formation from **IBA** and these results concur with that of  $^1\text{H}$  NMR.

## 2.7. Hydrogenation of 2-Chloropropanoic Acid

Antons showed that 2-chloropropionic acid (**2CPA**) hydrogenation generates 2-chloropropanol when Mohr's salt of the ruthenium catalyst is used.<sup>63</sup> In this work carbon supported ruthenium (Ru/C) was used for the hydrogenation of **2CPA** in aqueous medium. Although the initial expectation was to see the generation of 2-chloropropanol (**2CPOL**), the hydrogenation of **2CPA** only generated propanoic acid (**PA**) at 423 K and 1200 psi.

As **2CPA** was introduced in the reactor, the reactor pressure rapidly increased by 150 psi from the initial pressure (1200 psi), indicating that gas was being generated at 423 K. Furthermore, the collected samples were turning dark green with the progression of time. This suggested that HCl was produced in this reaction that in turn was leaching the metal components from the inside wall of the reactor (pH = 3.5 of the pre-reaction mixture; pH= 1 of the collected reaction mixture). Therefore, these reactions were repeated at 373 K to minimize the corrosion in the reactor. (Leaching of the reactor interior can be avoided by protective Teflon coating, but this measure can also significantly increase the time required for cooling of the reactor after the reaction.) Although the degree of leaching was lowered at 373 K, this reaction only produced **PA**

after six hours at both temperatures. **2CPA** rapidly reacted under these conditions to form **PA** in less than one hour at 423 K and less than two hours at 373 K.

The  $^1\text{H}$  NMR spectrum of **2CPA** ( $\delta$  1.656 3H(d)/[A]; 4.552 1H(q)/[B]) and **PA** ( $\delta$  1.064 3H(t)/[D]; 2.393 2H(q)/[E]) was referenced to t-butyl alcohol. The doublet of **2CPA** was monitored for concentration change. It is important to note that approximately 5 % of the starting material contained 2,2-dichloropropanoic acid ( $\delta$  2.223 3H(s)/[C]). The sample collected after one hour of reaction time, run at 423 K,

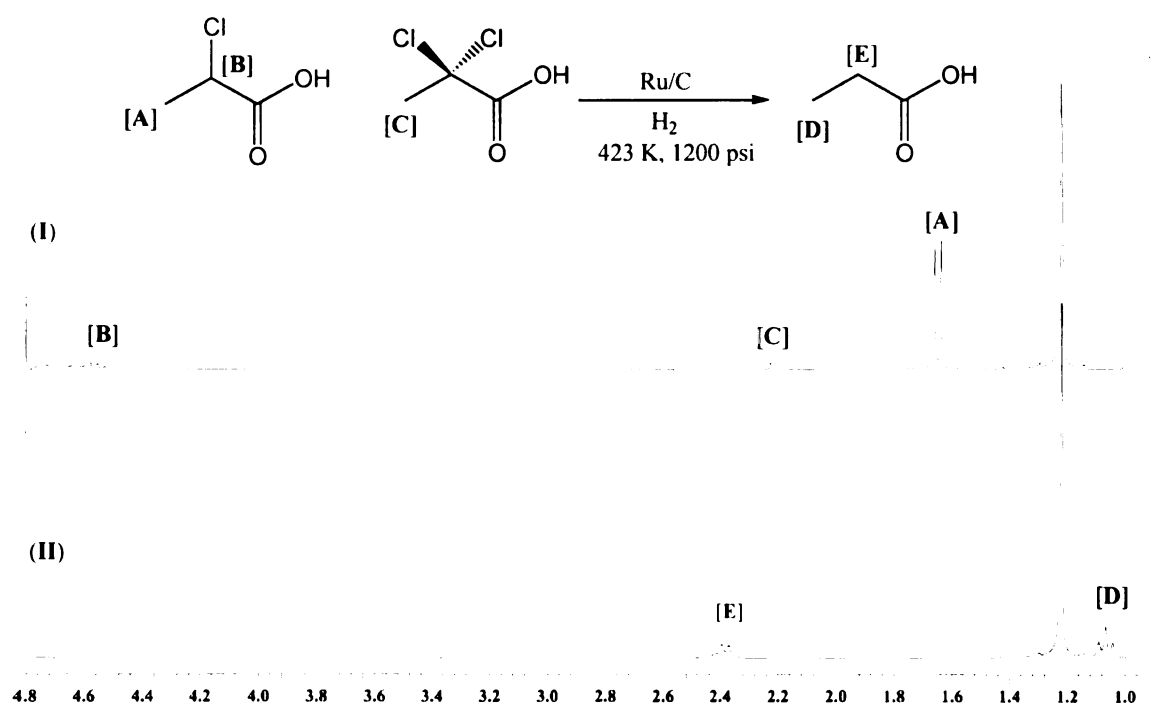


**Figure 2.10.** (I) is the  $^1\text{H}$  NMR spectrum of 2CPA pre-reaction mixture. (II) is taken after six hours and is the spectrum of PA. For stacked  $^1\text{H}$  NMR spectra detailing 2CPA hydrogenation, see Appendix 7.1.

contained only **PA** as confirmed by  $^1\text{H}$  NMR. The doublet of **2CPA** and the singlet of 2,2-dichloropropanoic acid were not observed on the spectrum, but characteristic **PA** peaks were evident (Figure 2.10). Furthermore, the concentration of **PA** did not change in six hours (for  $^1\text{H}$  NMR concentration profile, see Appendix 7.2). Analyzing the reaction samples of **2CPA** by HPLC presented a challenge as negative peaks were produced in the chromatogram, thus HPLC was not used for concentration determination.

The **2CPA** did not hydrogenate at the carboxy functionality. The generation of **PA**, under these reaction conditions, demonstrated that reaction only takes place at the C2 position of **2CPA**. At 423 K the conversion of **2CPA** is complete in 20 minutes and the selectivity to **PA** approaches 100%. At 373 K the conversion of **2CPA** is 73 % in one hour and in two hours it is completed with selectivity similar to that of the former reaction. Uncertainties were not determined in these reactions as they were run only once per temperature and concentration variation. At these pressures and temperatures a possible decarboxylation producing  $\text{CO}_2$  should also be considered, but **PA** concentrations were invariant in each sample.

Even more interesting is the behavior of this reaction in a control experiment run at 373 K without any catalyst. After two hours the presence of **PA** was evident but **2CPA** never completely reacted to form only **PA**. In addition, after two hours, a residual **LA** doublet and quartet peaks were observed. The characteristic **LA** peaks were no longer present in the  $^1\text{H}$  NMR spectrum after six hours.

One of the main questions is why **2CPA** reacts so quickly at the C2 position losing a chlorine atom, but it does not further react to hydrogenate the resulting **PA** to form **POL**. To address this problem, catalyst poisoning had to be considered.

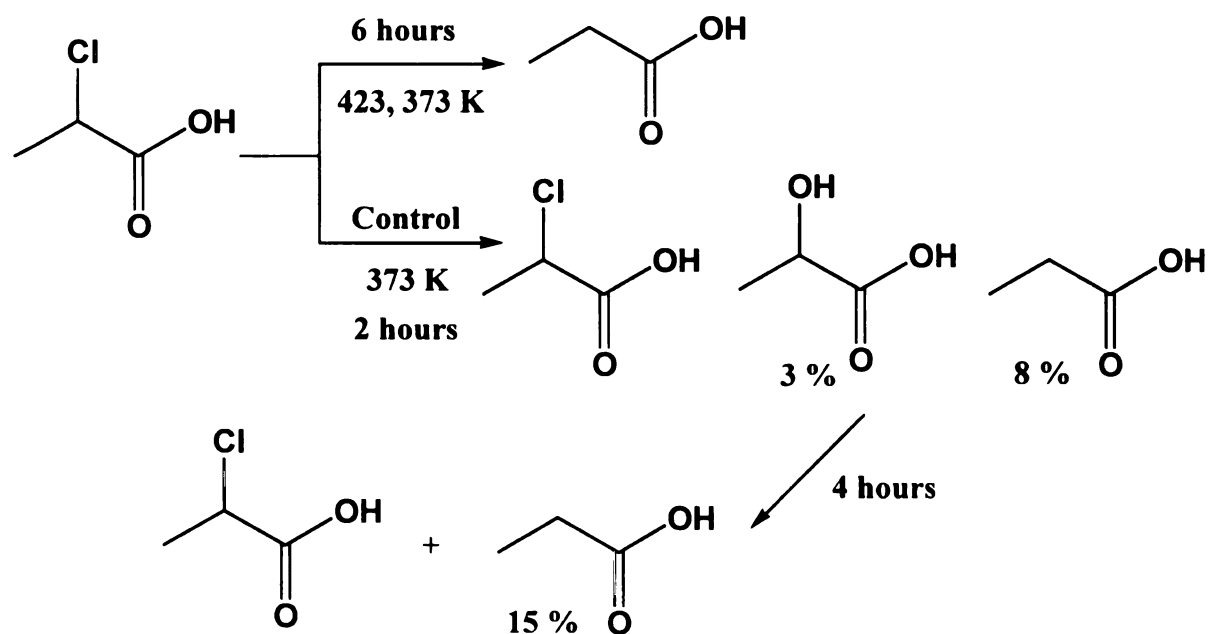
Qualitatively, it could be determined that HCl was generated because the samples that were removed from the reactor during the hydrogenation of **2CPA** were dark green. Then it was assumed that either the chloride or the proton of the acid poisons the catalyst.

To test this assumption, a hydrogenation reaction **LA** was run with added NaCl and a **PA** hydrogenation was carried out with added HCl. Because the presence of Cl<sup>-</sup> ion could inhibit the hydrogenation reaction, **LA**, an easily reducible species under normal hydrogenation conditions, should become difficult to reduce, if at all. In one control experiment **LA** was hydrogenated in the presence of one weight equivalent of Cl<sup>-</sup> (10 g of **LA** and 10 g of NaCl). In this reaction **LA** hydrogenation was not affected by the presence of chloride anion.

Testing for the effect of acid on the reaction, **PA** was selected instead of **LA** to avoid a possible dehydration reaction. Concentrated HCl (1 mL) was added to the aqueous reaction mixture of **PA** and was allowed to react in the reactor under conditions previously described for other substrates. **PA** hydrogenation was not changed by the addition of acid as the rates of conversion and production of **POL** were virtually the same as in the **PA** reduction by the regular protocol. Based on these results, a conclusion can be drawn that neither Cl<sup>-</sup> nor H<sup>+</sup> play a direct role in catalyst poisoning of these reactions.

The reactor itself may provide an ostensible explanation for the metal leaching. The stainless steel wall of the reactor is composed of an alloy that contains a variety of metals such as chromium that could be “washed out” of the reactor by HCl that is generated in these reactions. Conceivably, these metals could block the active sites on the catalyst surface and thus prevent the hydrogenation process at the carboxy functional group.

The formation of **PA** was evident in reactions at 423 and 373 K, but in a control experiment at 373 K and 1200 psi in which the catalyst was omitted, an appreciable amount of **PA** was still produced. Furthermore, **LA** formation was observed in the  $^1\text{H}$  NMR spectrum within two hours, but at the end of the six hour period it was no longer present in the reaction mixture. To explain the generation of **LA** under these conditions, water must attack **2CPA** at the C2 position where the chlorine is attached. Given that the chlorine can be easily removed in an  $\text{S}_{\text{N}}2$  mechanism from a substrate, water can carry out a nucleophilic attack at the C2 position. This attack may be facilitated by increased nucleophilicity of water at these pressures and temperatures. Scheme 2.5 provides a summary of **2CPA** hydrogenation reaction at various temperatures and in control conditions.



**Scheme 2.5.** Summary of **2CPA** hydrogenation reactions at varying temperatures and under controlled conditions.

## 2.8. Hydrogenation of Ethyl Lactate

As previously demonstrated by Adkins et al. the hydrogenation of ethyl lactate (**EL**) to propylene glycol (**PG**) goes with surprising ease.<sup>44,45</sup> In this project the hydrogenation of **EL** was carried out at 423 K and 1200 psi. In the <sup>1</sup>H NMR analysis of reaction samples, dioxane ( $\delta$  3.606 ppm) was used as the internal standard because the prominent singlet of t-butyl alcohol at 1.22 ppm, used for other reaction samples, overlaps with the doublet of **EL**. Unfortunately, this doublet was the only acceptable set of peaks for the concentration determination of **EL**.

**EL** has four easily distinguishable peaks on the <sup>1</sup>H NMR spectrum ( $\delta$  4.247 1H(q)/[**B**]; 4.084 2H(q)/[**C**]; 1.263 3H(d)/[**A**]; 1.117 3H(t)/[**D**]). The end products of **EL** hydrogenolysis are **PG** ( $\delta$  3.762-3.661 1H(m)/[**F**]; 3.414-3.242 2H(d/d)/[**G**]; 0.962 3H(d)/[**E**]) and **ETOH** ( $\delta$  3.500 2H(q)/[**J**]; 1.014 3H(t)/[**H**]) (Figure 2.11).

Doublet **A** of **EL**, multiplet **G** of **PG** and quartet **J** of ethanol were monitored for the concentration change (see Appendix 8.2 and 8.3 for concentration profile). As has been discussed in other sections, long base-line integration should be avoided to minimize error in concentration determination. In the case of **PG**, only peak **G**, which is doublet of doublet spanning a large base line, could be used for concentration determination. This is why there is a discrepancy between the HPLC and <sup>1</sup>H NMR results for the percent of product formation.

While <sup>1</sup>H NMR showed a 100 $\pm$ 10% conversion and over 100 $\pm$ 16% production of **PG**, HPLC results indicated only 82% conversion and 77% production of **PG** for the

same reaction. Selectivity from  $^1\text{H}$  NMR could not be determined due to unrealistic percentage values for **PG** formation.

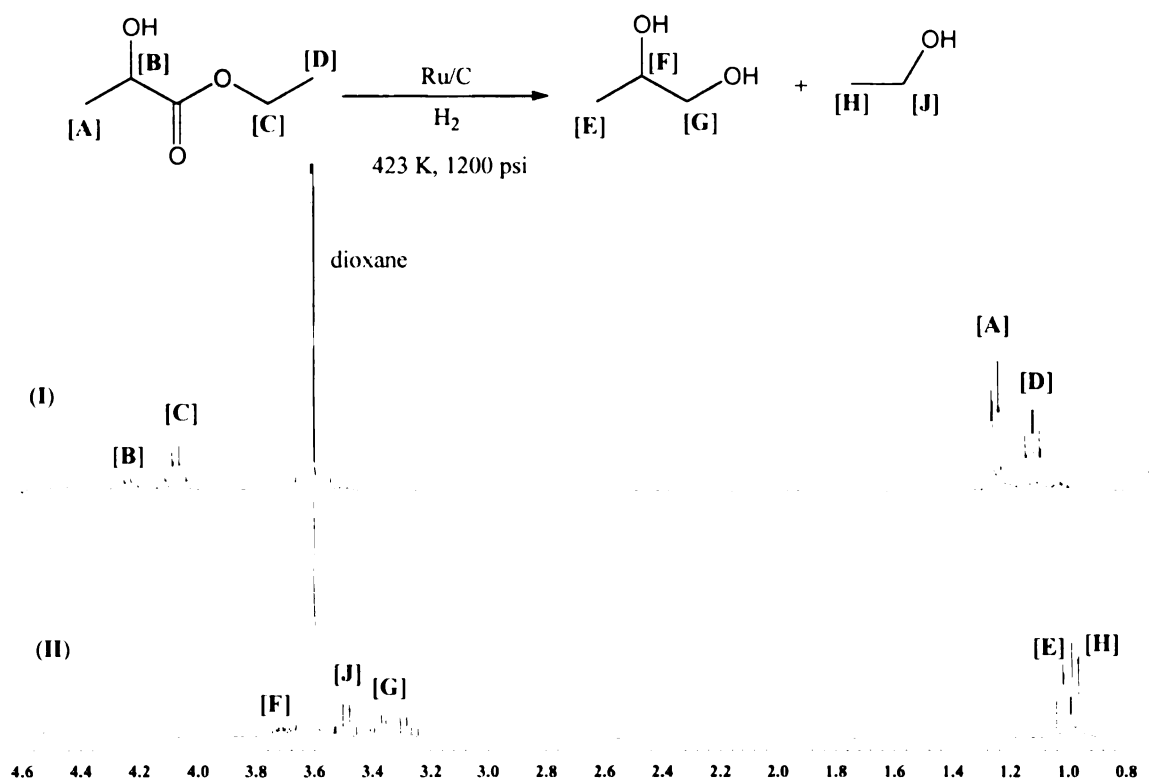


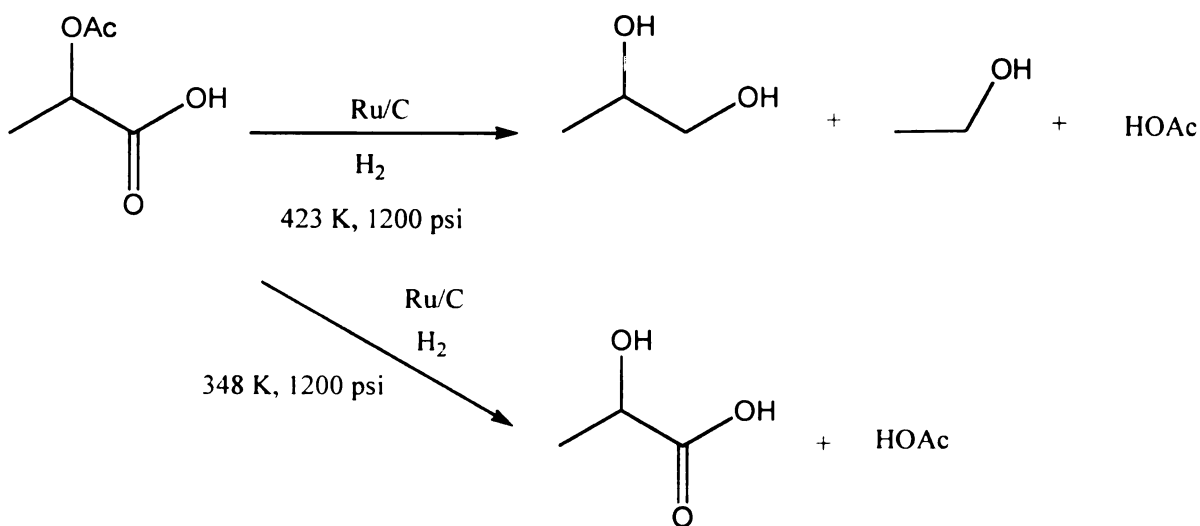
**Figure 2.11.**  $^1\text{H}$  NMR spectrum of **EL** hydrogenation. Spectrum I is **EL** and spectrum II is the mixture of **PG** and ethanol after a six hour reaction time. For stacked  $^1\text{H}$  NMR spectra detailing **EL** hydrogenation, see Appendix 8.1.

However, HPLC showed 92 % and 97 % selectivity for **PG** and ethanol, respectively. These are realistic values as excellent **PG** yields have been demonstrated by others.<sup>44,45</sup> Furthermore, a control experiment, under  $\text{H}_2$  not employing catalyst in aqueous medium, showed that only the hydrolysis product (**LA**) and ethanol are produced with 100 % estimated selectivity.

## 2.9. Hydrogenation of 2-Acetoxypropanoic Acid

The hydrogenation of 2-acetoxypropanoic (**2APA**) acid was run at two different temperatures (423, 348 K) and 1200 psi pressure. This reaction produced different results at different temperatures. While at 423 K, **PG**, ethanol and acetic acid (**HOAc**) were produced, reactions at 348 K only afforded **LA** and **HOAc** (Scheme 2.6).

The  $^1\text{H}$  NMR peaks of products and reactants of these reactions were referenced to t-butyl alcohol at 1.22 ppm. The starting material **2APA**, has two easily



**Scheme 2.6.** Hydrogenation of **2CPA** at 348 and 423 K and 1200 psi.

distinguishable peaks upfield and a weak-signal quartet close to the water peak ( $\delta$  5.011 1H(q)/[B]; 2.131 3H(s)/[C]; 1.481 3H(d)/[A]). The characteristic **PG** peaks ( $\delta$  3.905-3.789(m); 3.544-3.383(d/d) and 1.124(d)), ethanol quartet at 3.544 ppm and **HOAc** singlet at 2.058 ppm are prominent in the final sample collected after six hours (Figure 2.12).

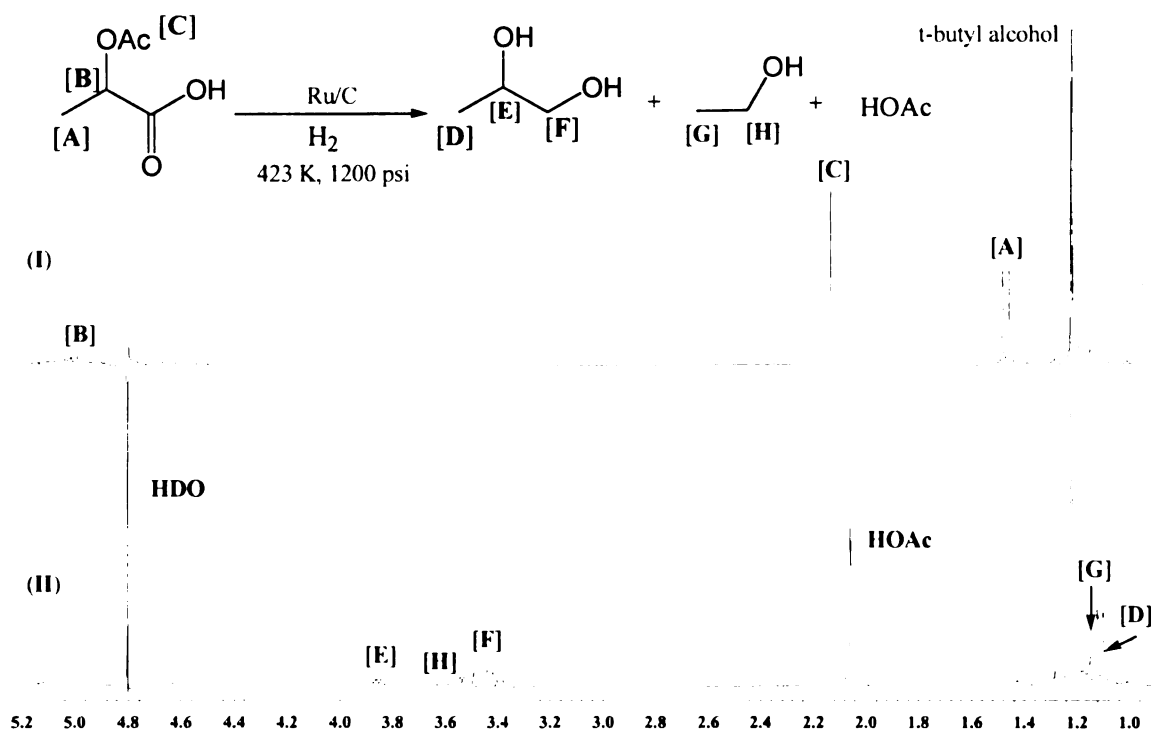


**Figure 2.12.** Hydrogenation of **2APA** at 423 K and 1200 psi produces **PG**, ethanol and **HOAc**. Spectrum **I** is the starting material (**2APA**) and Spectrum **II** is the product mixture after six hours. For stacked <sup>1</sup>H NMR spectra of **2APA**, see Appendix 9.1.

The concentration profile reveals an increase of concentration of **LA** in the first two hours and that the hydrolysis of the acetoxy group and the formation of ethanol is significantly faster than **PG** generation (see Appendix 9.2 and 9.3 for concentration profile). Previous work has demonstrated that acyl fragments are attached to the catalyst

surface longer than alkoxy fragments.<sup>26,29,35</sup> As hydrolysis of the ethoxy fragment of **2APA** takes place, followed by **LA** and **PG** formation, a mixed kinetics can be expected for this reaction.

The hydrogenation of **2APA** is also a relatively fast reaction compared to other acids such as propanoic acid, but **2APA**'s overall reactivity is also greater than those of **LA** or **GA**. <sup>1</sup>HNMR results of **2APA** reduction at 423 K showed a 100±9% conversion of 2-acetoxypropionic acid to form **PG** (74±11%). Although the weak signal of the **EtOH** quartet at 3.544 ppm is evident, the determination of its concentration came from HPLC analysis. An estimated 5 % of **EtOH** and 90 % **HOAc** are produced. The selectivity to **PG** is 70 % which was also confirmed by HPLC. A weak ethanol peak is present in the chromatogram that indicates an estimated 1%. It is reasonable to suggest that the rate of hydrolysis of the acetoxy functionality is significantly faster than the rate of its hydrogenation. This is consistent with prior findings in which the hydrogenation of acetic acid to ethanol was difficult, requiring stringent conditions.<sup>35</sup>

One of the problems with the hydrogenation of **2APA** is its hydrolyzing acetoxy group to form **HOAc** at relatively high temperatures. The acetoxy group hydrolyzed within two hours as it was confirmed by <sup>1</sup>HNMR, and the integration value of the developing singlet of **HOAc** after two hours did not change. Because the initial goal was to observe whether the highly electron-withdrawing acetoxy group is strongly activating in hydrogenation reactions, this temperature (423 K) had to be omitted. Hoping that the hydrolysis of the acetoxy group can be prevented or at least minimized at lower temperature, the hydrogenation of **2APA** was carried out at 348 K. It is important

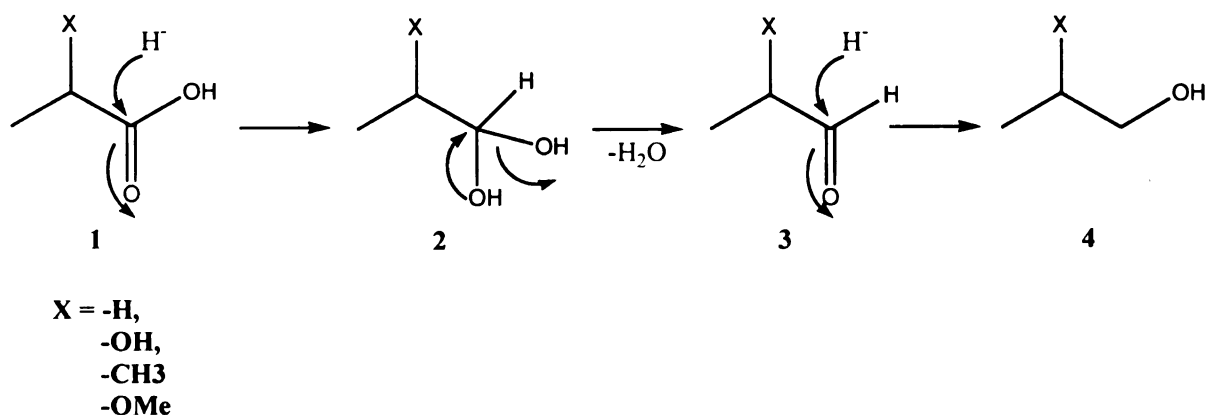
to retain the highly electron-withdrawing acetoxy group at the C2 position long enough to see its effect on the hydrogenation at the carboxy group.

If one was to assume that the a more electron-withdrawing group would increase reactivity, then one should see an increased rate of conversion of **2APA** to 2-acetoxy propanol or **PG** relative to **PA** or **LA** reduction. Unfortunately, even at 348 K, though not as fast as at 423 K, the hydrolysis of the acetoxy group was evident. Results of <sup>1</sup>HNMR clearly show a slower rate of acetic acid formation and the generation of **LA** as the other product of this reaction. But because this temperature is below the optimal range, no propylene glycol was formed in this reaction (Scheme 2.6)

A control experiment, under H<sub>2</sub> and without catalyst, showed that hydrolysis products (**LA** and **HOAc**) are generated exclusively from **2APA** in two hours. This result can be used to conclude that the hydrolysis of **2APA** is unaffected by the presence of the catalyst.

## 2.10. Compiled Results

A general mechanism describing the hydrogenation reaction of organic acids is described in the scheme below. The organic chemical process in these reactions can be understood by hydride delivery at the carboxy carbon (1) to generate the hemiacetal.



**Scheme 2.7.** The reaction mechanism for alcohol formation from  $\alpha$ -substituted organic acids in aqueous medium under heterogeneous catalytic conditions.

intermediate (2). Hemiacetal forms aldehyde (3) that in turn undergoes another hydride delivery to form alcohol (4). Hydrogenation at the C2 carbon of **2CPA** and **2APA** by hydride delivery may be an  $S_N2$  process. However, arguments can be made that insertion of hydrogen followed by  $\beta$  elimination can be an alternative mechanism. The hydrogenation of **2APA** is more easily understood as it is hydrolyzed by water to form **LA** under these conditions. The **LA** in turn can hydrogenate, as described in scheme 2.1.

In the general procedure 10 weight % aqueous mixtures were described to react with 1 weight % catalyst mixture (2.16 g/100 g of pre-reaction mixture). The activated carbon-supported ruthenium contained only 5% ruthenium. Thus in these reactions, only 0.05 gram of ruthenium was used as the active catalyst. This naturally translates into a non-uniform molar ratio of catalyst to substrate. For example, the results indicate that the percent conversion **2MPA** was slower than that of **IBA**, but one must also remember that the catalyst ratio to **2MPA** was also greater than the ratio between the catalyst and **IBA**. However, even a higher catalyst loading for **2MPA** hydrogenation did not produce better conversion rates compared to **IBA** reductions.

The results of carbon-supported ruthenium-catalyzed hydrogenation reactions are summarized in table 2.1 (<sup>1</sup>HNMR) and 2.2 (HPLC) and these results are plotted in Figure 13-16. Note that some of the values in the table are designated with \*, meaning that they incurred integration or instrumental error. Instrumental error was only determined for HPLC analysis from a series of identical concentration ethanol internal standards. The relative error, however, was only 0.15% which is negligible. The ethanol standards produced an average response factor of 3370142±6534. The magnitude of the standard deviation is negligible relative to the average counts of the ethanol standard. One can conclude that instrumental error did not play a significant role in any discrepancy that may have arisen from HPLC analysis. Only one HPLC analysis was carried out per type of reaction except for **GA** which was not analyzed by HPLC. Therefore, uncertainties from HPLC, other than instrumental error, could not be determined. Table 2.3 summarizes the selectivity values and rate data and relative rates of main product formation.

Substrate	2CPA	LA	GA	EL	2MPA	MA	2APA	IBA	PA
Main Product	PA	PG	EG	PG	2MPOL	2METOH	PG	IBOL	POL
% Conv. (1 hr.)	100*	32	29	41	12	48	65	20	5
% Conv. (2 hr.)	100*	61	41	68	21	66	93	27	20
% Conv. (3 hr.)	100*	73	45	78	29	78	100	35	22
% Conv. (4 hr.)	100*	89	76	84	41	84	100	40	32
% Conv. (5 hr.)	100*	100	100	90	39	88	100	48	35
% Conv. (6 hr.)	100*	100	100	100	43	86	100	52	35
% Prod. (1 hr.)	121*	30	22	63*	16	19	32	5	12
% Prod. (2 hr.)	106*	55	32	81*	34	33	53	10	13
% Prod. (3 hr.)	94*	77	44	89*	31	37	60	14	19
% Prod. (4 hr.)	98*	74	52	99*	47	41	73	18	13
% Prod. (5 hr.)	96*	83	61	108*	50	46	66	21	15
% Prod. (6 hr.)	108*	82	62	105*	55	46	74	25	18

**Table 2.1.** Compiled  $^1\text{H}$  NMR results of Ru/C-catalyzed aqueous phase hydrogenations. This table only shows the main products of reactions. Hydrogenation of 2APA also generated HOAc and EL hydrogenation generated large quantity of EtOH. Values designated with a \* indicate a relatively large degree of uncertainty. Reactions of 2MPA also produced MeOH, POL and residual PG.

Substrate	LA	EL	2MPA	MA	2APA	IBA	PA
Main Product	PG	PG	2MPOL	2METOH	PG	IBUOL	POL
% Conv. (1 hr.)	7*	33	3	21	*	15	1
% Conv. (2 hr.)	32	55	15	35	*	24	8
% Conv. (3 hr.)	64	69	30	44	*	32	20
% Conv. (4 hr.)	75	76	30	51	*	39	21
% Conv. (5 hr.)	83	75	38	57	*	46	23
% Conv. (6 hr.)	87	82	48	64	*	52	33
% Prod. (1 hr.)	1*	33	7	12	17	6	4
% Prod. (2 hr.)	21	59	17	24	31	11	8
% Prod. (3 hr.)	46	62	24	31	38	15	9
% Prod. (4 hr.)	60	72	36	36	46	18	12
% Prod. (5 hr.)	60	97	43	41	46	19	14
% Prod. (6 hr.)	67	77*	47	44	51	25	14

**Table 2.2.** Compiled HPLC results of Ru/C-catalyzed aqueous phase hydrogenations. This table only shows the main products of reactions. Hydrogenation of **2APA** also generated **HOAc** and **EL** hydrogenation generated large quantity of **EtOH**. Values designated with a \* indicate a relatively large degree of uncertainty. Reactions of **2MPA** also produced **MeOH**, **POL** and residual **PG**. The **GA** was not analyzed by HPLC.

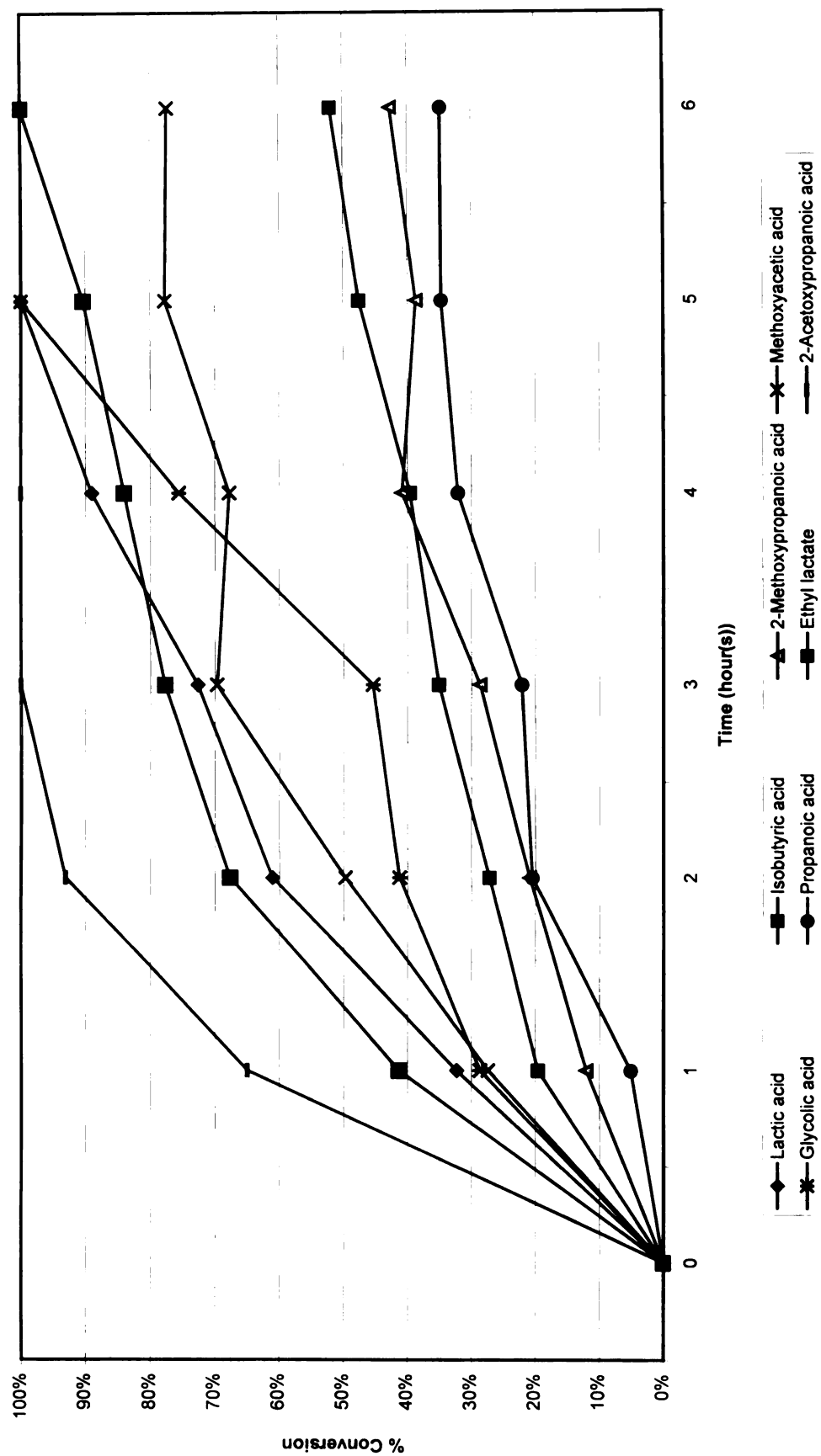
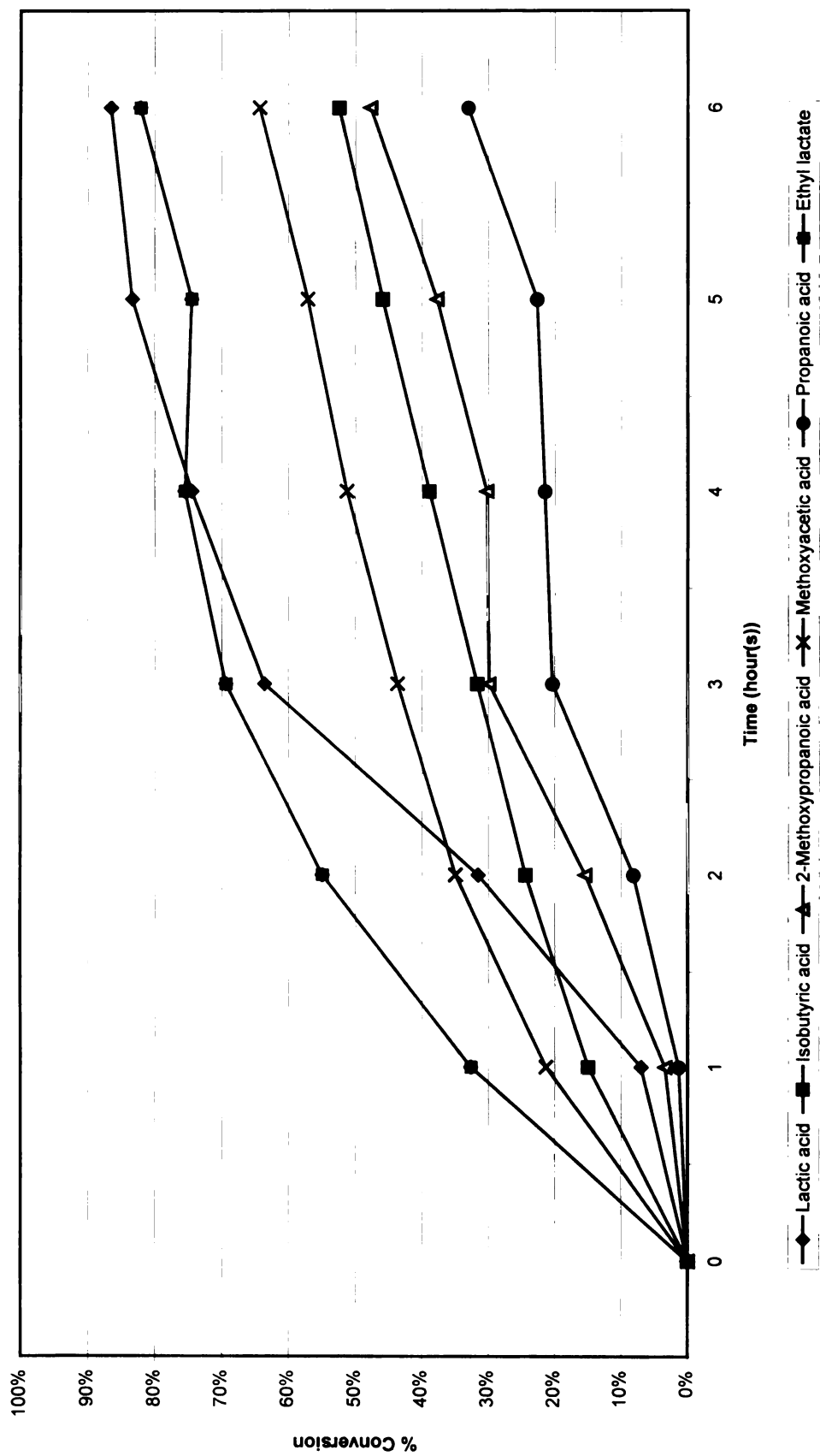
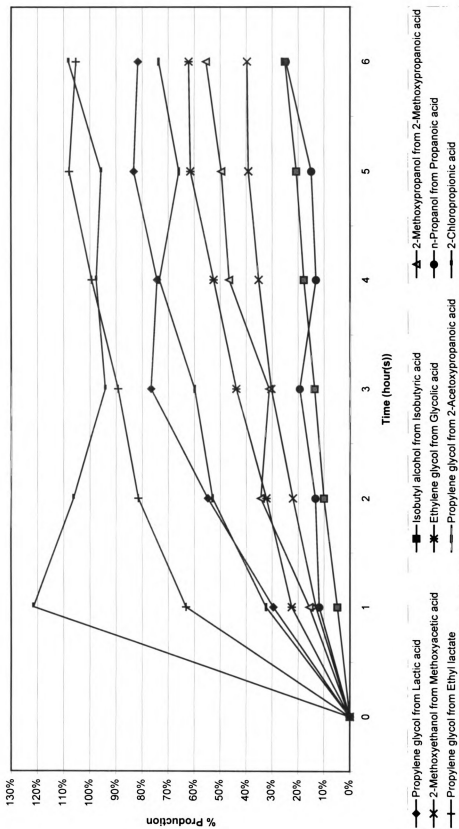


Figure 2.13. Percent conversion of LA, ISOB, 2MPA, MA, GA, PA, EL and 2APA in aqueous-phase hydrogenation reactions at 423 K and 1200 psi, as determined by <sup>1</sup>H NMR.



**Figure 2.14.** Percent conversion of LA, ISOB, 2MPA, MA, PA and EL in aqueous-phase hydrogenation reactions at 423 K and 1200 psi, as determined by HPLC.



**Figure 2.15.** Percent production of PG from L.A, IBUOL from IBA, 2MPOL from 2MPA, 2MEOH from MA, EG from GA, POL from PA, PG from EL, PG from 2APA and 2CPA producing PA in aqueous-phase hydrogenation reactions at 423 K and 1200 psi, as determined by <sup>1</sup>H NMR.

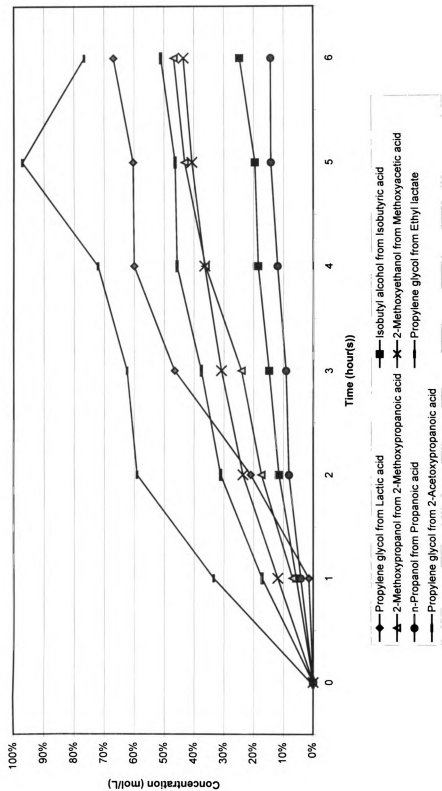


Figure 2.16. Percent production of PG from LA, IBUOL from IBA, 2MPOL from 2MPA, 2MEOH from MA, POL from PA, PG from EL and PG from 2APA in aqueous-phase hydrogenation reactions at 423 K and 1200 psi, as determined by HPLC.

Substrate	Main Product	% Selectivity to Main Product	k'(acid) (1/hr)	k(product) (1/hr)	Relative Rate of Product Formation
2-Chloropropanoic Acid (2CPA)	Propanoic Acid (PA)	100	1.0E1	1.0E1	250
2-Acetoxypopropanoic Acid (2APA)	Propylene Glycol (PG)	74	1.4	9.9E-1	25
Ethyl Lactate (EL)	Propylene Glycol (PG)	100	4.6E-1	4.6E-1	12
Lactic Acid (LA)	Propylene Glycol (PG)	82	5.4E-1	4.4E-1	11
Glycolic Acid (GA)	Ethylene Glycol (GA)	62	3.1E-1	1.9E-1	5
Methoxyacetic Acid (MA)	2-Methoxy Ethanol	53	2.6E-1	1.4E-1	4
Isobutyric Acid (IBA)	Isobutyl Alcohol (IBUOL)	48	1.2E-1	5.6E-2	1
2-Methoxypropanoic Acid (2MPA)	2-Methoxypropanol (2MPA)	100*	9.6E-2	9.6E-2	2
Propanoic Acid (PA)	n-Propanol (POL)	51	7.8E-2	4.0E-2	1

**Table 2.3.** The calculated  $^1\text{H}$  NMR results for the aqueous-phase Ru/-catalyzed hydrogenation of organic acids and esters at 423 K and 1200 psi. The calculations are described in the Analytical Methods of the Experimental section. The relative rates of product formation are the ratios of k(product).

## Conclusion

The effects of vicinal substituents on the aqueous-phase hydrogenations of lactic acid and ester derivatives were studied. Electron-withdrawing and/or hydrogen bonding substituent are thought to activate the substrate upon hydrogenation. Based on the results of this study, it is clear that hydrogen bonding has a profound effect on the rate of hydrogenation, but the electron-withdrawing ability of a vicinal functional group of an organic acid also seem to have a significant influence on the selectivity to the corresponding alcohol (see results in Table 2.3). As observed for lactic acid, glycolic acid and ethyl lactate, their reactivity and selectivity must be due to the vicinal hydroxy functional group. One can theorize that this behavior may be because the fixed geometry of these compounds, due H-bonding, facilitates the adsorption to the catalyst surface.

Substrates bearing a methoxy functional group vicinal to the carboxy functionality have demonstrated lower activity than their H-bonding analogues. To answer the initial question of H-bonding versus electron-withdrawing, it is clear that the non-hydrogen-bonding but electron-withdrawing vicinal methoxy substituents did not accelerate the reaction rate as much as the -OH groups do. However, these methoxy-substituted acids still showed good to excellent selectivities to the corresponding alcohol products (see Table 2.3). In addition, the appreciably lower reactivity of 2-methoxypropanoic acid compared methoxyacetic acid is suggestive that effects other than H-bonding or electron-withdrawal may effect reactivity toward hydrogenation.

Steric hindrance has been an important issue in organic chemistry and it should also be considered in catalytic hydrogenations. For example, the methoxy group of

**2MPA** can be thought of simply as a sterically bulky group near the carboxy functionality. Having both methoxy and methyl groups at the C2 position, **2MPA** might be expected to react slower than **MA** which lacks a C2 methyl group. Indeed, **MA** reacts at three-fold greater rate as compared to **2MPA**.

The steric argument is weakened, however, by the case of **IBA** that reacts twice as fast as **PA** or even **2MPA**. The **IBA** has 2 methyl groups at the C2 position, it lacks electron-withdrawing and vicinal H-bonding functional group, yet the rate of conversion to **IBUOL** is much faster than that of **PA**. This phenomenon needs to be studied and pyvalic acid should be the next candidate for hydrogenation to see how the addition of one more methyl group affects this reaction. It is conceivable that there is yet an unknown mechanism that may take place at the catalyst surface that could explain such discrepancy. The relative rate of alcohol product formation is only marginally greater for **IBA** hydrogenation. Taking the uncertainty values into account, **IBA** shows virtually identical product formation rate with **PA**.

Based on both HPLC and <sup>1</sup>HNMR methods, it is clear that the increasing order of reactivity with respect to hydrogenation at the carboxyl functional group to the corresponding alcohol is as follows: **PA < 2MPA < IBA < MA < GA < LA < EL**. The rate of conversion of substrates, however, showed a somewhat different order: **PA < IBA < 2MPA < MA < APA < LA < EL**.

The conversion of **2CPA** to **PA** cannot be ranked in the same category with the rest of the compounds listed because it did not undergo hydrogenation at the carboxyl functional group. Furthermore, **2APA** hydrogenation is also inconclusive as competing hydrolysis and hydrogenation take place.

The percent production of main products in the results table (Table 2.3) was not entirely conclusive for a few compounds. The analysis for the hydrogenation of ethyl lactate, for example, automatically incurred an error by having to integrate a **PG** multiplet near the internal standard. Integration across long base line substantially added to the integral value of the peaks. The **2CPA** also presented a challenge as an appreciable amount of chromium metal had been dissolved from the inside of the reactor. However, Teflon coating of the reactor may completely eliminate leaching, thus hydrogenation may progress and the formation of n-propanol can be expected. HPLC was not useful for **2CPA** because negative peaks in the chromatogram could not be integrated into meaningful counts to calculate the concentrations. In addition, the acidic HPLC column quickly hydrolyzed **2APA** it showed up at the **LA** spot in the chromatogram and had very similar response factor. Therefore, percent production of **PG** from **2APA** had to be calculated from the **LA** that was the hydrolysis product of **2APA**.

# Experimental

## General Outline for the Hydrogenation Reactions

Except for 2-methoxy propanoic acid all compounds were purchased from Aldrich and used as is. The hydrogenation reactions of 10 weight percent aqueous solutions of substrates were run in high pressure Model 4560 Parr Mini Reactor (Image 1) with one weight percent activated carbon-supported ruthenium catalyst under 1200 psi H<sub>2</sub> pressure and at 423, 373 or 348 K. As described in the previous section, the type of substrate used in a given hydrogenation reaction determined the choice of temperature. For example, a highly acidic substrate, such as 2-chloropropanoic acid, was reacted at 373 K to minimize damage to the inside metal surface of the reactor. Prior to each hydrogenation experiment, about a 1-2 mL sample was saved from the 10 weight percent aqueous pre-reaction mixture and designated as a “prerun” sample. The prerun sample was used to determine the initial concentration of the reaction mixture by <sup>1</sup>H NMR or HPLC before it was introduced in the reactor. <sup>1</sup>H NMR and HPLC concentration of a prerun sample was recalculated, using simple dilution calculation ( $M_1 \times V_1 = M_2 \times V_2$  where  $M$  = concentration of compound,  $V$  = volume of compound), to obtain the actual concentration of the stock solution. Ideally, the absolute concentration and the <sup>1</sup>H NMR or HPLC-determined concentration of the stock solution ought to be identical.

## **Procedure for Handling the Reactor**

Before the hydrogenation reaction of a substrate, the internal parts of the reactor were scrupulously cleaned and dried to avoid side reactions resulting from residual compounds from previous experiments. The Ru/C catalyst (one weight percent relative to the reaction mixture) was placed in the reaction chamber. After the reactor was assembled, it was flushed three times with H<sub>2</sub> or He gas at approximately 200 psi pressure to remove any impurities from the reactor chamber and valves or any parts that would otherwise be in contact with the reaction mixture. It is important to note that the flushing must be done at a slow rate to avoid blowing the catalyst out the valves of the reactor. After reducing the catalyst at 423 K and 300 psi pressure over a three hour period, the reactor was allowed to cool down to RT and depressurized to 0 psi. The reactor was heated up again to the desired temperature (348, 373 or 423 K). The reaction mixture was poured into a charge vessel previously cleaned and flushed three times with H<sub>2</sub> gas at 200 psi. The charge vessel containing the reaction mixture was flushed twice with H<sub>2</sub> at approximately 200 psi to remove all air. The charge vessel was then secured to the reactor and charged up to 250 psi. The control valve between the charge vessel and the reactor was opened to allow the transfer of aqueous substrate into the reactor at this pressure. The pressure of the connected charge vessel and reactor was increased up to 300 psi. The control valve between the reactor and the charge vessel was then turned off and the charge vessel was vented before it was disassembled from the reactor. The digital monitor interfaced with the reactor indicated the accurate pressure and temperature inside the reactor. A metal-jacketed condenser was secured to the

reactor through the valve used for the charging the vessel. The condenser was quickly flushed with N<sub>2</sub> gas and used for collecting 1-2 mL of sample from the reactor under pressure. This sample was designated as “prerunpot” and its concentration should be very close to the initial (prerun) concentration of the stock solution. Prerunpot sample must be collected as quickly as possible to minimize product formation. Finally, the reactor pressure was raised to 1200 psi and the reaction was “officially” started. Approximately 1-2 mL of sample was collected periodically using the condenser (normally samples were collected each hour). After each sample collection, the condenser was flushed with N<sub>2</sub> gas for a few minutes and the pressure of the reactor was readjusted to 1200 psi. The collected samples were filtered by Millex sterile syringe driven filter units and were labeled accordingly. The inside pressure of the reactor was recorded as the reaction proceeded. When the hydrogenation reaction was ended, the reactor was slowly cooled down by removing its heating mantle and adjusting the temperature to RT. The reactor was slowly vented from the gas and carefully opened and washed for later use.

There are important considerations in operating a high pressure reactor as it poses potential danger to its operator and surroundings. As a precaution, after charging the reactor, the main control valve and the main gas tank should be turned off. When introducing high pressure gas through a gas line to the reactor, gas must pass through several control valves which should be opened one at a time. The gas tank and the reactor should be checked periodically for possible leaking and the metal stirring impeller must be properly installed to avoid damage to the reactor. The Teflon seals in the reactor head should be periodically checked and replaced if needed. Finally, the reactor should

be periodically cleaned with 20 % aqueous acetone solution under pressure and higher than room temperature to remove all contaminants.

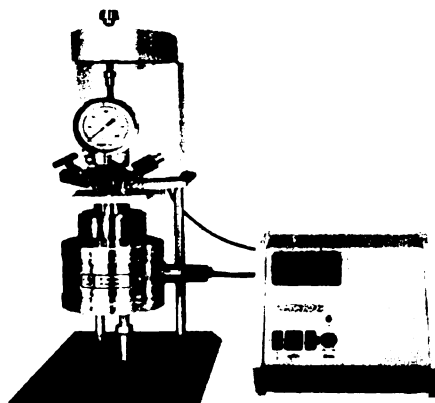


**Image 1.** The Series 4560 Parr Mini Reactor interfaced with a control panel that monitors both pressure and temperature.

## Analytical methods

HPLC and  $^1\text{H}$  NMR were used to determine the absolute concentrations of each sample. Each  $^1\text{H}$  NMR sample was prepared from 10  $\mu\text{L}$  of dioxane or t-butyl alcohol internal standard and 20  $\mu\text{L}$  of a reaction sample and diluted to one mL by  $\text{D}_2\text{O}$ . The stock solutions of the internal standards were prepared such that their 10  $\mu\text{L}$  aliquots diluted to one mL would make exactly 0.020 M concentration. After identifying the composition of each reaction mixture by  $^1\text{H}$  NMR, the well-defined resonances, preferably with lowest degree of splitting, were used to calculate the concentration of

each sample. It was also important to use an internal standard that does not overlap with any reactant and product peaks and has only a singlet. In general one should integrate a set of the lowest number of peaks of a given compound to avoid long base-line integration and thus minimize error in the concentration calculation. In fact, when possible, singlets should be used for concentration determination. To determine the concentrations of the reactants and products in a reaction mixture, all peaks were integrated and their values were reset, based on the integral value of the internal standard (t-butyl alcohol set at 900; dioxane set at 800). The concentration of the standard was normalized to 100 hydrogen atoms, and this value was inversely related to the normalized integration value of a given product or reactant to obtain its <sup>1</sup>H NMR concentration. For example, the integration value of a non-overlapping doublet belonging to the methyl group of lactic acid is found at 1.41 ppm and can be used to calculate the lactic acid concentration with respect to the reaction time by the equation below:

$$\frac{\frac{0.020 \text{ M t-BuOH}}{900 \text{ t-BuOH singlet}}}{9} = \frac{\frac{x \text{ M of LA}}{300 \text{ LA doublet}}}{3} \quad x = 0.020 \text{ M}$$

The resulting <sup>1</sup>H NMR concentration was recalculated by dilution method to obtain the actual concentration of the reactant or product in the reaction mixture.

The HPLC samples were prepared from 100 μL of solutions of reaction mixtures or stock solutions of standards diluted to 1.00 mL using HPLC grade water. The stock solutions were prepared as approximately one weight percent HPLC grade aqueous

solutions (0.1g of substrate/10 g of solution). These standards were all products and reactants that were identified by <sup>1</sup>HNMR in the various hydrogenation reactions. Each standard having different HPLC response factor gave different number of counts (for standard concentration and response factor see Appendix 10). The absolute concentration of a standard was divided by the corresponding number of peak area (counts) giving a conversion factor that in turn was multiplied by the peak area (counts) of the corresponding compound from a reaction sample, as shown below:

$$\frac{C(\text{standard})_i}{(\text{PA of standard})_i} = (\text{CF of standard})_i = \frac{C_i}{(\text{PA})_i}$$

**C<sub>i</sub> = Concentration of Species i**

**C(standard)<sub>i</sub> = Concentration of standard<sub>i</sub>**

**CF = Conversion Factor**

**PA = Peak Area**

Ethanol was used as the internal standard and was prepared the same way as previously described for reaction standards. Ethanol samples were inserted in the HPLC tray between sets of reaction samples to monitor the concentration variation between measurements. The peak areas of the ethanol internal standard showed negligible standard deviation (see previous section).

The percent conversion of the substrate was calculated from the concentration of the substrate as described below:

$$\text{Conversion \%} = \left( 1 - \frac{C(\text{substrate})_t}{C(\text{substrate})_0} \right) \times 100$$

The percent production of the product derived from the starting material was calculated as described below:

$$\text{Product \%} = \left( \frac{\text{C(product)}_t}{\text{C(substrate)}_o} \right) \times 100$$

The selectivity for a reaction product was calculated from the concentrations of the starting material and the concentration of the reaction product as:

$$\text{Selectivity \%} = \left( \frac{\text{C(product)}_t}{\text{C(substrate)}_o - \text{C(substrate)}_t} \right) \times 100 \quad \text{only if } \text{C(product)}_o = 0$$

The concentration profiles of the reactions were plotted as concentration of reactant or product versus time. The data points were fitted with an exponential decay curve, using the Kaleidograph program. This program is designed to calculate the rate constant of a reaction, thus the rate constant ( $k'_{(\text{substrate})}$ ) was obtained. The  $k'_{(\text{substrate})}$  value was used to calculate  $k_{(\text{product})}$  of a corresponding product of a reaction as:

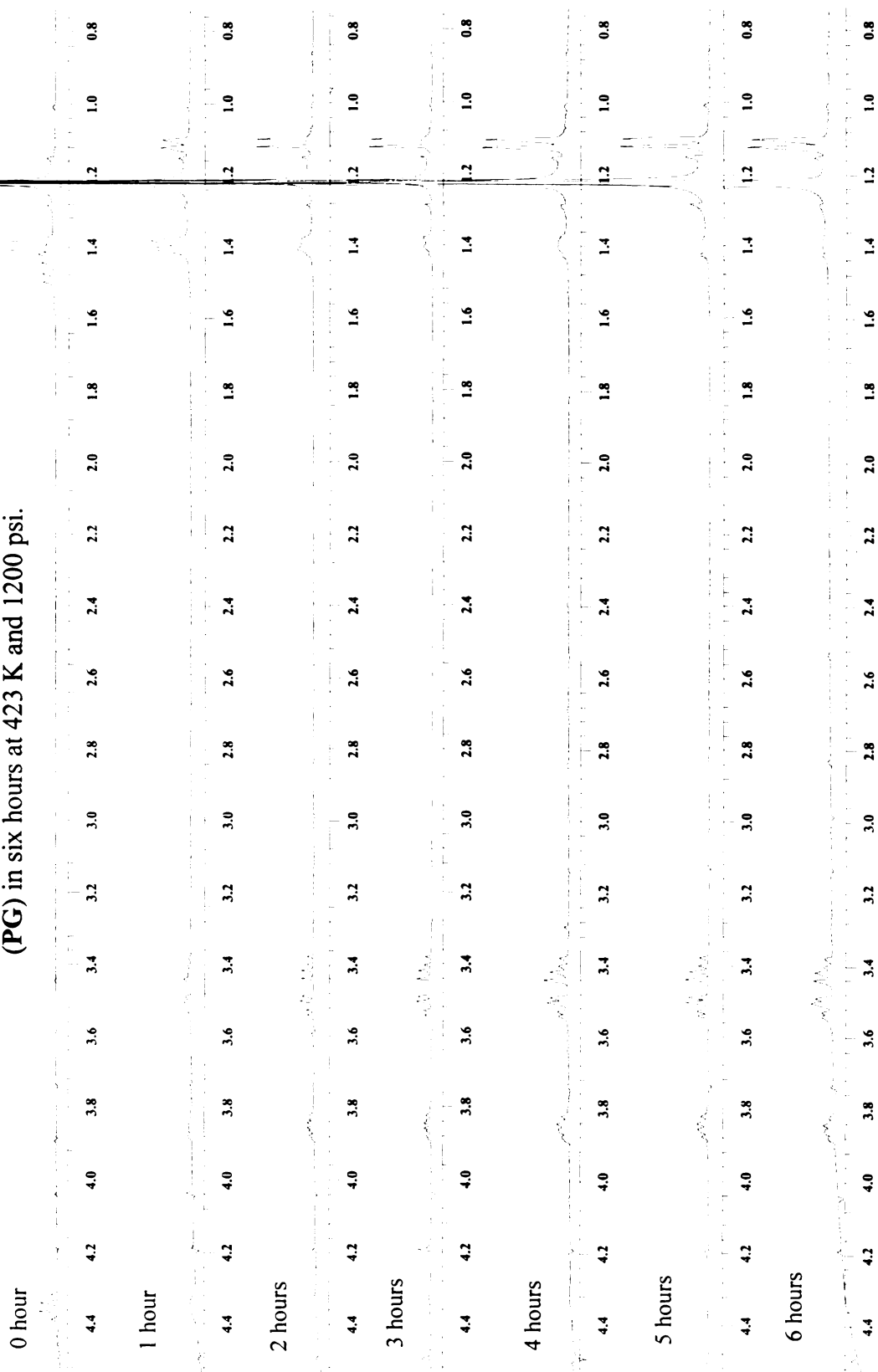
$$k_{(\text{product})} = k'_{(\text{substrate})} \times (\text{selectivity})$$

Hence the calculated  $k_{(\text{product})}$  allowed the determination of relative rates of the reactions.

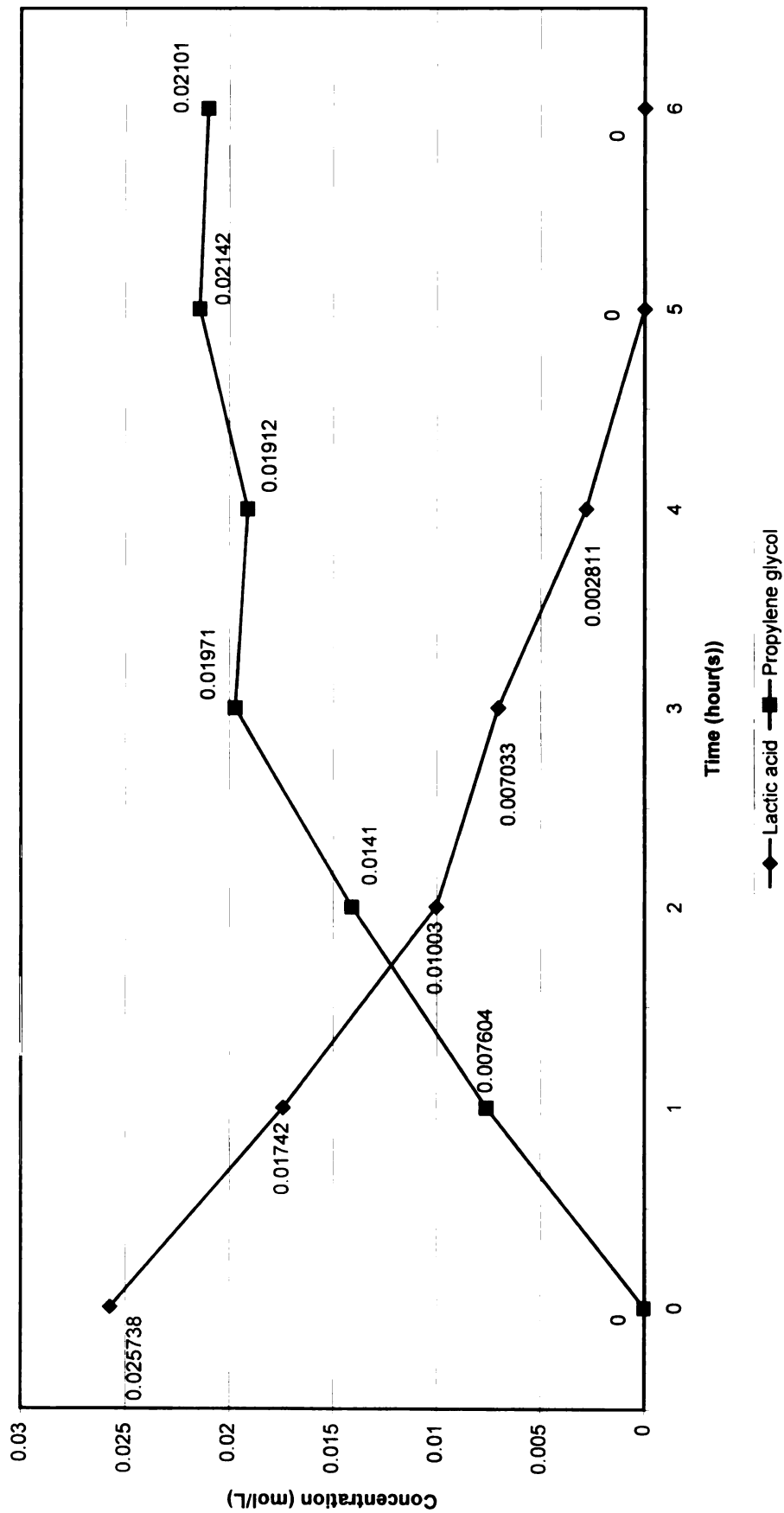
## **Preparation of 2-methoxypropionic acid**

The preparation of 2-methoxypropanoic acid (**2MPA**) was carried out as described in the literature, with a couple of minor modifications.<sup>66</sup> These modifications involved washing and drying NaH in excess of 100% over the stoichiometric amount of the starting material (ethyl lactate) by hexanes and dry THF in the open. Approximately 1.1 equivalent of pure and dry NaH was collected and used for the deprotonation of ethyl lactate in dry THF. Although the literature procedure described the use of a continuous extractor for final extraction, ordinary extraction technique was applied 30 times. The yield was slightly above the literature value.

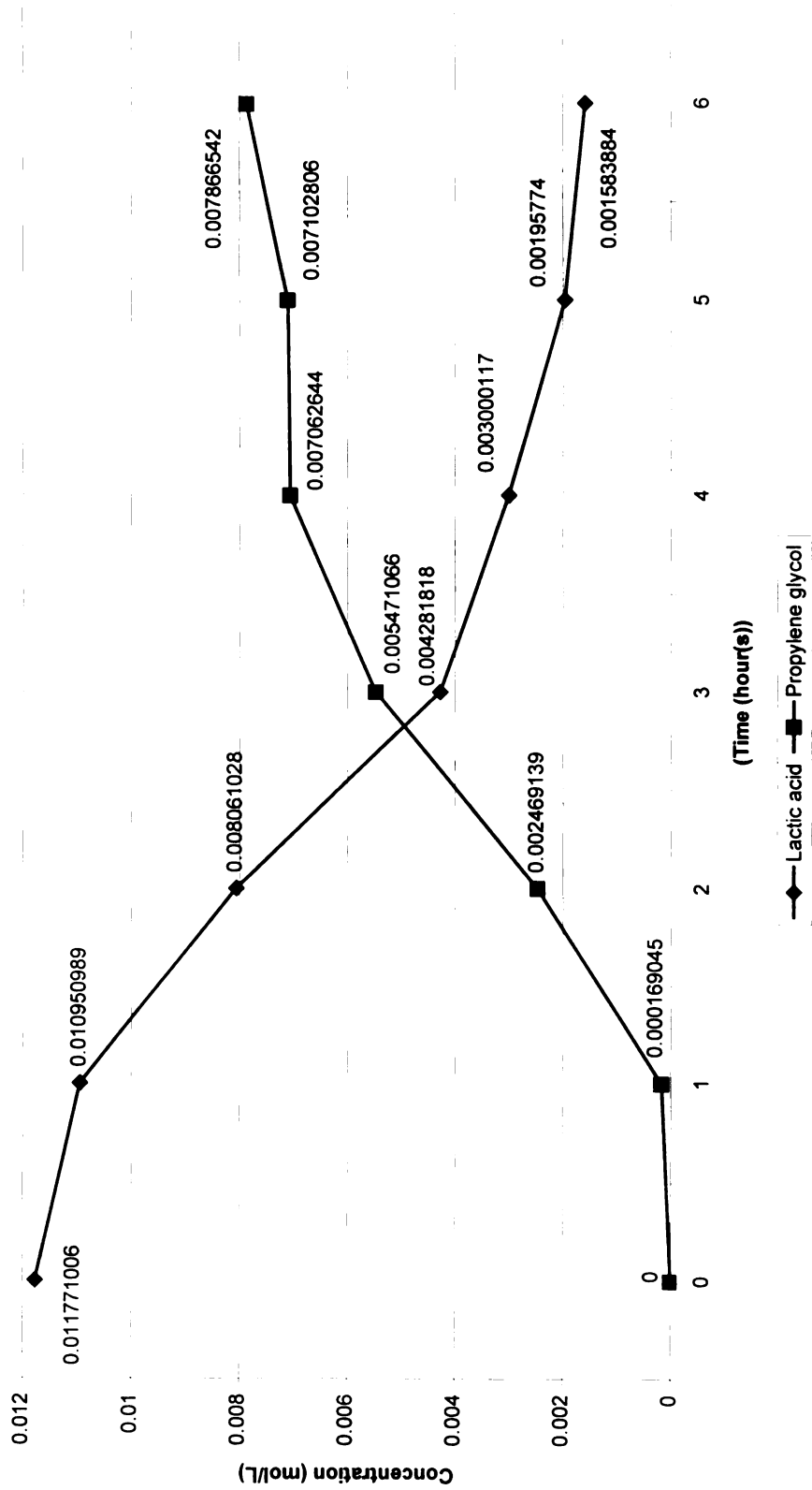
**Appendix 1.1.**  $^1\text{H}$  NMR spectra of Ru/C-catalyzed aqueous phase hydrogenation of lactic acid (LA) to propylene glycol (PG) in six hours at 423 K and 1200 psi.



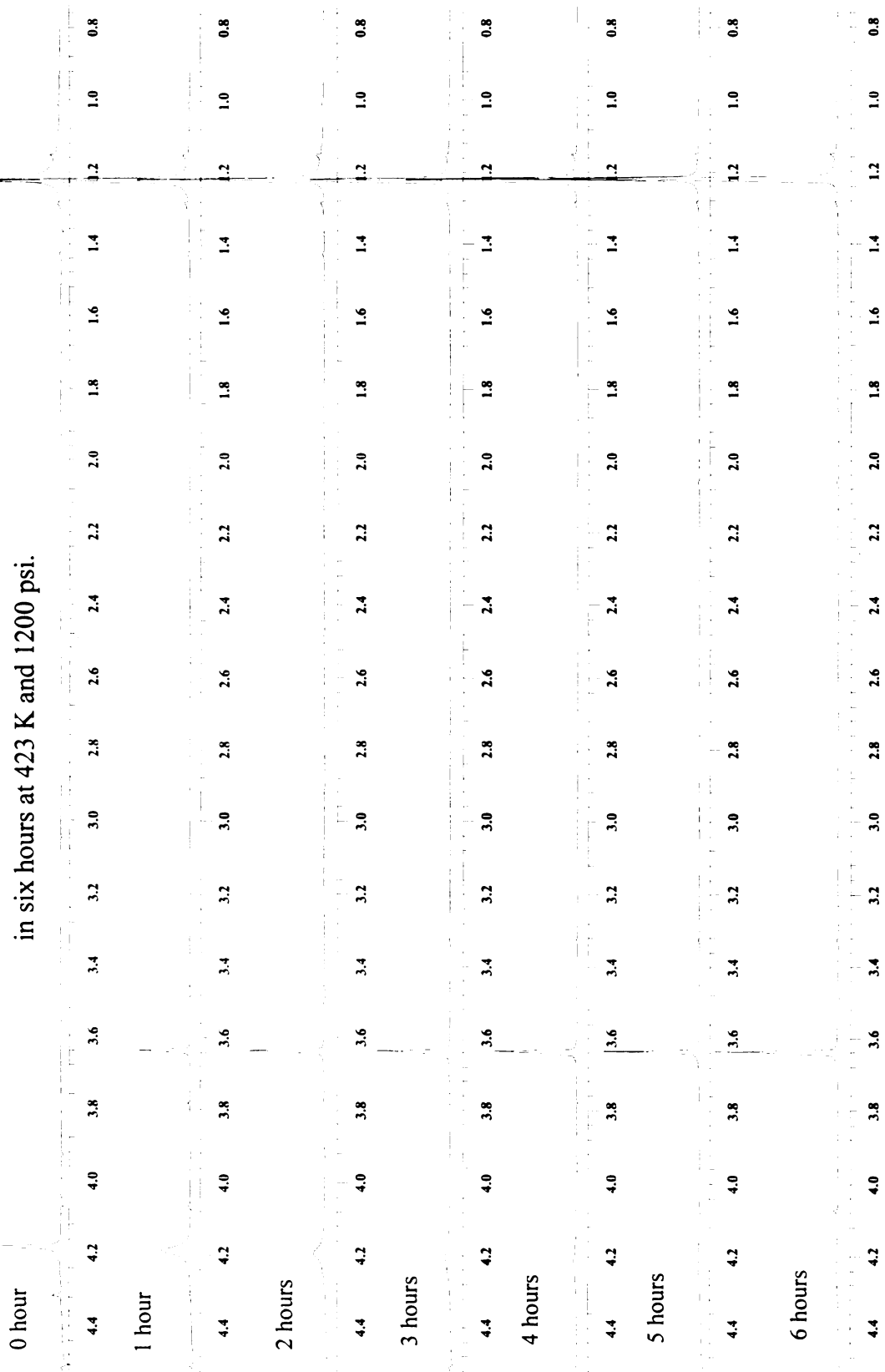
**Appendix 1.2.** Concentration profile of the hydrogenation reaction of lactic acid at 423 K and 1200 psi determined by proton NMR



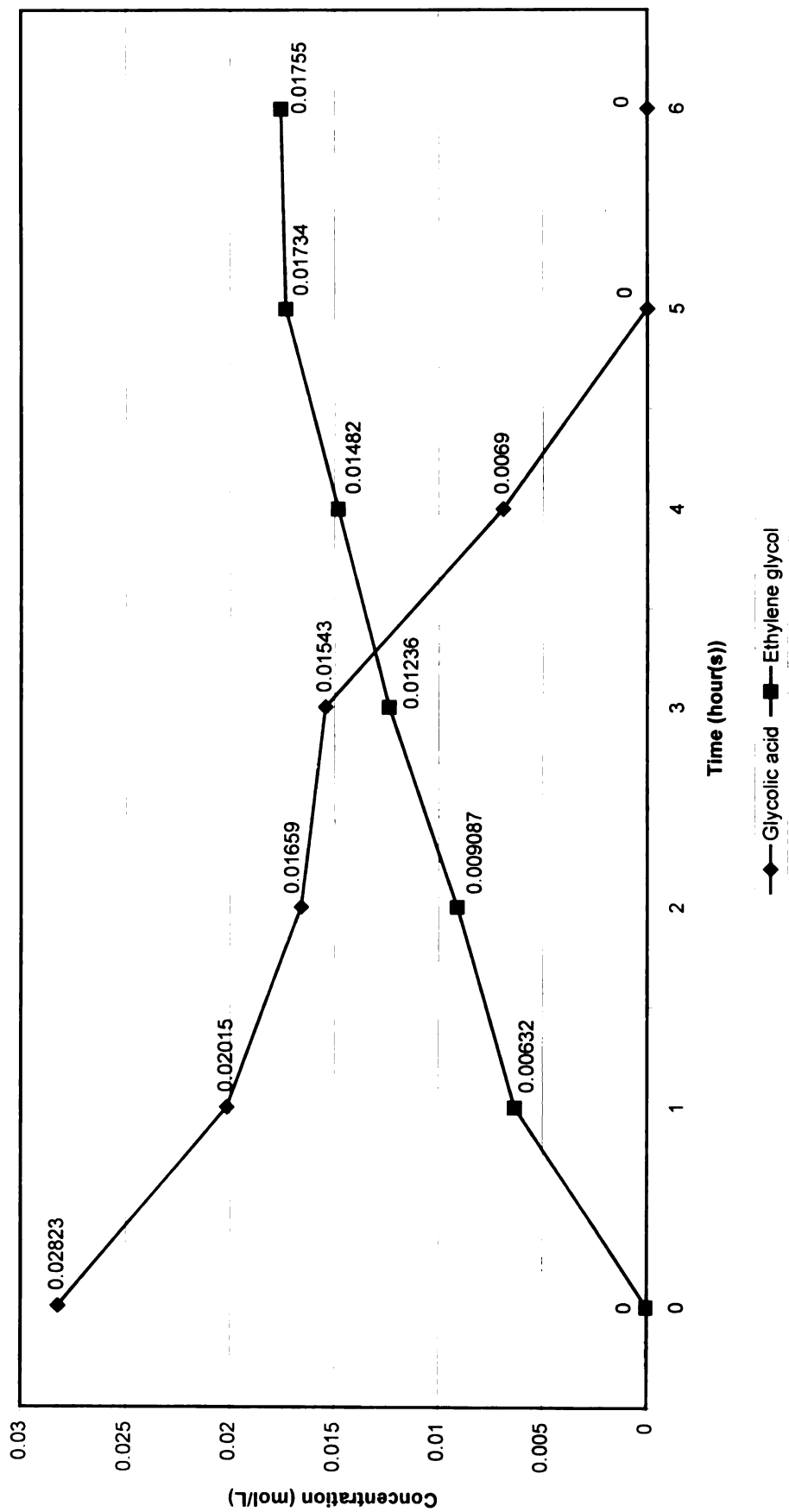
**Appendix 1.3.** Concentration profile of the hydrogenation reaction of Lactic Acid at 423 K and 1200 psi determined by HPLC



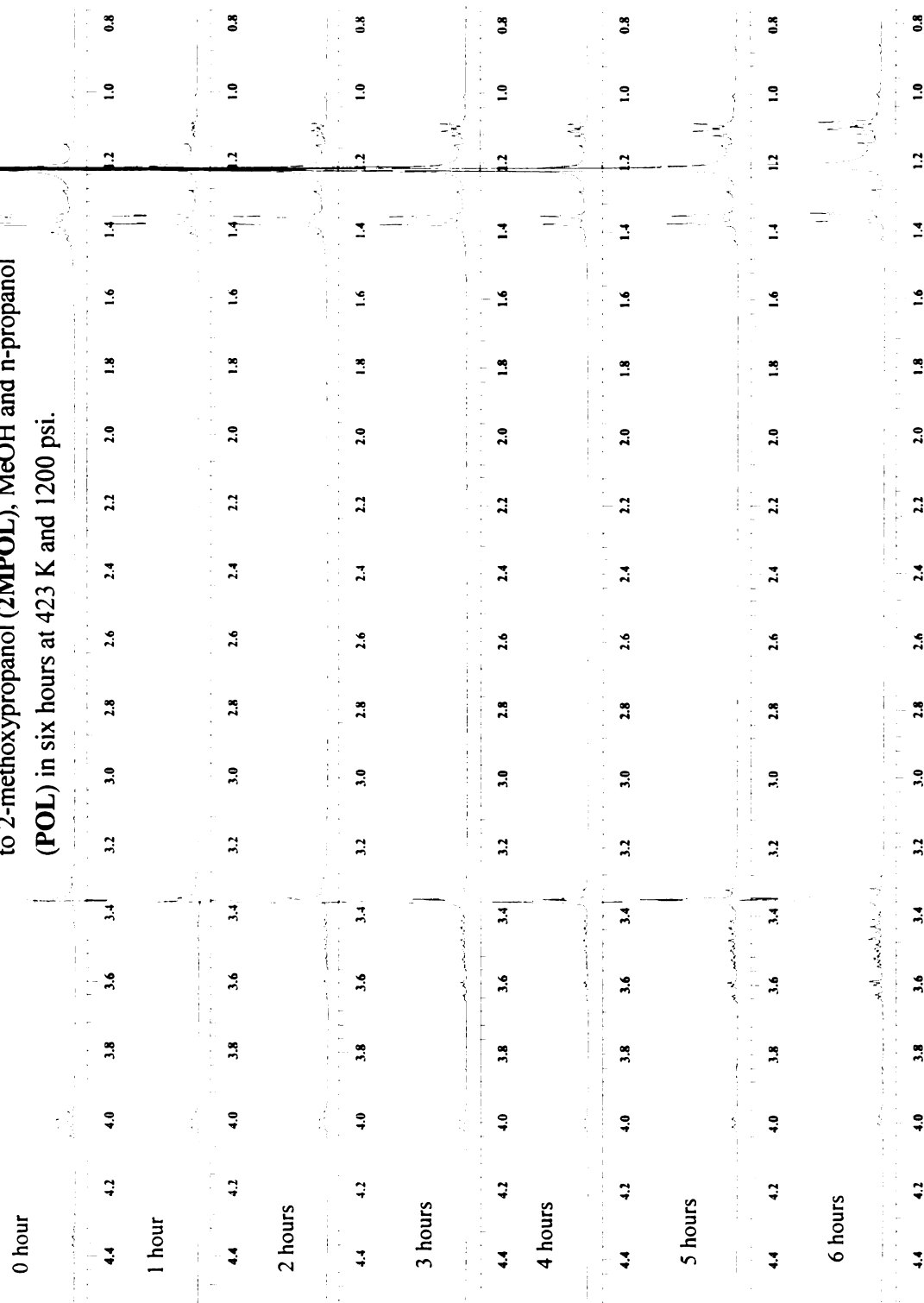
**Appendix 2.1. <sup>1</sup>H NMR spectra of Ru/C-catalyzed aqueous phase hydrogenation of glycolic acid (GA) to ethylene glycol (EG) in six hours at 423 K and 1200 psi.**



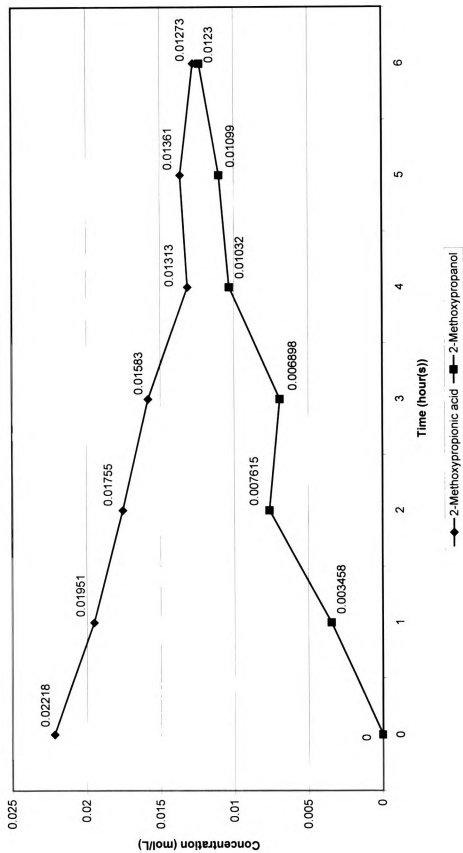
**Appendix 2.2.** Concentration profile of the hydrogenation reaction of glycolic acid at 423 K and 1200 psi determined by proton NMR



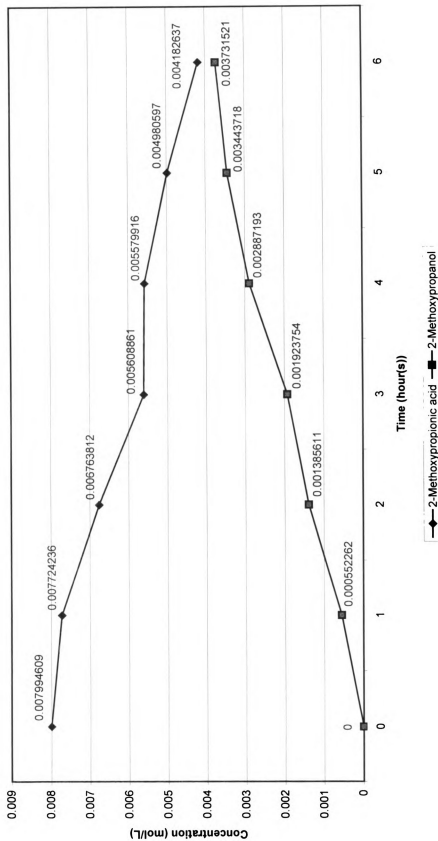
**Appendix 3.1.  $^1\text{H}$  NMR spectra of Ru/C-catalyzed aqueous phase hydrogenation of 2-methoxypropanoic acid (2MPA) to 2-methoxypropanol (2MPOL), MeOH and n-propanol (POL) in six hours at 423 K and 1200 psi.**



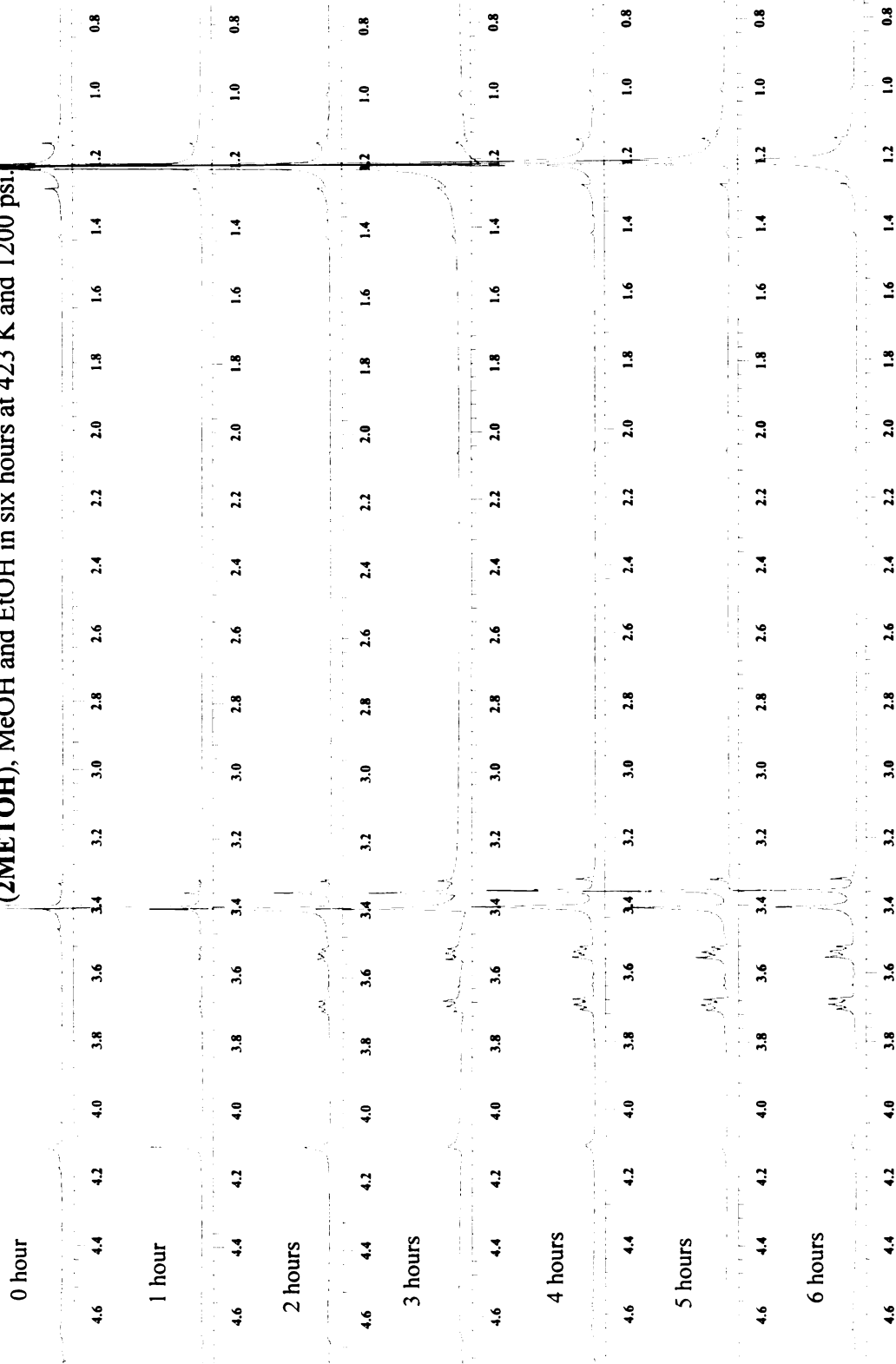
**Appendix 3.2.** Concentration profile of the hydrogenation reaction of 2-methoxypropanoic acid at 423 K and 1200 psi by proton NMR



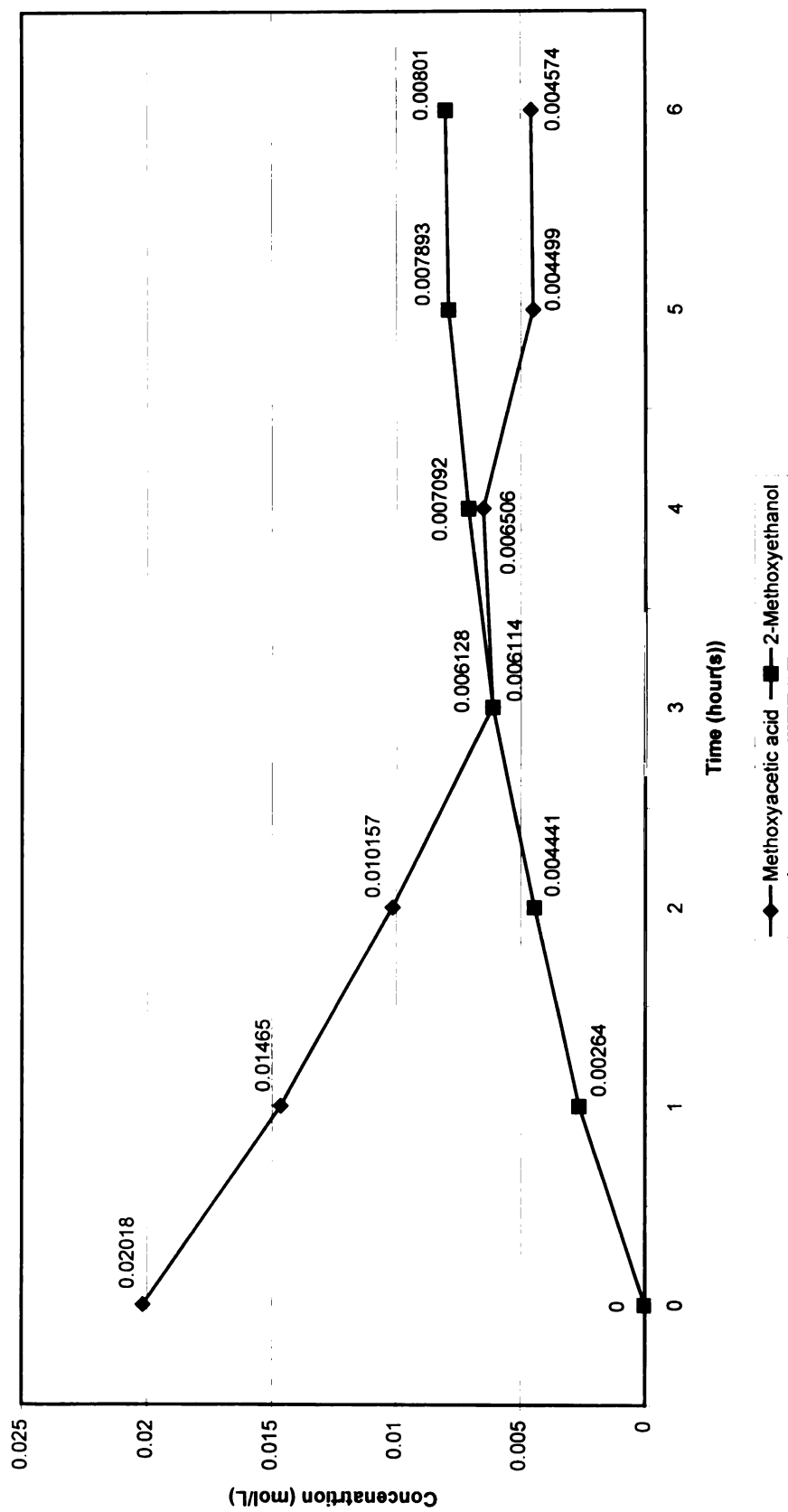
**Appendix 3.3.** Concentration profile of the hydrogenation reaction of 2-methoxypropanoic acid at 423 K and 1200 psi determined by HPLC



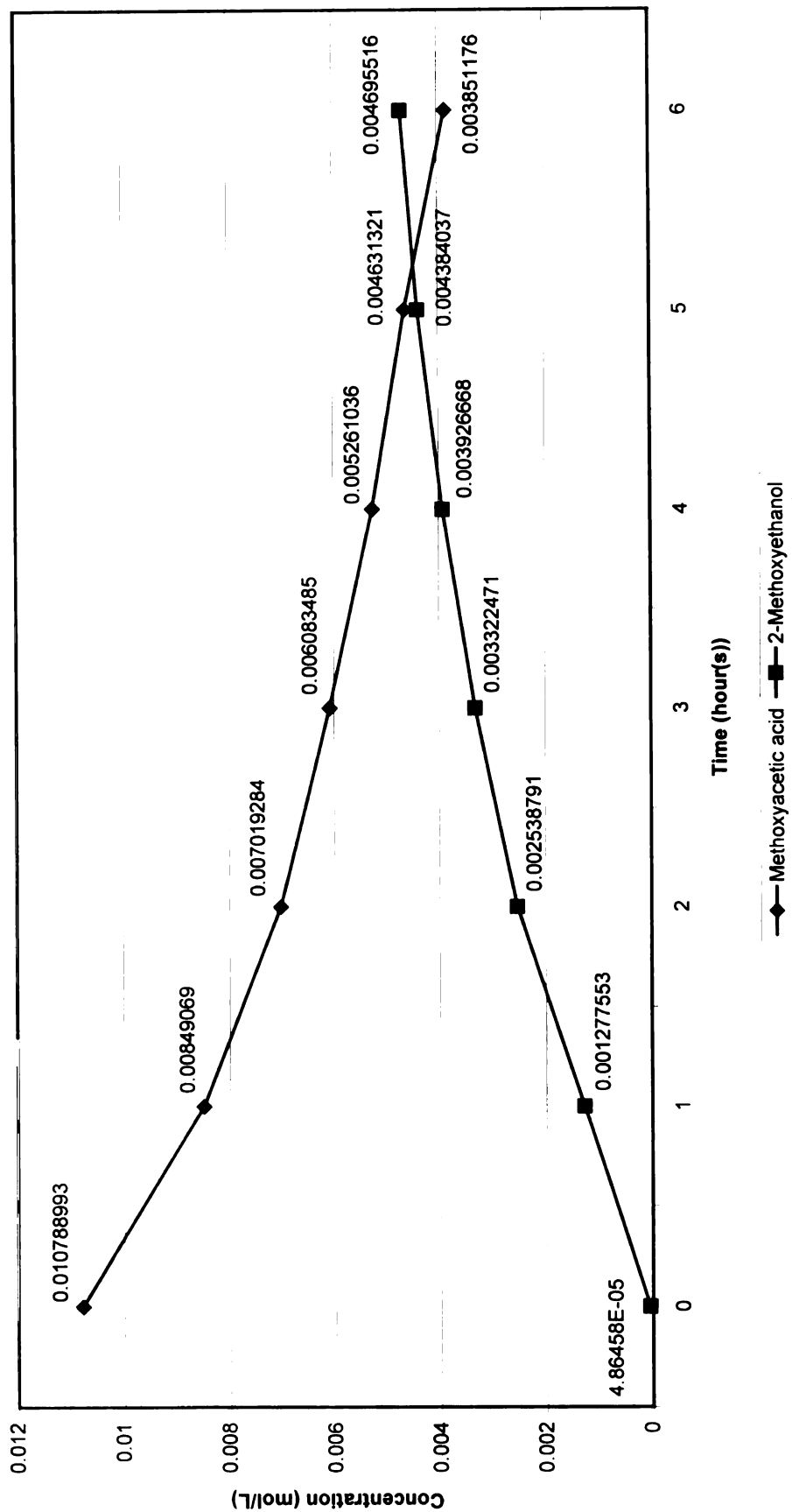
**Appendix 4.1. <sup>1</sup>H NMR spectra of Ru/C-catalyzed aqueous phase hydrogenation of methoxyacetic acid (MA) to 2-methoxyethanol (2METOH), MeOH and EtOH in six hours at 423 K and 1200 psi.**



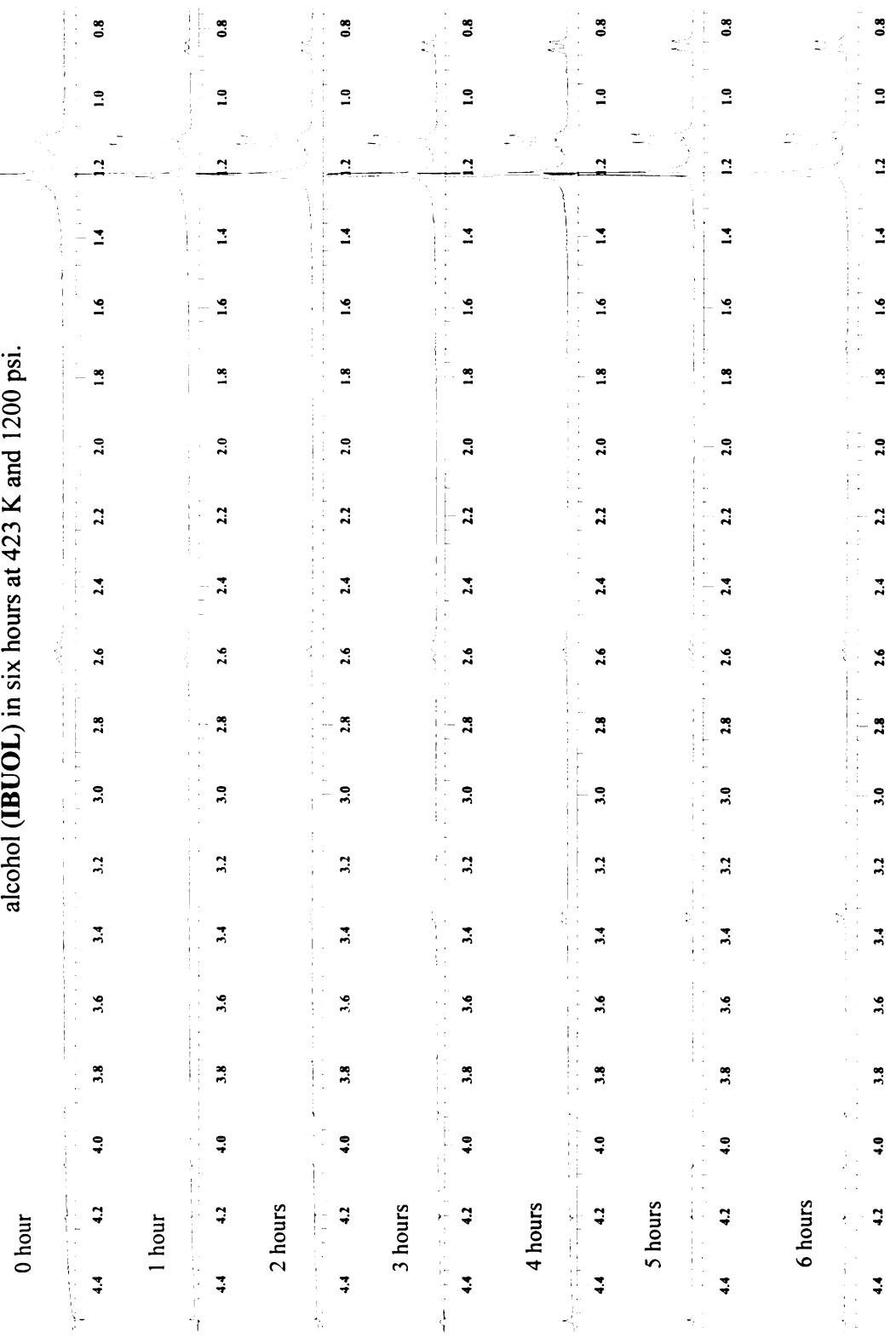
**Appendix 4.2.** Concentration profile of the hydrogenation reaction of methoxyacetic acid at 423 K and 1200 psi determined by proton NMR



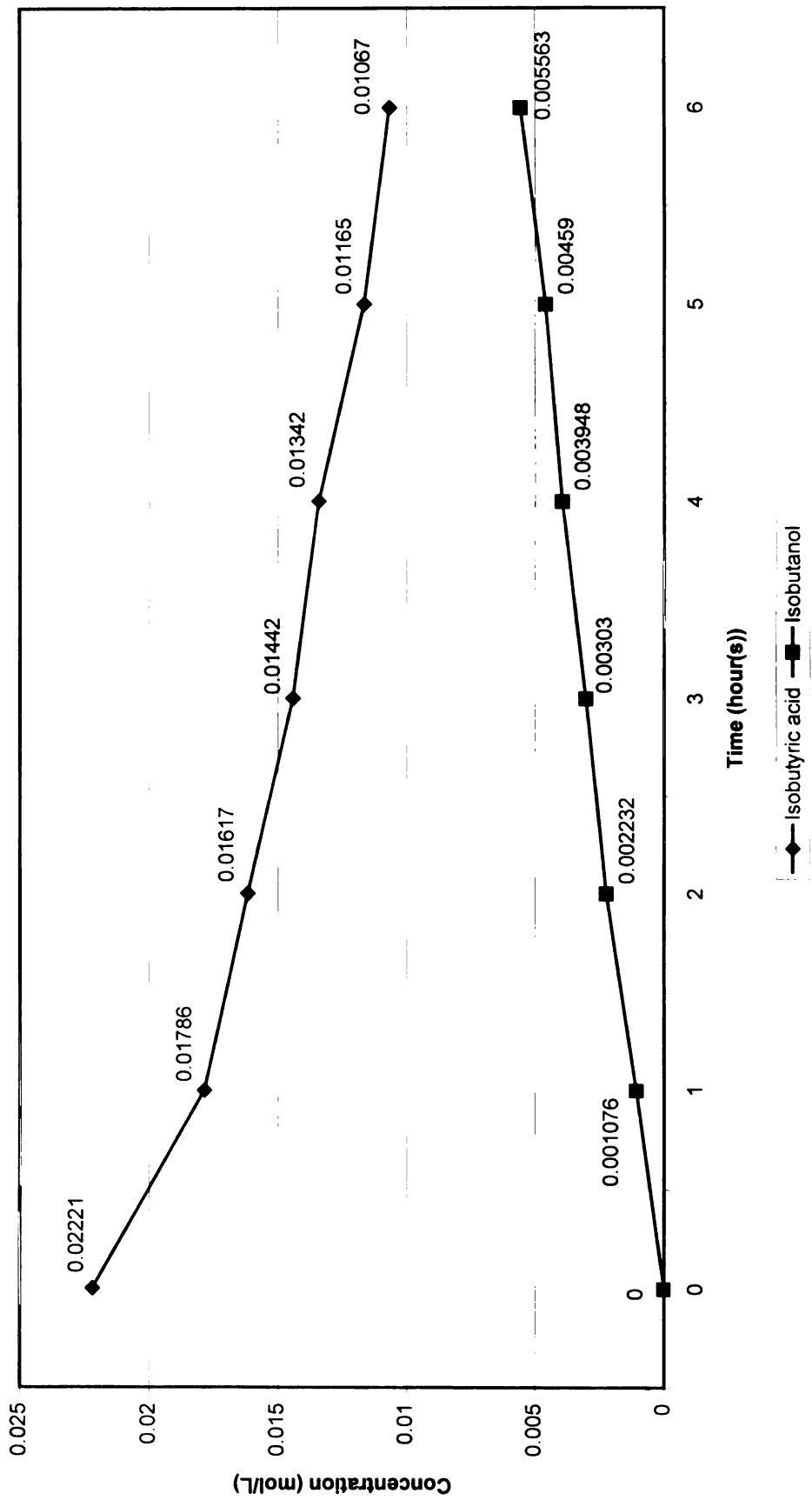
**Appendix 4.3.** Concentration profile of the hydrogenation reaction of methoxyacetic acid at 423 K and 1200 psi determined by HPLC



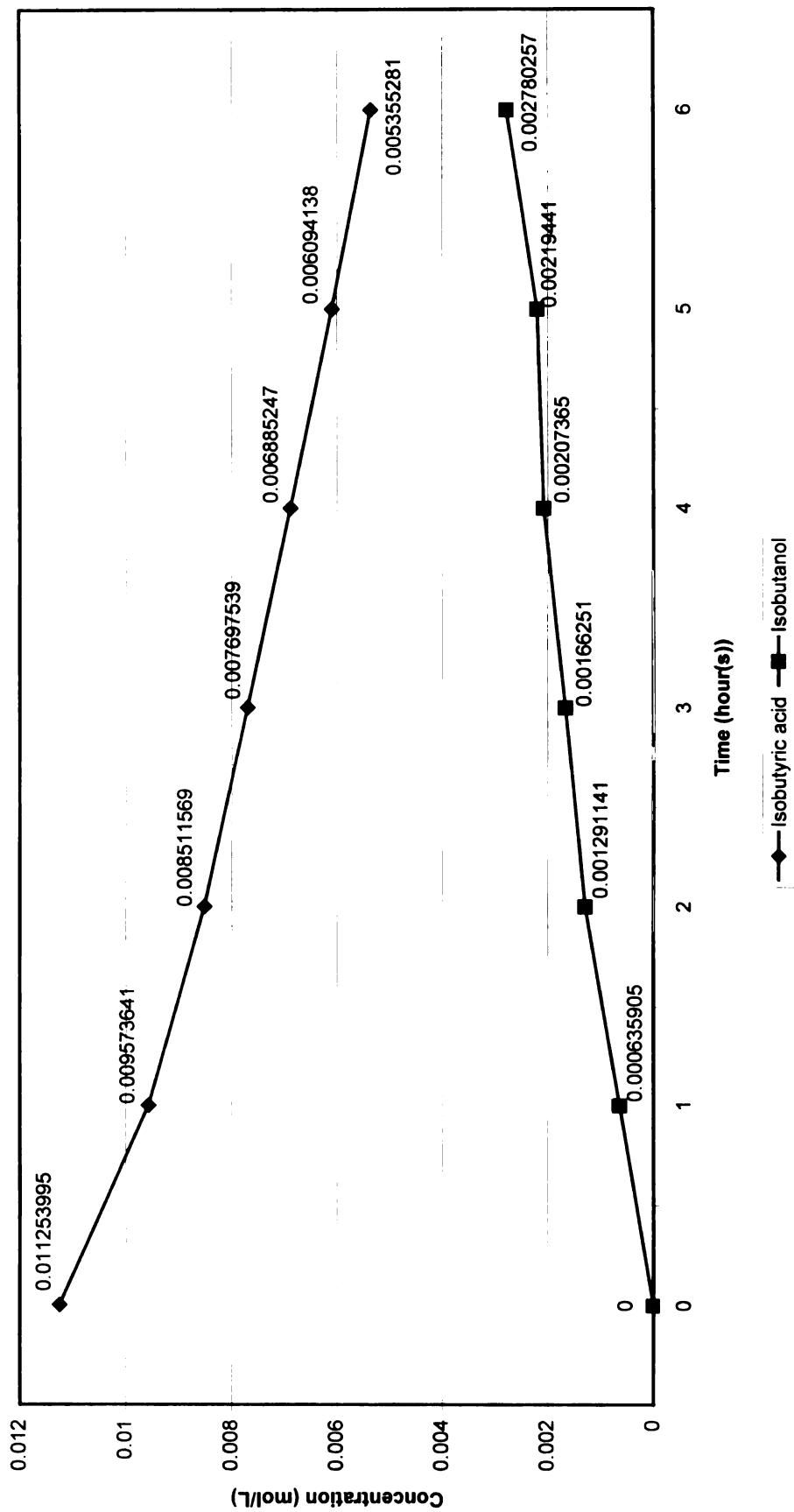
**Appendix 5.1. <sup>1</sup>H NMR spectra of Ru/C-catalyzed aqueous phase hydrogenation of isobutyric acid (IBA) to isobutyl alcohol (IBUOL) in six hours at 423 K and 1200 psi.**



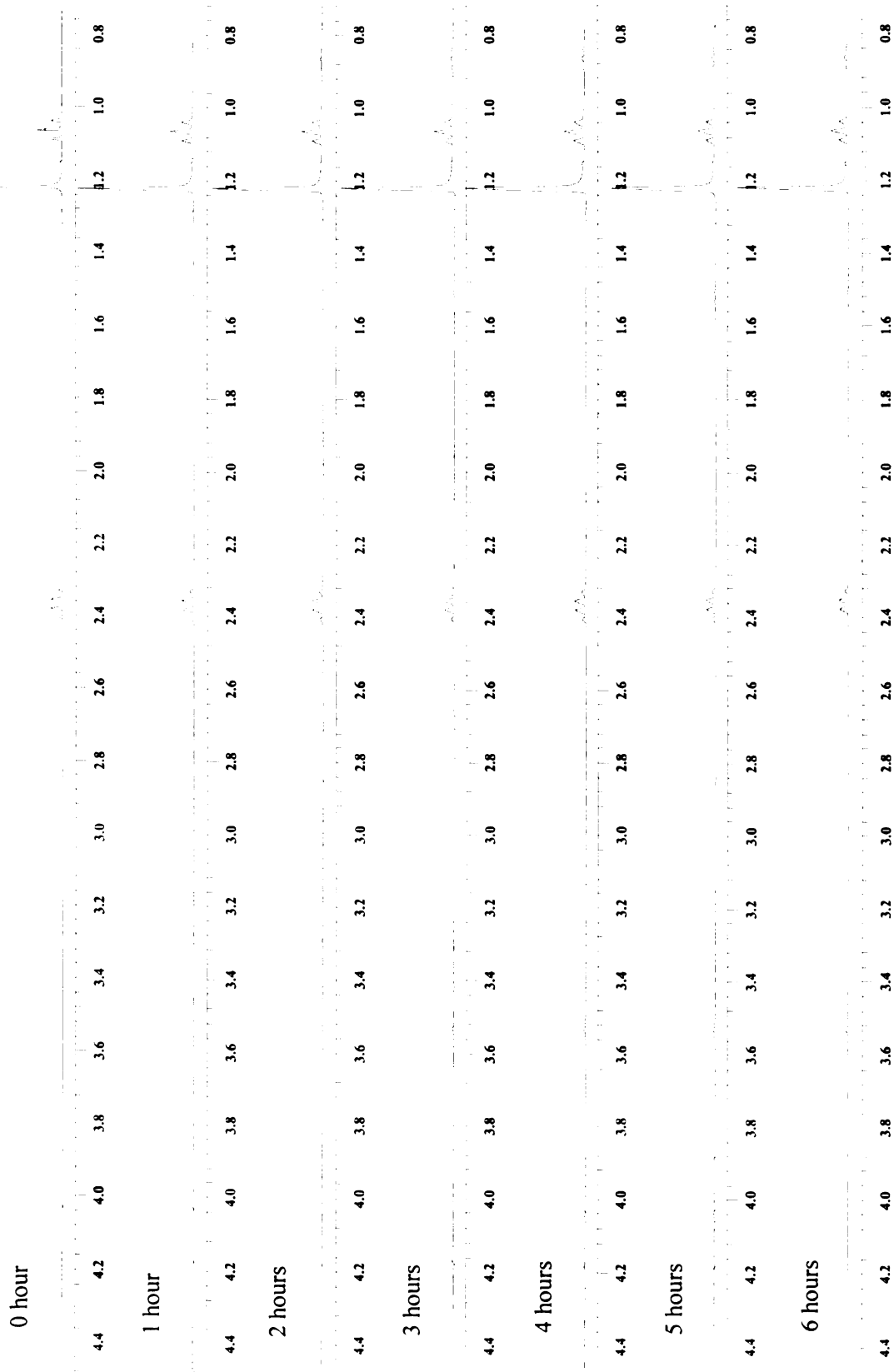
**Appendix 5.2.** Concentration profile of the hydrogenation reaction of isobutyric acid at 423 K and 1200 psi determined by proton NMR



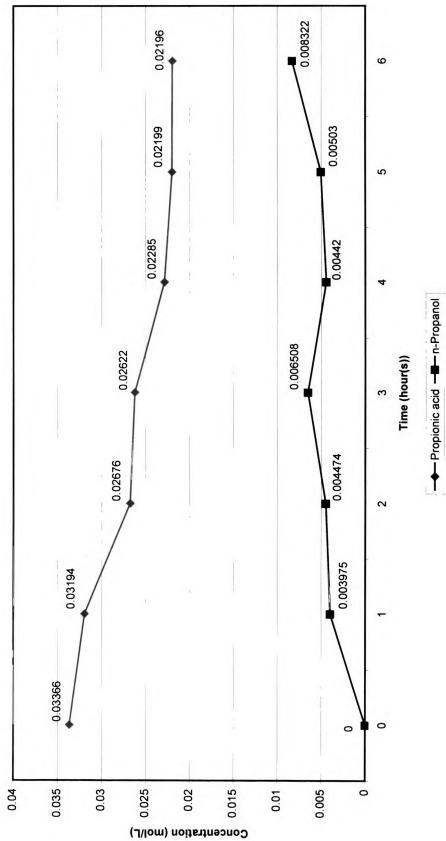
Appendix 5.3. Concentration profile of the hydrogenation reaction of isobutyric acid at 423 K and 1200 psi determined by HPLC



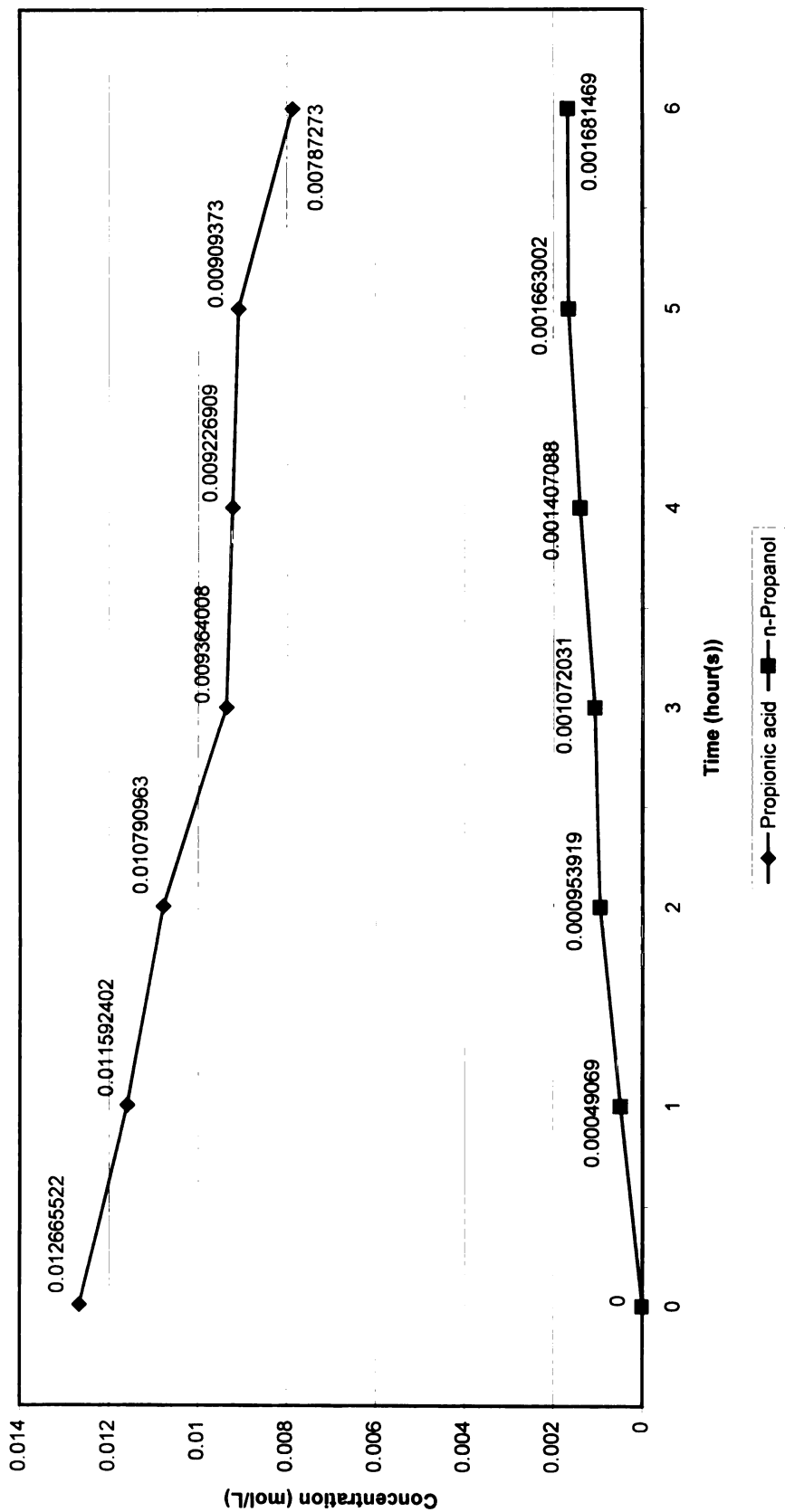
**Appendix 6.1.**  $^1\text{H}$  NMR spectra of Ru/C-catalyzed aqueous phase hydrogenation of propanoic (PA) to n-propanol (POL) in six hours at 423 K and 1200 psi.



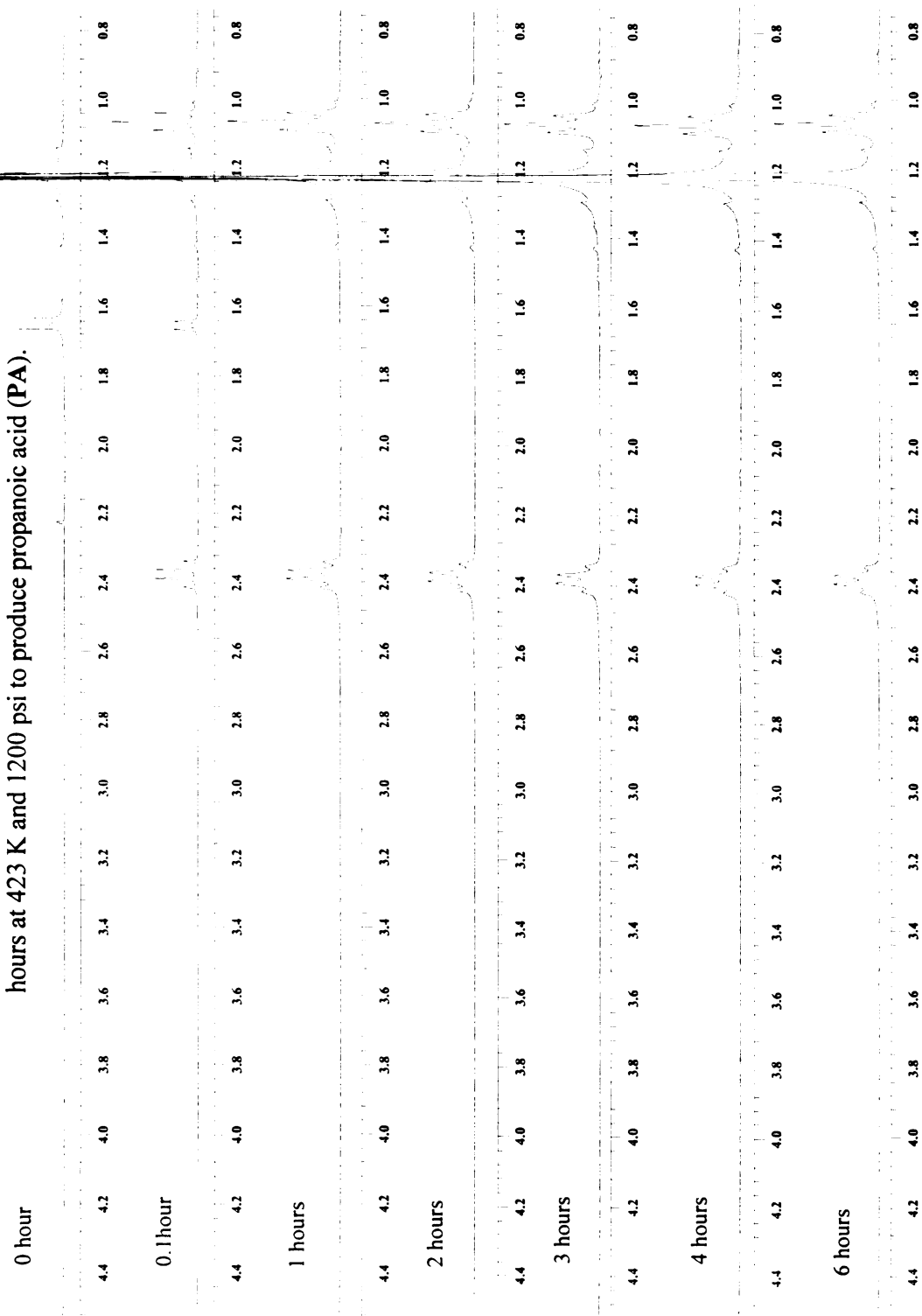
**Appendix 6.2.** Concentration profile of the hydrogenation reaction of propionic acid at 423 K and 1200 psi determined by proton NMR



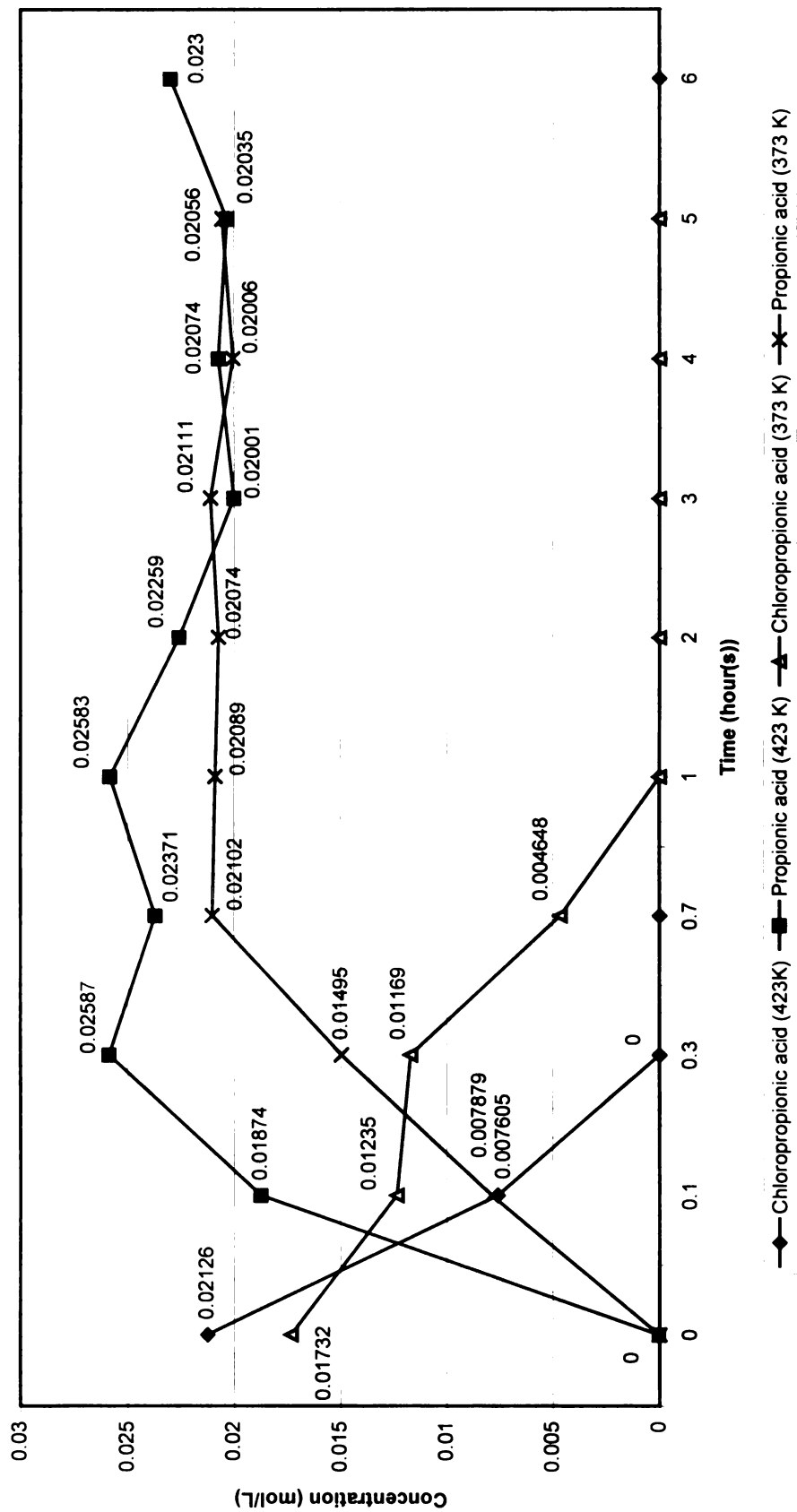
**Appendix 6.3.** Concentration profile of the hydrogenation reaction of propanoic acid at 423 K and 1200 psi determined by HPLC



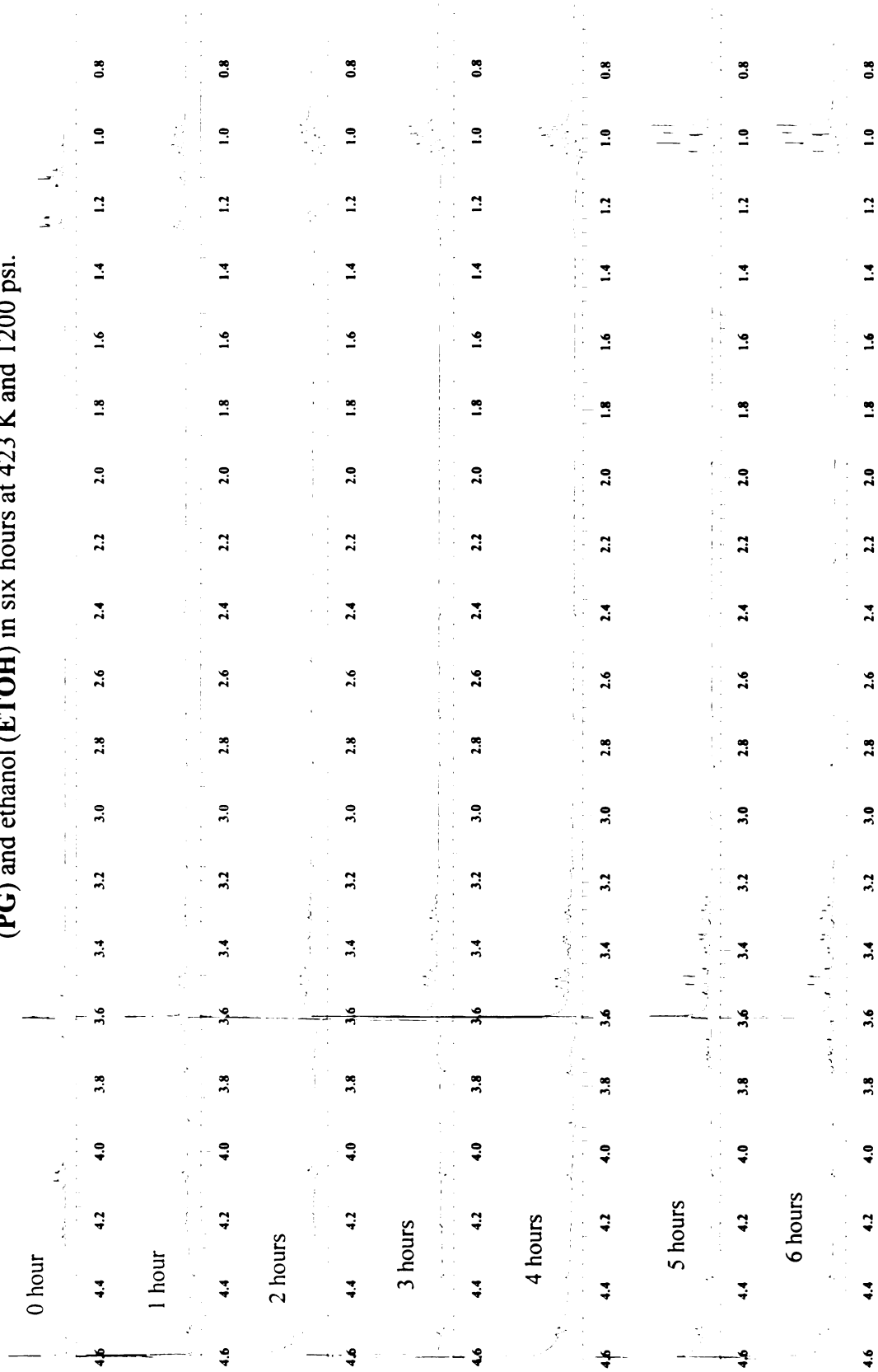
**Appendix 7.1.  $^1\text{H}$  NMR spectra of Ru/C-catalyzed aqueous phase hydrogenation of 2-chloropropanoic acid (2CPA) in six hours at 423 K and 1200 psi to produce propanoic acid (PA).**



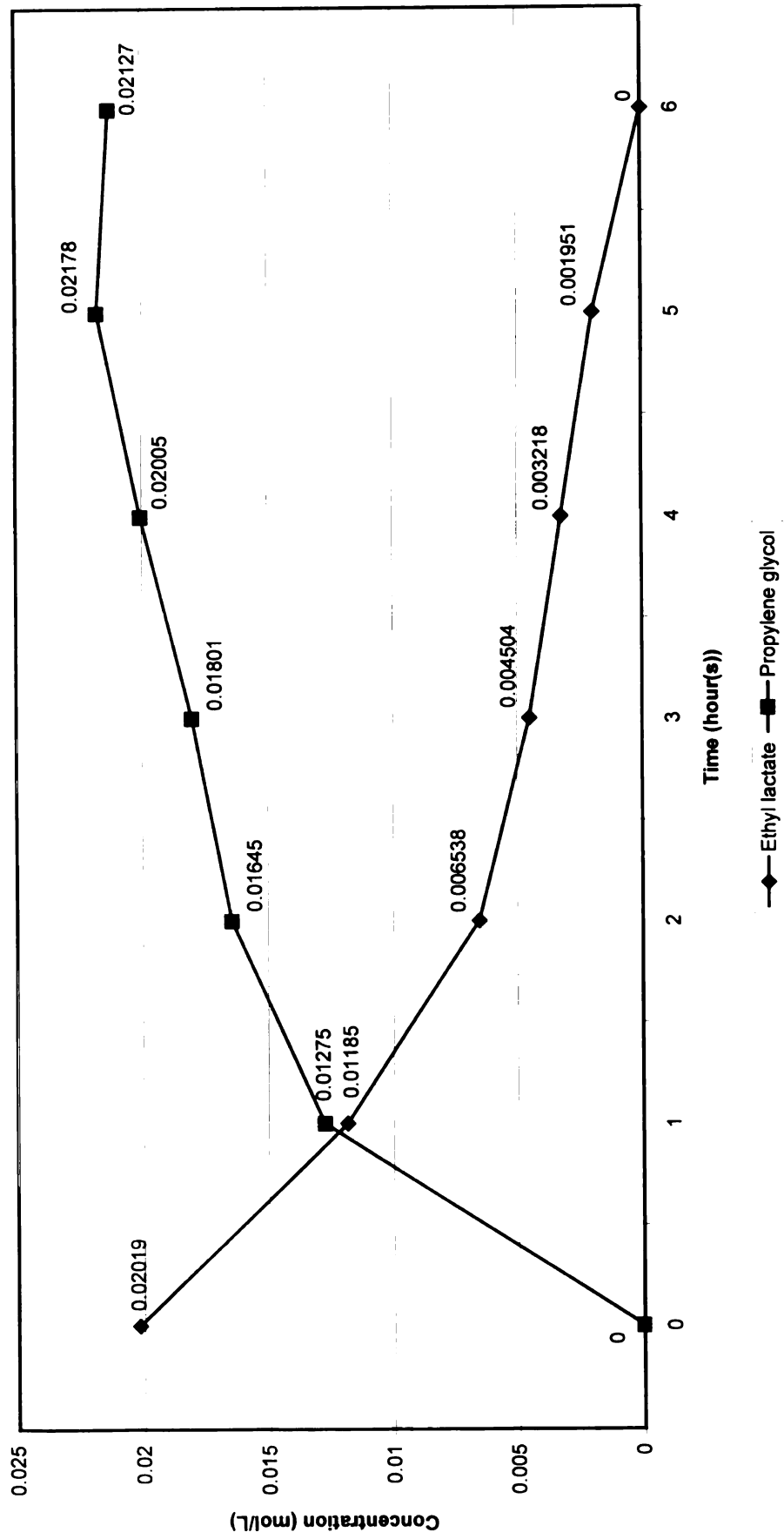
**Appendix 7.2.** Concentration profile of the hydrogenation of 2-chloropropionic acid at 423 and 373 K



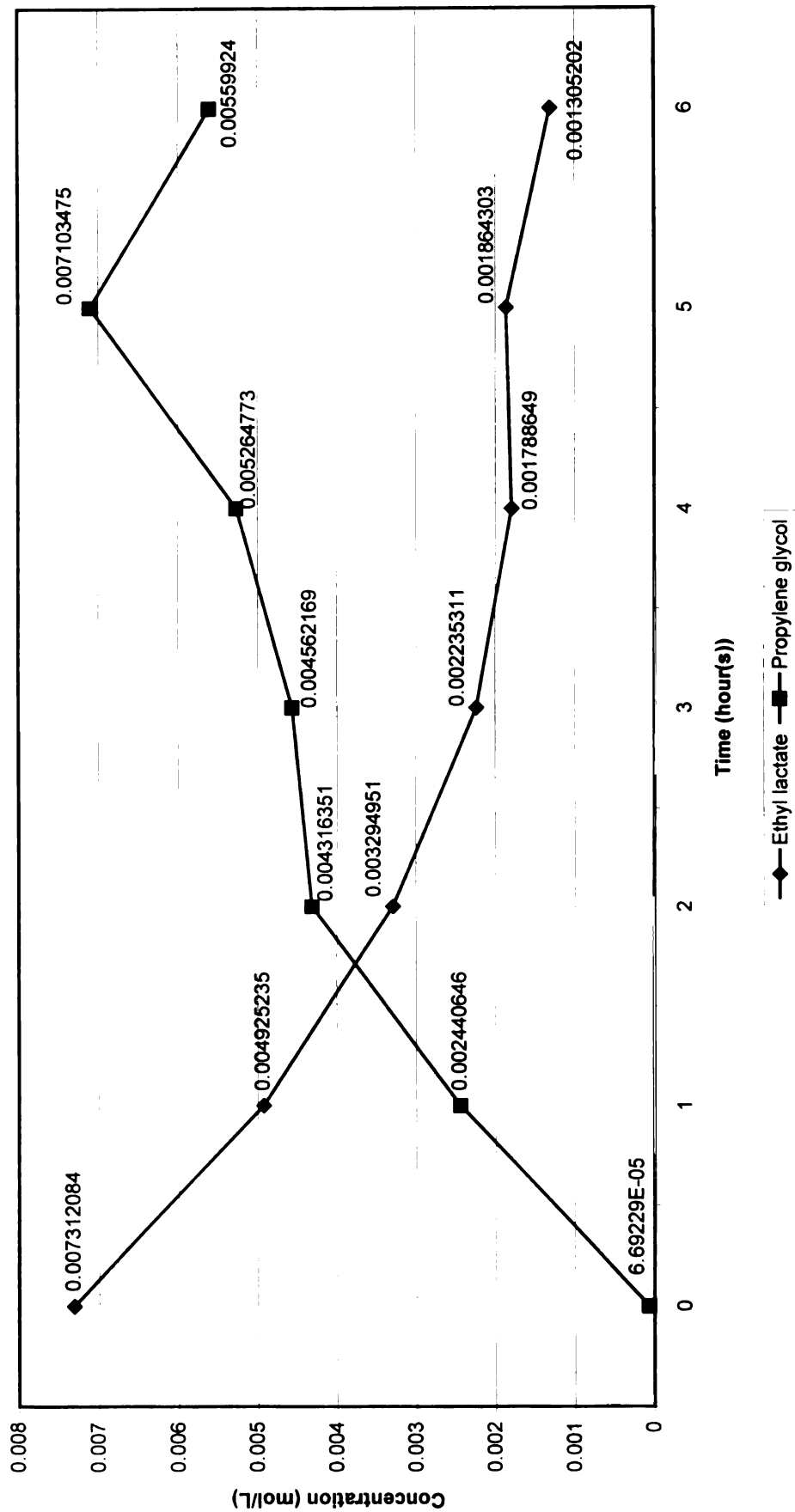
**Appendix 8.1.  $^1\text{H}$  NMR spectra of Ru/C-catalyzed aqueous phase hydrogenation of ethyl lactate (EL) to propylene glycol (PG) and ethanol (ETOH) in six hours at 423 K and 1200 psi.**



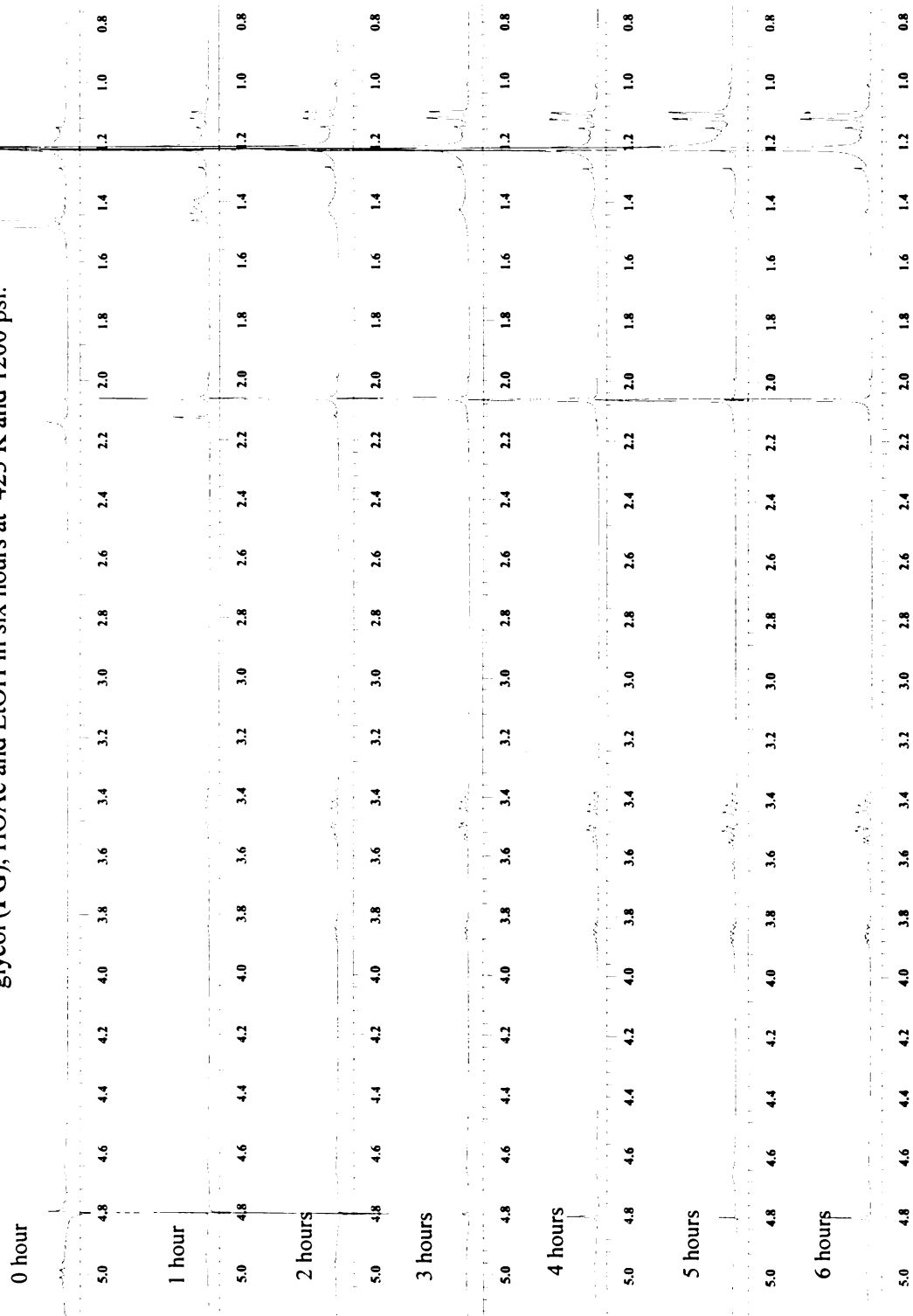
**Appendix 8.2.** Concentration profile of the hydrogenation of ethyl lactate at 423 K and 1200 psi determined by proton NMR



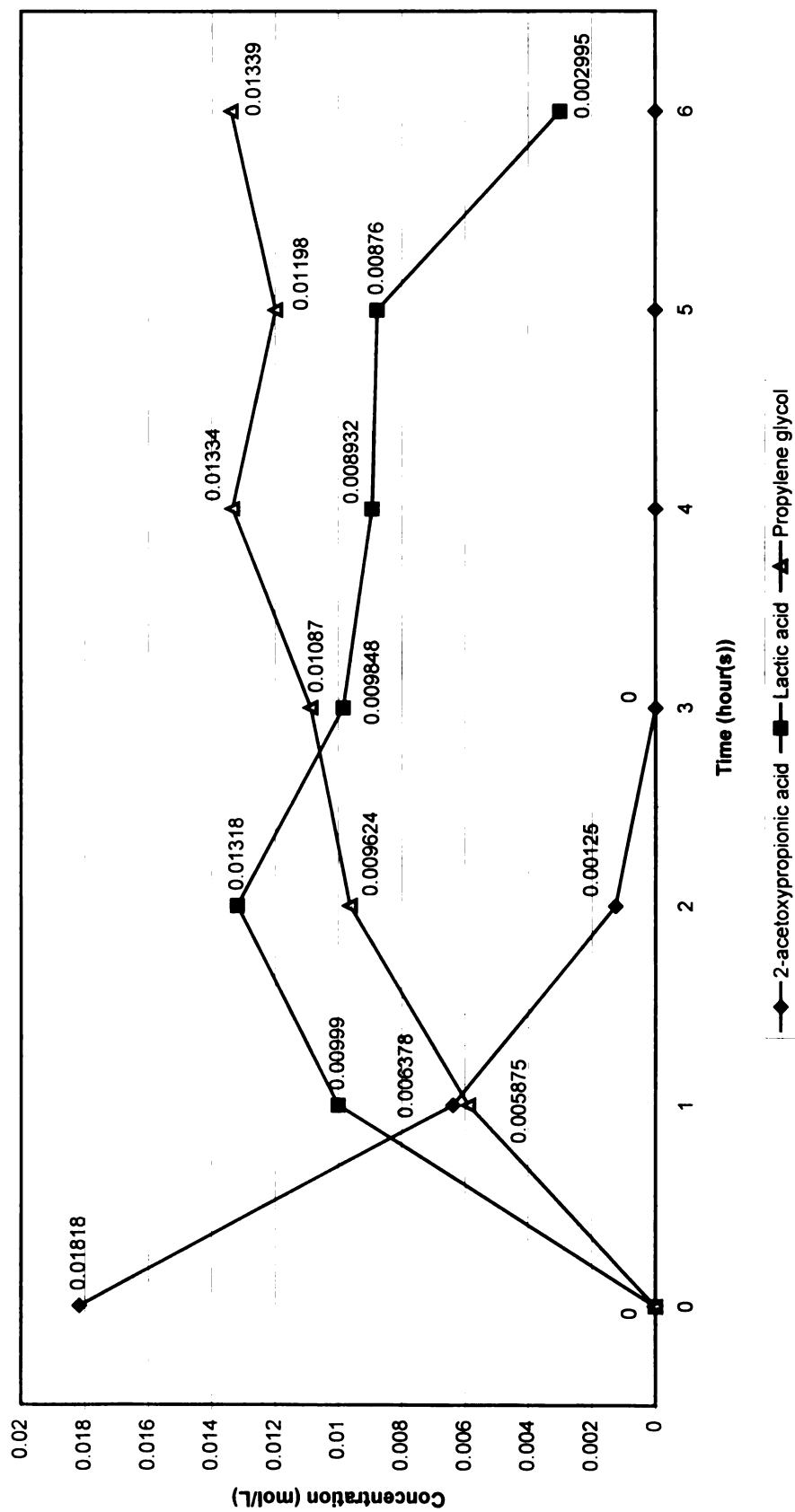
**Appendix 8.3.** Concentration profile of the hydrogenation of ethyl lactate at 423 K and 1200 psi determined by HPLC



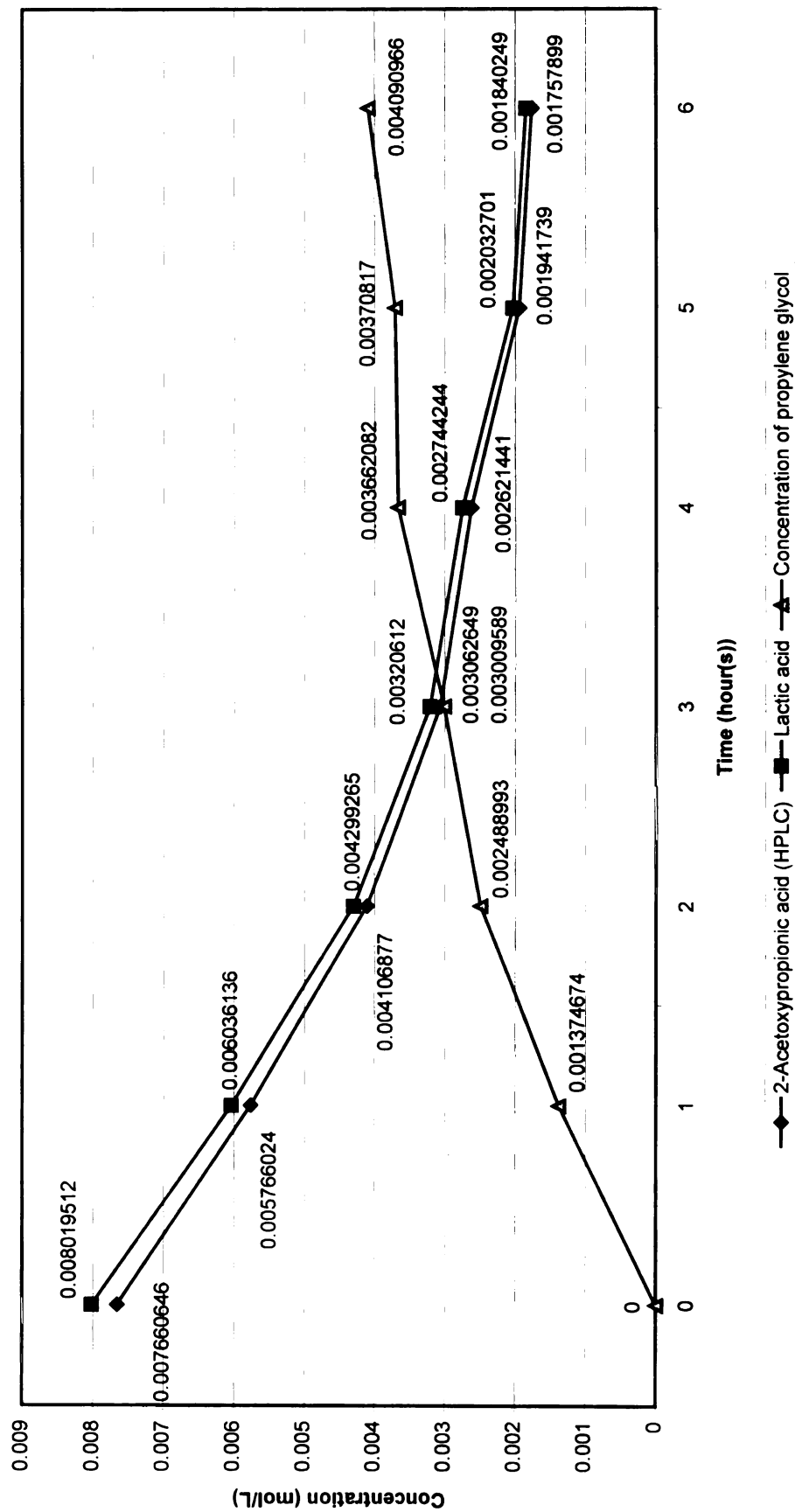
**Appendix 9.1. <sup>1</sup>H NMR spectra of Ru/C-catalyzed aqueous phase hydrogenation of 2-acetoxypropanoic acid (2APA) to propylene glycol (PG), HOAc and EtOH in six hours at 423 K and 1200 psi.**



**Appendix 9.2.** Concentration profile of the hydrogenation of 2-acetoxypropanoic acid at 423 K and 1200 psi determined by proton NMR



**Appendix 9.3.** Concentration profile of the hydrogenation of 2-acetoxypropionic acid at 423 K and 1200 psi determined by HPLC



**Appendix 10.** Table of HPLC standards (prepared as  $\approx 0.1$  g of standard/10 g of solution) and their corresponding peak area (counts).

<b>HPLC Standard</b>	<b>Conc. of Stock Solution. (mol/L)</b>	<b>HPLC Peak Area (Counts)</b>
Lactic Acid (LA)	1.59E-2	4535399
Propylene Glycol (PG)	1.78E-2	6514324
Ethyl Lactate (EL)	9.14E-3	4846357
Ethanol (EtOH)	2.76E-2	3384916
Propanoic Acid (PA)	1.74E-2	4833463
n-Propanol (POL)	1.72E-2	4218308
Methanol (MEOH)	3.74E-2	1029536
2-Acetoxypropanoic Acid (2APA)	8.73E-3	3218327
Acetic Acid (HOAC)	2.00E-2	3562055
2-Chloropropanoic Acid (2CPA)	1.01E-2	4975447
2-Methoxypropanoic Acid (2MPA)	9.85E-3	3738495
Chloropropanol	1.41E-2	6299451
Glycolic Acid (GA)	1.84E-2	3722936
Ethylene Glycol (EG)	2.17E-2	5500556
Methoxyacetic Acid (MA)	1.31E-2	4674990
2-Methoxyethanol (2METOH)	1.54E-2	4424119
Isobutyric Acid (IBA)	1.30E-2	4567477
Isobutanol (IBUOL)	1.57E-2	5300779

## Bibliography

- (1) Association, N. C. G.: St Louis, Missouri, 2000.
- (2) Jackson, J. E.; Miller, D. J.; Kovacs, D. G. *Publication being submitted 2002*.
- (3) Noyori, R.; Okhuma, T. *Angew. Chem. Int. Ed.* **2001**, *40*, 41-67.
- (4) Singh, U. K.; Vannice, A. M. *Appl. Catal. A: General* **2001**, *213*, 1-24.
- (5) Baiker, A. *Chem. Rev.* **1999**, *99*, 453-473.
- (6) Augustine, R. *Catalysis Today* **1997**, *37*, 419-440.
- (7) Thompson, H. W.; Naipawer, R. E. *J. Am. Chem. Soc* **1973**, *95*, 6379-6382.
- (8) Thompson, H. W. *J. Org. Chem.* **1971**, *36*, 2577-2582.
- (9) Fried, J.; Edwards, A. *Organic Reactions in Steroid Chemistry*; Van Nostrand Reinhold, 1976; Vol. 1.
- (10) Cram, D. J.; Abd Elhafez, F. A. *J. Am. Chem. Soc* **1952**, *74*, 5828-5851.
- (11) Noyori, R. *Asymmetric Catalysis in Organic Synthesis*; Wiley: New York, NY, 1994.
- (12) Akabori, S.; Izumi, Y.; Fuji, Y.; Sakurai, S. *Nature* **1956**, *178*, 323-340.
- (13) Singh, U. K.; Landau, R. N.; Sim, Y.; Leblond, C.; Blackmond, D. G.; Tanielyan, S.; Augustine, R. L. *J. Catal.* **1995**, *154*, 91-104.
- (14) Sun, Y.; Wang, J.; Leblond, C.; Landau, R. N.; Blackmond, D. G. *J. Catal.* **1996**, *161*, 759-771.
- (15) Sun, Y.; Landau, R. N.; Wang, J.; Leblond, C.; Blackmond, D. G. *J. Am. Chem. Soc* **1996**, *118*, 1348-1353.
- (16) Sun, Y.; Wang, J.; Leblond, C.; Reamer, R. A.; Laquidara, J.; Sowa, J. R. J.; Blackmond, D. G. *J. Org. Chem.* **1997**, *548*, 65-72.
- (17) Blaser, H.-U.; Jalett, H.-P.; Garland, M.; Studer, H.; Hhies, A.; Wirth-Tijani, J. *J. Catal.* **1998**, *173*, 282-292.

- (18) Singh, U. K.; Vannice, A. M. *J. Catal.* **2000**, *191*, 165-180.
- (19) Wehrli, J. T.; Baiker, A. J. *J. Mol. Catal.* **1989**, *57*, 1989-1998.
- (20) Blaser, H.-U.; Jalett, H.-P.; Wiehl, J. *J. Mol. Catal.* **1991**, *68*, 215-228.
- (21) Struyk, J.; Scholten, J. J. F. *Appl. Catal.* **1990**, *62*, 151-173.
- (22) West, R. *J. Am. Chem. Soc.* **1959**, *81*, 1615-1625.
- (23) Pauling, L. *Proc. R. Soc. London Ser. A* **1949**, *196*, 343-348.
- (24) Boudart, M. *Adv. Catal.* **1969**, *20*, 153-159.
- (25) Broadbent, H. S.; Campbell, G. C.; Bartley, W. J.; Johnson, J. H. *J. Org. Chem.* **1959**, *24*, 1847-1854.
- (26) Turek, T.; Trimm, D. L.; Cant, N. W. *Catal. Rev. Sci. Eng.* **1994**, *36*, 645.
- (27) CRC Handbook **1992**.
- (28) Christiansen J. A. In *US Patent* 1,302,011, **1919**.
- (29) Evans, J. W.; Casey, P. S.; Mainwright, M. S.; Trimm, D. L.; Cant, N. W. *Appl. Catal.* **1983**, *7*, 31-41.
- (30) Evans, J. W.; Tonner, S. P.; Mainwright, M. S.; Trimm, D. L. *Chem. Eng. Today* **1983**, 509-516.
- (31) Cerveny, L.; Havlicek, V. *Sb. Vys. Sk. Chem.-Technol. Praze, C: Org. Chem. Technol.* **1988**, *C30*, 125-141.
- (32) Sorum, P. A.; Onsager, O. T. *Proc. Int. Congr. Catal.* **1984**, *8*, 233-244.
- (33) Kim, K. M.; Woo, H. C.; Cheong, M.; Kim, J. C.; Lee, K. H.; Lee, J. S.; Kim, Y. G. *Appl. Catal. A: Generalo* **1992**, *83*, 15-30.
- (34) Gormley, R. J.; Rao, V. U. S.; Soong, Y.; Micheli, E. *Appl. Catal. A: Generalo* **1992**, *87*, 81-101.
- (35) Monti, D. M.; Cant, N. W.; Trimm, D. L.; Mainwright, M. S. *Journal of Catalysis* **1986**, *100*, 17-27.
- (36) Lazier, W. A. In *US Patent* 2079414, 1937.

- (37) Yan, T. Y.; Albright, L. F.; Case, L. C. *Ind. Eng. Chem. Res. Prod. Res. Dev.* **1965**, *4*, 101-110.
- (38) Grey, R. A.; Pez, G. P.; Wallo, A.; Corsi, J. J. *Chem. Soc. Chem. Commun.* **1980**, 783-784.
- (39) Grey, R. A.; Pez, G. P. In *US Patent 4,232,170*, 1979.
- (40) Evans, J. W.; Mainwright, M. S.; Cant, N. W.; Trimm, D. L. *J. Catal.* **1984**, *88*, 203-213.
- (41) Ferreti, O. A.; Bournonville, J. P.; Mabillon, G.; Martino, G.; Candy, J. P.; Basset, J.-M. *J. Mol. Catal.* **1991**, *67*, 283-294.
- (42) Claus, P.; Lucas, M.; Lucke, B. *Appl. Catal. A: General* **1991**, *79*, 1-18.
- (43) Agarwal, A. K.; Mainwright, M. S.; Trimm, D. L.; Cant, N. W. *J. Mol. Catal.* **1988**, *45*, 247-254.
- (44) Adkins, H.; Billica, H. R. *J. Am. Chem. Soc.* **1948**, *70*, 3121-3125.
- (45) Adkins, H.; Bowden, E. *J. Am. Chem. Soc.* **1934**, *56*, 689-691.
- (46) Thomas, D. J.; Wehrli, J. T.; Mainwright, M. S.; Trimm, D. L. *Appl. Catal. A: General* **1992**, *86*, 101-114.
- (47) Turek, T.; Trimm, D. L.; Black, D. S.; Cant, N. W. *Appl. Catal. A: General* **1994**, *116*, 137-150.
- (48) Kohler, M. A.; Cant, N. W.; Mainwright, M. S.; Trimm, D. L. In *Proc. 9th International Congress on Catalysis*; The Chemical Institute of Canada, Ottawa: Calgary, 1988, p 1043.
- (49) Monti, D. M.; Cant, N. W.; Trimm, D. L.; Mainwright, M. S. *J. Catal.*, *100*, 28.
- (50) Thomas, D. J.; Stambach, M. R.; Cant, N. W.; Mainwright, M. S.; Trimm, D. L. *Ind. Eng. Chem. Res.* **1990**, *29*, 204.
- (51) Couteau, W.; Dungalhoeff, M. L.; Hendrickx, A.; Verbeest, R. In *Ger. Patent 2 553 959*: Germany, 1976.
- (52) Bradley, M. W. *Belg. Patent 892 958* **1982**.
- (53) Sharif, M.; Turner, K. In *Eur. Patent Appl. 143 634*, 1986.

- (54) Kouba, J. A.; Zletz, A. In *US Patent 4 613 707*, 1986.
- (55) Adkins, H.; Folkers, K. *J. Am. Chem. Soc* **1932**, *54*, 1145-1154.
- (56) Arnold, F. R.; Lazier, W. A. In *US Patent 2,116,552*: USA, 1938.
- (57) Guyer, A.; Bieler, A.; Jaberg, K. *Helv. Chim. Acta* **1947**, *30*, 39.
- (58) Adams, P. T.; Selff, R. E.; Tolbert, B. M. *J. Org. Chem.* **1952**, *74*, 2416-2423
- (59) Rayadhyaksha, R. A.; Karwa, S. L. *Chem. Eng. Sci.* **1984**, *41*, 1765-1770.
- (60) Kitson, M.; Williams, P. S. In *US Patent 4,777,303*; BP Chemicals Ltd.: USA, 1988.
- (61) Kitson, M.; Williams, P. S. In *US Patent 4,826,795*; BP Chemicals Ltd.: USA, 1989.
- (62) Kitson, M.; Williams, P. S. In *US Patent 4,804,791*; BP Chemicals Ltd.: USA, 1989.
- (63) Antons, S. In *US Patent 5,731,479*; Bayer Aktiengesellschaft: USA, 1998.
- (64) Antons, S. In *US Patent*; Bayer Aktiengesellschaft: USA, 2002.
- (65) Zhang, Z.; Jackson, J. E.; Miller, D. J. *Appl. Catal. A: General* **2001**, *219*, 89-98.
- (66) Yonezava, Y.; Hino, T.; Tokita, Y.; Matsuda, K.; Ikeda, T. *Tetrahedron*. 1997, **53**(24), 14287-14296.

MICHIGAN STATE UNIVERSITY LIBRARIES



3 1293 02328 8123